



ISOTROPIC DAMAGE PHENOMENA IN SATURATED POROUS MEDIA: A BEM FORMULATION

EDUARDO TOLEDO DE LIMA JUNIOR

Ph.D. Thesis

ESCOLA DE ENGENHARIA DE SÃO CARLOS
UNIVERSIDADE DE SÃO PAULO

ÉCOLE NORMALE SUPÉRIEURE DE CACHAN

2010

EDUARDO TOLEDO DE LIMA JUNIOR

ISOTROPIC DAMAGE PHENOMENA IN SATURATED POROUS MEDIA: A BEM FORMULATION

A thesis submitted in partial satisfaction of the
requirements for the degree of
Doctor of Philosophy
in

Civil Engineering
of the

ESCOLA DE ENGENHARIA DE SÃO CARLOS
UNIVERSIDADE DE SÃO PAULO

and

Mechanics – Mechanical Engineering – Civil Engineering
of the

ÉCOLE NORMALE SUPÉRIEURE DE CACHAN

Supervisors

Wilson Sergio Venturini, Full Professor *(in memorian)*
Humberto Breves Coda, Associate Professor

Escola de Engenharia de São Carlos
Universidade de São Paulo

Ahmed Benallal, Research Director

École Normale Supérieure de Cachan

São Carlos, 2010

REPRODUCTION AND RELEASE OF THE WHOLE CONTENT OR PART OF THIS THESIS ARE AUTHORIZED, BY ANY ELECTRONIC OR CONVENTIONAL WAY, FOR STUDY AND RESEARCH PURPOSES, SINCE THE SOURCE IS CITED

Card catalog prepared by the Section of Information
Treatment of Library Service - EESC / USP

Lima Junior, Eduardo Toledo
L732i Isotropic damage phenomena in saturated porous media: a bem formulation / Eduardo Toledo Lima Junior ; advisors Ahmed Benallal, Humberto B. Coda. - São Carlos, 2010.

Thesis (Doctoral Program and the Graduate Area of Concentration in Civil Engineering) – Escola de Engenharia de São Carlos da Universidade de São Paulo and École Normale Supérieure de Cachan, 2010.

1. Saturated porous media. 2. Isotropic damage. 3. Boundary element method. I. Title.

To Wilson Sergio Venturini

ACKNOWLEDGEMENTS

To Professor Wilson S. Venturini for the direction since the M.Sc. course, for his trust in my work, and for his great consideration and generosity. A brave man,with a brilliant mind.

To Professor Humberto B. Coda for his attention, friendship and valuable contributions throughout the work, especially in recent months, when he officially took over the direction of the thesis.

To Researcher Ahmed Benallal for his direction and opportunity to study in the Laboratory of Mechanics and Technology (LMT Cachan).

To Professor Euclides de Mesquita Neto for his contributions to the Ph.D. qualifying examination.

To Professors Sergio P. B. Proença and Rodrigue Desmorat, for their assistance and discussions.

To Masaki Kawabata Neto, Maria Nadir Minatel and Rosi A. J. Rodrigues on behalf of the general staff of the Structural Engineering Department (SET-EESC-USP).

To Aurore Patey, Catherine Génin, Evelyne Dupré and Nancy Michaud, on behalf of the general staff of LMT Cachan and International Relations Department (SRI-ENS Cachan).

To the colleagues of SET-EESC-USP and LMT Cachan, for the ever pleasing times we shared.

To my friend Wilson W. Wutzow for his help in the development of the thesis, since its inception.

To my friends Caio G. Nogueira, Manoel Dênis C. Ferreira, Edson D. Leonel, Jefferson L. Silva and Rodrigo R. Paccola for their discussions on the topics related to the thesis.

To all my good friends, in Brazil and France, there is no need to mention names because they know who they are.

To Beverly Young, for the text translation.

To The Coordination for the Improvement of Higher Education Personnel (CAPES), to the State of São Paulo Research Foundation (FAPESP) and to Île-de-France Region, for the financial support in Brazil and France.

To my parents, Eduardo and Josilma, and my brother Guilherme, for their endless love, kindness and unconditional support. I am blessed.

To my fiancée Mônica, for her love, companionship, and the support she gave me throughout the thesis. We both lived the "Ph.D. experience" together, from the beginning. I am doubly blessed. To her mother and sister, Ligia and Marina, for their loving care, as my family in São Paulo.

I thank God, for the gift of life.

ABSTRACT

This work is devoted to the numerical analysis of saturated porous media, taking into account the damage phenomenon on the solid skeleton. The porous media is taken into poroelastic framework, in full-saturated condition, based on the Biot's Theory. A scalar damage model is assumed for this analysis. An implicit Boundary element Method (BEM) formulation, based on time-independent fundamental solutions, is developed and implemented to couple the fluid flow and the elasto-damage problems. The integration over boundary elements is evaluated by using a numerical Gauss procedure. A semi-analytical scheme for the case of triangular domain cells is followed to carry out the relevant domain integrals. The non-linear system is solved by a Newton-Raphson procedure. Numerical examples are presented, in order to validate the implemented formulation and to illustrate its efficiency.

***Keywords**: Saturated Porous Media, Isotropic Damage, Boundary Element Method.*

RESUMO

Este trabalho trata da análise numérica de meios porosos saturados, considerando danificação na matriz sólida. O meio poroso é admitido em regime poroelástico, em condição saturada, com base na teoria de Biot. Um modelo de dano escalar é empregado nesta análise. Uma formulação implícita do Método dos Elementos de Contorno (MEC), baseada em soluções fundamentais independentes do tempo, é desenvolvida e implementada de forma a acoplar os problemas de difusão de fluido e de elasto-dano. A integração sobre os elementos de contorno é feita através da quadratura de Gauss. Um esquema semi-analítico é aplicado sobre células triangulares para avaliar as integrais de domínio do problema. A solução do sistema não linear é obtida através de um procedimento do tipo Newton-Raphson. Apresentam-se exemplos numéricos a fim de validar a formulação implementada e demonstrar sua eficiência.

***Palavras-chave**: Meios Porosos Saturados, Dano Isotrópico, Método dos Elementos de Contorno.*

RÉSUMÉ

Ce travail est consacré à l'analyse numérique des milieux poreux saturés, en tenant compte le phénomène d'endommagement sur le squelette solide. Le milieu poreux est pris dans le cadre poro-élastique, dans un état complètement saturé, d'après la théorie de Biot. Un modèle scalaire d'endommagement est supposé pour cette analyse. Une formulation implicite de la Méthode des éléments de frontière, basée sur des solutions fondamentales indépendantes du temps, est développé et implantée numeriquement pour coupler les problèmes de l'écoulement de fluide et de l'elasticité endommageable. L'intégration sur des éléments de frontière est realisée en utilisant la méthode numérique de Gauss. Un schéma semi-analytique pour le cas des cellules triangulaires de domaine est suivie pour évaluer les intégrales de domaine pertinentes. Le systéme non-linéaire est résolu par une procédure de Newton-Raphson. Des exemples numériques sont présentés, afin de valider la formulation implantée et pour illustrer son efficacité.

***Mots-clés**: Milieux Poreux Saturés, Endommagement Isotropique, Méthode des Éléments de Frontière.*

TABLE OF CONTENTS

1. INTRODUCTION

1.1. OVERALL CONSIDERATIONS AND OBJECTIVES 15
1.2. METHODOLOGY 16
1.3. BRIEF LITERATURE REVIEW 16
1.3.1. Poromechanics and Linear Poroelasticity 16
1.3.2. Strain Localization and Continuum Damage Mechanics 17
1.3.3. Porous Media Subjected to Damage 18
1.3.4. Integral Equations and BEM Applied to Poroelasticity and to Damage Mechanics 19
1.4. THESIS STRUCTURE 21

2. ASPECTS ON POROMECHANICS AND CONTINUUM DAMAGE MECHANICS

2.1. OVERALL CONSIDERATIONS 23
2.2. DESCRIPTION OF A SATURATED POROUS MEDIUM 23
2.3. BEHAVIOR OF THE SKELETON 24
2.3.1. Motion of a Continuum. Displacement. Deformation Gradient 24
2.3.2. Porosity. Void Ratio 26
2.3.3. Strain Tensor 26
2.4. BEHAVIOR OF THE FLUID PHASE 28
2.4.1. Particle Derivative 28
2.4.2. Relative Flow Vector of a Fluid Mass. Filtering Vector. Fluid Mass Content 30
2.5. MASS BALANCE 30
2.5.1. Eulerian Continuity Equations 30
2.5.2. Lagrangean Continuity Equations 31
2.6. MOMENTUM BALANCE 33
2.6.1. The Hypothesis of Local Forces 33
2.6.2. Momentum Balance 34
2.6.3. The Dynamic Theorem 34
2.7. STRESS TENSOR 34
2.8. EQUILIBRIUM EQUATION 36
2.9. PARTIAL STRESS TENSOR 37
2.10. ASPECTS ON THE CONTINUUM DAMAGE MECHANICS 38
2.10.1. Damage Variable and Effective Stress 39
2.10.2. Isotropic Local Damage Model (Marigo, 1981) 40
2.10.3 Comments on Strain Localization 41

3. PORO-DAMAGE FORMULATION AND BEM IMPLEMENTATION

3.1. OVERALL CONSIDERATIONS 45
3.2. PORO-DAMAGE FORMULATION 45
3.2.1. Constitutive Laws 45
3.2.2. Fluid Transport Law 48
3.2.3. Fluid Continuity Equation 49
3.2.4. Equilibrium Equation 50
3.2.5. Rates of the Variables 50
3.3. INFLUENCE OF DAMAGE ON THE POROELASTIC PARAMETERS 50
3.4. ASPECTS ON THE BOUNDARY ELEMENT METHOD 51
3.4.1. Boundary Elements and Discretization 52
3.4.2. Domain Discretization 54
3.5. BEM FORMULATION 57
3.5.1. Integral Formulation for the Solid Phase 57
3.5.2. Integral Formulation for the Fluid Phase 63
3.5.3. Time-dependent Integral Formulation 65
3.5.4. Algebraic System 67
3.5.5. Solution Procedure 72
3.5.6. Algorithm to Evaluate the Damage Level 75

4. NUMERICAL EXAMPLES

4.1. OVERALL CONSIDERATIONS 79
4.2. LINEAR POROELASTICITY EXAMPLES 79
4.2.1. One-dimensional Consolidation 79
4.2.2. Plane Consolidation 82
4.2.3. Poroelastic Response under Different Loading Conditions 86
4.3. EXAMPLES ON THE ADOPTED DAMAGE MODEL 87
4.3.1. Characterization and Parametric Analysis of the Model 88
4.3.2. Solid under Cyclic Loading 89
4.3.3. Solid with Defect under Uniaxial Tension 91
4.4. EXAMPLES ON POROELASTICITY COUPLED TO DAMAGE 93
4.4.1. Poroelastic Column Subject to Damage 93
4.4.2. Poroelastic Plane Domain subjected to Damage 100
4.4.3. Brief Comments on the Shallow and Deep Foundation Structures 104

CONCLUSION AND PERSPECTIVES 108
BIBLIOGRAPHY 111

Chapter 1

Introduction

1.1. OVERALL CONSIDERATIONS AND OBJECTIVES

The complexity of the problems currently encountered in engineering leads to a growing demand for quality personnel, infrastructure and available analytical methods. In the field of structural engineering, there have been several initiatives to improve the theoretical and numerical representation of the behavior of structural parts and systems. The development of numerical models enables a more realistic evaluation of the in-service behavior of structures and failure modes, quantifying the deterioration of components and determining the loading threshold limits in projects.

Among the various topics of interest, the mechanical behavior of porous materials stands out. These are multiphase materials, composed of a deformable solid matrix and a porous space, which may contain liquid and gas fluids. The interaction between the solid and fluid phases defines the mechanical response of the medium to the external forces, through solid skeleton deformations and the fluid flow into the pores. This thesis addresses the porous media fully saturated by a single fluid.

The study of porous materials is relevant in several areas, such as soil and rock mechanics, diffusion of contaminants, biomechanics and petroleum engineering.

The cases in which a non-linear mechanical behavior of materials occurs, as for instance damage and plasticity, are of great interest to the mechanics of materials and structures. The rupture process of a body is progressive, starting with a state of micro-cracking that localizes and develops into a state of effective crack opening, which can in fact induce rupture. The phenomenon identified between the onset of microcracking and fracture is called damage.

The damage models predict the gradual loss of strength and stiffness of the material when loaded. In its constitutive law, it exhibits regions in which resistant strain levels decrease with increasing strain. Under a possible unloading condition, the stiffness loss remains constant, so that no residual strain accumulates.

Considering the increasing complexity of mechanical models developed for engineering problems, the constant search for robust numerical formulations is vital, which can provide reliable results with the least possible computational effort. Thus in this context, the Boundary Element Method (BEM) is an interesting choice to obtain numerical solutions in various applications.

The behavior of a saturated porous medium is sought to be understood from the interaction between the mechanical response of the solid phase and the fluid flow through the porous space. This work proposes to investigate the degradation of brittle and quasi-brittle materials from a known isotropic damage model. Thus, one of the objectives is to incorporate that damage law into the solid matrix of the porous medium, in order to analyze the influence of

the dissipative phenomena in the global response of the system, including it in the mechanical properties. The main objective of this thesis is the development of a nonlinear BEM formulation that enables the application of the aforementioned model.

1.2. METHODOLOGY

The behavior of a saturated porous medium from the formulation presented in Coussy (2004) is described, which is derived from Biot's work (1941, 1955), taking as state variables the strain in the solid matrix and the pore pressure acting on the fluid. A laminar fluid flow is assumed, which is governed by Darcy's law. The Lagrangian kinematic description is adopted here.

The loss of stiffness from the damage process is assessed using an isotropic model, applicable to brittle and quasi-brittle materials, proposed by Marigo (1981). The scalar state variable is introduced, which represents the deterioration level in the solid matrix.

The expression for the free energy potential of the poroelastic system is defined, with the internal variables as the strain in the solid skeleton and the porosity. The damage scalar variable is introduced into this expression, in order to incorporate the damage process to the problem.

A nonlinear transient BEM formulation is developed, by coupling the models of the method applied to the fluid diffusion and the plane elasticity in the presence of damage. The Betti's reciprocal theorem is used to obtain the integral equations, using time-independent fundamental solutions. The integration on the boundary elements is performed numerically, using a Gauss-type procedure and a semi-analytical scheme is used to evaluate the domain integrals of the problem.

The temporal integration of the constitutive equations is carried out implicitly. With the non-linear damage law, the consistent tangent operator is deduced and the algebraic equilibrium equations are evaluated using the Newton-Raphson procedure.

1.3. BRIEF LITERATURE REVIEW

1.3.1. Poromechanics and Linear Poroelasticity

The first studies on the subject are credited to Terzaghi (1923), who described the mechanism for transferring an axial load applied to a soil column. This one-dimensional model did not foresee the occurrence of lateral strains. In 1936, Rendulic generalized Terzaghi's theory for a three-dimensional case. However, it was Biot (1941) who presented the first well-accepted model for settlement, or consolidation, in three-dimensional media,

considering isotropic and incompressible fluid. Biot proposes the analysis of a porous medium saturated by the superposition of two continuous media: the solid skeleton and the fluid phase that fills the pores. Biot (1955) later improved his own model by extending it to compressible fluids, considering anisotropy for both the solid skeleton as well as for the fluid, formulating Darcy's law in a generalized way. In 1956, Biot incorporated viscoelasticity of the solid medium into this theory.

Several studies emerged in the 1940s that proposed analytical solutions for particular geometry problems and loading conditions. Biot and Clingan (1941, 1942), McNamee and Gibson (1960, 1963), and Schiffman and Fungaroli (1965) can be cited. The behavior of underground aquifers was studied in Verruijt (1969). Rice and Cleary (1976) sought to relate the poroelastic parameters proposed by Biot, using concepts of soil and rock mechanics. In this work the response differences of a saturated porous medium under drained and undrained conditions are discussed.

Among the more recent works, we highlight those developed by Coussy, presented in a book that was published in 1995. In this publication, the poroelastic and poroplastic models are described and justified by the rigorous consideration of thermodynamic effects involved. Detournay and Cheng (1993), Coussy *et al*. (1998), Wang (2000) and Coussy (2004) should are also mentioned.

A study on saturated media, alternative to Biot's work (1941, 1955), was presented in Auriault and Sanchez-Palencia (1977). From the hypothesis, inherent in the homogenization schemes, that the microscopic structure is periodically reproduced in the domain of the problem, the authors proposed a model for a media saturated by a viscous and incompressible fluid. Other authors have explored the theme from this micromechanical approach, citing Chateau and Dormieux (1998) that addressed partially saturated media, and Lydzba and Shao (2000) that examined the role of microstructure to define the material properties.

1.3.2. Strain Localization and Continuum Damage Mechanics

Kachanov (1958) was the first work that introduced the concept of damage. This work investigated a problem of uniaxial creep for metals subjected to high temperatures, and the damage variable was introduced to describe the ability of a cross section to transfer a load. The continuum damage mechanics (CDM) was formalized based on the thermodynamics of irreversible processes, in the works of Lemaitre and Chaboche (1985) and Lemaitre (1992). In thermodynamics, a consistent physical meaning emerges for the variables that describe the material degradation, always associating them to an energetic process.

Materials that exhibit softening behavior are subject to the problem of strain localization. From a mathematical point of view, this phenomenon leads to some drawbacks regarding the existence and uniqueness of a solution to the problem. The topic was addressed in Benallal *et al*. (1991). Comi *et al*. (1995) presented a study on the strain localization for pure compression in brittle materials (concrete). The different influences of the formulation of elasto-plastic damage model on the compression localization are analyzed. Pijaudier-Cabot and Benallal (1993) described the localization conditions for a material following a non-local damage constitutive relationship. Theoretical studies on localization are also found in Benallal *et al.* (1992) and Jirásek (2002).

The traditional damage models, formulated under local theory, do not capture the effects introduced by the strain localization phenomenon. Thus, some strategies were proposed to regularize the solutions obtained with these local models, based on the concept of a characteristic length for each material. It is assumed that this length limits the range that is subject to localization.

More robust nonlocal damage theories have also been presented. Bazant (1991) argued, based on micromechanics concepts, that at a certain point the damage can be assessed by weighting the deformations measured in the vicinity of this point. Pijaudier-Cabot and Bazant (1987) discuss, regarding a simplified damage model, the influence of a non-local variable calculated as an integral over a representative volume of the same variable defined locally. The same authors in Pijaudier-Cabot and Bazant (1988) present the same non-local integral, stating that other quantities should be considered besides the deformation, as for instance the damage measure.

1.3.3. Porous Media Subjected to Damage

Many authors have addressed the effects of micro-cracking and damage in porous media. As in damage models for solids, there are energy approaches (CDM) based on thermodynamic principles and micromechanical approaches, which usually rely on homogenization processes to express the properties of the material at a macroscopic scale. Some works that use both methods are mentioned, in addition to experimental studies.

Cheng and Dusseault (1993) proposed a model based on CDM and on Darcy's law, and a damage evolution law from microscopic and macroscopic experimental results on rocks. Bary's thesis (1996), on the study of concrete dams, presents an anisotropic damage model based on thermodynamics, and also a numerical analysis using finite elements, with an experimental calibration of material parameters. Shao *et al*. (1997) and Bart *et al*. (2000) present a damage variable defined in terms of the density of distributed microcracks, using

fracture mechanics results to assess the damage evolution. The expressions that measure the influence of damage on the material properties are also presented.

Souley *et al*. (2001) experimentally measured the permeability changes induced by damage on sandstones, incorporating these findings into an anisotropic damage model. Numerical analyses related to the experiments of Souley *et al*. (2001) are presented in Rutqvist (2009). Other experimental analyses on the occurrence of damage in porous media and the consequent alteration of its mechanical and hydraulic properties are found in Tang *et al*. (2002) and Ghabezloo *et al*. (2009).

A viscoelastic model for the stable and unstable damage evolution is presented and validated, based on laboratory results of tests conducted on granite and sandstone, by Hamiel *et al*. (2006). Dormieux and Kondo (2004) analyzed changes in the permeability of a saturated medium from a self-consistent homogenization scheme. A critical value of microfissuration density parameter is defined, besides verifying a sudden increase in the permeability coefficient. Dormieux *et al*. (2006) studied the evolution of anisotropic damage in saturated media, also from a micromechanical point of view. Another model regarding damage evolution that considers anisotropy is found in Zhou (2006).

A mixed model of anisotropic damage, based on energy principles and micromechanics results is presented in Arson (2009) and Arson and Gatmiri (2009), with applications on partially saturated media, considering temperature effects.

1.3.4. Integral Equations and BEM Applied to Poroelasticity and to Damage Mechanics

Studies on integral equations are known to exist since the early nineteenth century, which are the basis for the Boundary Element Methods. However, the first classical theory of integral equations, in which the kernels were defined and integrable, is credited to Fredholm (1903). Fredholm (1906) was a pioneer in the solution of boundary value problems in elastostatics using the linear integral formulation. From this work, the use of integral equations remained limited to theoretical formulations with an indirect approach. In these, the solution to the problem was obtained by fictitious sources applied to the contour, which after its determination, allowed calculating the physical variables of the problem. In 1967, Rizzo presented the first direct formulation for the numerical treatment of integral equations, in which the kernels contain the variables of the problem.

Based on the technique presented by Rizzo (1967), several authors addressed the problem, citing the works of Cruse (1969, 1973, 1974) that addressed the general problems of two and three-dimensional elasticity, and Rizzo and Shippy (1968) that proposed to introduce sub-regions in the treatment of non-homogeneous areas.

The so-called boundary methods made headway after Lachat's thesis, submitted to the University of Southampton in 1975, in which the author introduced the simplicity and elegance the method lacked, bestowing upon it a greater generality. With Lachat's developments, the techniques for solving integral equations were then interpreted as a numerical method. It is reported that Brebbia (1978[a], 1978[b]) was the first to refer to the technique as "Boundary Element Method" in his works. In these studies, obtaining the integral equations was performed by using the Weighted Residual Method, with the appropriate choice of the weighting function. After the first book, published by Brebbia (1978[a]), the method began to be studied intensively in several research centers.

Telles and Brebbia (1979, 1980[a], 1980[b]) showed BEM being used in elastic and viscoplastic problems, with the introduction of strain or stress fields in the equation. Venturini (1982, 1984, 1988) and Venturini and Brebbia (1983, 1988) applied the Boundary Element Method to geotechnical problems, including in the modeling of materials with discontinuities.

In the field of porous media, Cleary (1977) can be cited as a pioneering work, presenting the first integral equations for poroelasticity, based on the direct formulation, proposed by Rizzo (1967). Time-dependent fundamental solutions for soil consolidation were presented in Aramaki and Yasuhara (1981) and Kuroki *et al*. (1982). In 1984[a], Cheng and Liggett formulated an integral equation for poroelasticity applying the Laplace transform. The authors incorporated the propagation of cracks to the problem in Cheng and Liggett (1984[b]).

Also in the 1980s and 1990s, there were other important works on the application of direct BEM formulations to the problem of poroelasticity, citing Cheng and Predeleanu (1987), Nishimura and Kobayashi (1989), Dargush and Banerjee (1989, 1991) and Borba (1992). A more complete treatise on the fundamental solutions and integral equations for the poroelastic problem was presented by Cheng and Detournay (1998).

Later, Park and Banerjee (2002) analyzed the three-dimensional problem of soils consolidation by developing particular integrals. Cavalcanti and Telles (2003) presented time independent fundamental solutions applied to the analysis of saturated media. As for works that address poroplasticity, Wutzow (2008) can be cited, which incorporated stiffeners into the solid matrix. Kamalian *et al*. (2008) and Maghoul *et al*. (2010) present fundamental solutions in time domain for media under saturated and unsaturated conditions.

Among the earliest known BEM formulations for the analysis of damage mechanics problems, Herding and Kuhn (1996), Garcia *et al*. (1999), Lin *et al*. (2002) and Sladek *et al*. (2003) are cited. Also cited are Botta *et al*. (2005), Venturini and Botta (2005) and Benallal *et al*. (2006). Several of these works incorporate strategies to deal with numerical instabilities associated with the problem of strain localization.

Some studies on numerical analysis of porous media subject to damage, based on the Finite Element Method, should be cited. A damage evolution law for geomaterials was proposed in Cheng and Dusseault (1993). Selvadurai (2003) incorporated isotropic damage to saturated porous media, presenting empirical expressions for permeability variation due to damage process. Selvadurai and Shirazi (2004) addressed the problem of a spherical cavity filled with fluid. Vasconcelos (2007) incorporated an isotropic damage formulation to a FEM code applied to saturated geomaterials.

The solution to nonlinear problems from the Newton-Raphson method and the resulting use of consistent tangent operators is widespread in the scientific community and can be found in Simo and Taylor (1985) and Simo and Hughes (1992). Other works that address BEM versions for non-linear models are: Bonnet and Mukherjee (1996), Poon *et al.* (1998), Fudoli (1999) and Benallal *et al.* (2002).

1.4. THESIS STRUCTURE

The items discussed in this thesis are arranged throughout the text as described below:

Chapter 2 presents a brief review of the poromechanics, showing how the heterogeneous medium is described, and also the problem formulation, which is based on the classical continuum mechanics. The continuum damage mechanics is considered briefly and the local damage model adopted in this work is presented. The strain localization phenomenon is commented and, although not addressed in this thesis, a non-local model able to deal with the problem is presented.

Chapter 3 presents the model developed for the damage on the solid matrix of the saturated porous media. Expressions to evaluate the influence of the damage process on the mechanical and flow properties of the material are proposed. These are some aspects of the boundary element method, and the nonlinear formulation of the method developed for the computational implementation of the model is presented. The algorithm of damage evolution is described, and also the deduction of the consistent tangent matrix is shown.

Chapter 4 presents some numerical applications in order to validate the model and illustrate the operation of the code developed.

The equations in the text of the thesis are written in indicial or tensorial notation, using the one that is more illustrative, depending on the context in which it is inserted. Some equations are presented in both notations, when deemed necessary.

Chapter 2

Aspects on Poromechanics and Continuum Damage Mechanics

2.1. OVERALL CONSIDERATIONS

The mechanics of porous media addresses materials whose mechanical behavior is significantly influenced by the presence of fluid phases. The response of the material is through its deformations when subject to external actions and pressure changes in the fluid. In rocks, for example, two mechanisms have a core importance in this interaction process between the phases (Detournay and Cheng, 1993): An increase in the pore pressure induces the rock to dilate, whereas a compression in the rock results in increased pore pressure, in the case of confined fluid. Considering the non-confinement, the excess pore pressure, which is imposed by the compression of the rock, is gradually dissipated during the fluid diffusion process and a new deformation distribution is created in the body. Thus, it is observed that the rock is more deformable in drained conditions.

A basic idea to be considered in the study of porous media is that their response to certain external actions is not immediate. The deformations occur over time in the phenomenon known as settlement or consolidation. The observations and the need to explain this phenomenon propel further studies on porous media.

The damage mechanics predicts the loss of strength and stiffness of a solid, due to irreversible microscopic processes, such as: decohesion, relative slipping of crystal structure, phase changes, etc. Some of these processes are caused by existing microdefects or microcracks in the material, which provide a microstrain concentration in its neighbourhood.

This chapter presents a brief description on poromechanics, mostly based on the works of Coussy (2004) and Wang (2008). Assuming that the solid matrix is subject to a damage process, some comments are made about the mechanics of continuous damage, specifying how it is considered in the mathematical formulation. For additional details, Lemaitre and Chaboche (1985) and Voyiadjis and Kattan (2005) can be referenced.

2.2. DESCRIPTION OF A SATURATED POROUS MEDIUM

Let us assume a porous medium, composed of a solid matrix, and a porous space in which the pores are interconnected. It is through this connected porous space that the transport of fluid mass occurs. Any two points in its domain can be connected by a generic arc totally contained in it, so that the fluid phase in that space can be treated as a continuum. There may also be closed pores included in the solid matrix, in which the occurrence of flow is not considered, at least not in the timescale considered in this theory. Hence, from this point of the text, the term “pore” is applied to the effective pores of the connected space, while the disconnected pores will be treated as part of the solid matrix.

Therefore, it is understood that the saturated porous medium is described by the superposition, temporal and spatial, of two continuous media: The first represents the solid skeleton and the second, the fluid phase. Usually, the deformation of the porous media is described in relation to the skeleton deformation, which can actually be observed and shows a more accessible physical meaning.

An infinitesimal volume of porous medium can be represented by the composition of two elementary material particles (Figure 2.1), one that is solid – which also contains occlusions and disconnected pores – and one that is fluid. Considering that the porous medium is heterogeneous at a microscopic level, its treatment as a continuous medium requires the choice of a macroscopic scale, in which the internal constitution of the material can be neglected, when analyzing the physical phenomenon of interest. Therefore, the continuity hypothesis admits the existence of an infinitesimal control volume of representative dimensions at a macroscopic scale, in the study of all phenomena involved in the intended application.

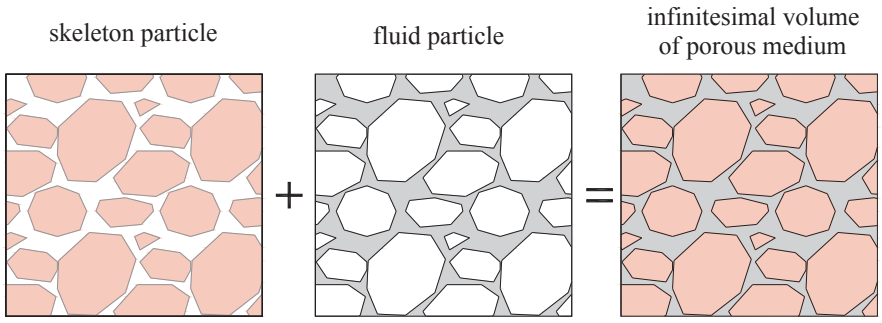

Figure 2.1 – Definition of the porous medium by the superposition of the fluid and solid phases

2.3. BEHAVIOR OF THE SKELETON

If there are external forces or pressure variations in the fluid, the solid skeleton deforms. This deformation is analyzed according to the classical theory foreseen in the continuum mechanics, whose main concepts are briefly described below.

2.3.1. Motion of a Continuum. Displacement. Deformation Gradient

Consider a solid body occupying a determined region of space, at a time $t = 0$. In this initial configuration, a particle is represented by its position vector $\mathbf{X}$ of components X_i, in a Cartesian coordinate system, of orthonormal basis e_i $(i = 1,2,3)$. After deforming, in time t, the body is in a current configuration, with its reference particle represented by the position vector $\mathbf{x}$ of components $x_i(X_j, t)$ as shown in Figure 2.2. One can then write:

$$\mathbf{X} = X_i e_i \; ; \; \mathbf{x} = x_i(X_j, t) e_i \tag{2.1}$$

the displacement vector $\mathbf{u}$ of a particle is defined, from its initial position $\mathbf{X}$ to the current position $\mathbf{x}$ as:

$$\mathbf{x} = \mathbf{X} + \mathbf{u} \tag{2.2}$$

Supposing two particles, positions $\mathbf{X}$ and $\mathbf{X} + d\mathbf{X}$ in the initial configuration. After the deformation, the infinitesimal material vector $d\mathbf{X}$ becomes $d\mathbf{x}$, and connects the two particles in their current positions $\mathbf{x}$ and $\mathbf{x} + d\mathbf{x}$. Any vector material $d\mathbf{X}$ is transported to its corresponding deformed $d\mathbf{x}$ by a linear application called the deformation gradient $\mathbf{F}$, as follows·

$$d\mathbf{x} = \mathbf{F} \cdot d\mathbf{X} \tag{2.3}$$

$$\mathbf{F} = \nabla_X \mathbf{x} \; ; \; F_{ij} = \frac{\partial x_i}{\partial X_j} \tag{2.4}$$

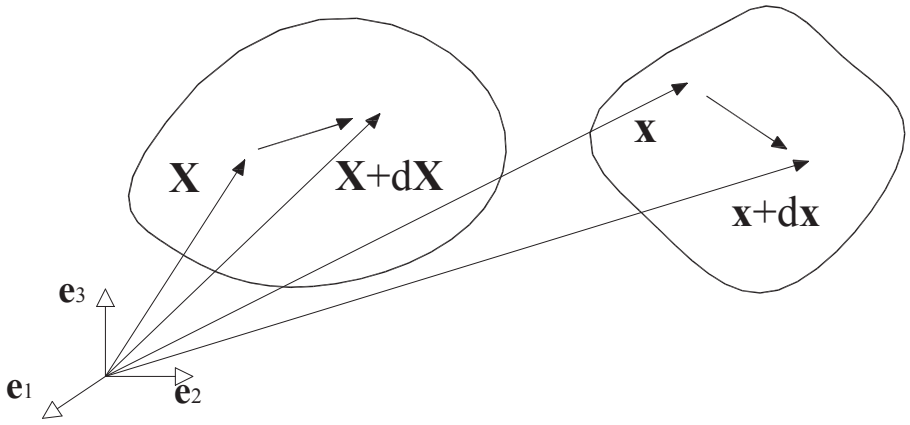

Figure 2.2 - Initial and current configurations

Note that the operator refers ∇_X to the initial configuration. The inverse and transposed forms of tensor $\mathbf{F}$ are written as:

$$d\mathbf{X} = \mathbf{F}^{-1} \cdot d\mathbf{x} \; ; \; d\mathbf{x} = d\mathbf{X} \cdot \mathbf{F}^{T} \tag{2.5}$$

The deformation gradient is expressed in terms of displacement as follows.

$$\mathbf{F} = \boldsymbol{I} + \nabla_X \mathbf{u} \; ; \; F_{ij} = \delta_{ij} + \frac{\partial u_i}{\partial X_j} \tag{2.6}$$

The second-order identity tensor is represented by $\boldsymbol{I}$, which is equivalent to the kronnecker delta δ_{ij}, in indicial notation.

Lagrangian and Eulerian kinematic descriptions. A continuum deformation can be described in two ways. The first one, called Eulerian or spatial, takes the current position of a particle as reference, expressing the variables depending on $\mathbf{x}$ and t. In the Lagrangian, or material description, the particles are described as a function of the initial position $\mathbf{X}$ and time t.

2.3.2. Porosity. Void Ratio

Let an infinitesimal volume $d\Omega_t$ of the porous medium, written in the current configuration. The volume occupied by the fluid phase equals $n\, d\Omega_t$, with n the Eulerian porosity. Considering that this reference volume changes with deformation, the Eulerian porosity is not well suited to quantify the volume variation withstood by the pore space. Therefore, the Lagrangian porosity ϕ is defined, which deals with the current porous volume in relation to the initial volume $d\Omega_0$.

$$\phi\, d\Omega_0 = n\, d\Omega_t \tag{2.7}$$

In order to quantify the degree of compactness of a porous material, an Eulerian variable is defined, the void ratio e. This is the relationship between the porous volume and the solid matrix volume:

$$e = \frac{n}{1-n} \tag{2.8}$$

2.3.3. Strain Tensor

During the deformation, the infinitesimal vectors in the deformed configuration undergo changes in their lengths and angles. These changes can be measured by the Green-Lagrange strain tensor, identified by $\boldsymbol{\Delta}$. Take two vectors $d\mathbf{X}$ and $d\mathbf{Y}$, taken in $d\mathbf{x}$ and $d\mathbf{y}$ after deformation, respectively. The variation of their scalar product is written using (2.3), as follows,

$$d\mathbf{x}\cdot d\mathbf{y} - d\mathbf{X}\cdot d\mathbf{Y} = 2d\mathbf{X}\cdot\boldsymbol{\Delta}\cdot d\mathbf{Y} \tag{2.9}$$

$\boldsymbol{\Delta}$ can be defined in terms of the deformation gradient, based on equation (2.5):

$$\boldsymbol{\Delta} = \frac{1}{2}\left(\mathbf{F}^{T}\cdot\mathbf{F} - \boldsymbol{I}\right) \tag{2.10}$$

A system of main orthogonal directions is taken to its final configuration, rotated by a tensor called the rotation gradient $\mathbf{R}$, which can be isolated in a polar decomposition of tensor $\mathbf{F}$:

$$\mathbf{F} = \mathbf{D} \cdot \mathbf{R} \tag{2.11}$$

In this decomposition, tensor $\mathbf{D}$ contains all information necessary to measure the deformation, resulting in another expression of the Green-Lagrange deformation:

$$\boldsymbol{\Delta} = \frac{1}{2}\left(\mathbf{D}^2 - \boldsymbol{I}\right) \tag{2.12}$$

Using the equation (2.6), tensor $\boldsymbol{\Delta}$ can also be defined as a function of the displacement vector, as shown below.

$$\boldsymbol{\Delta} = \frac{1}{2}\left(\nabla_X \mathbf{u} + \nabla_X{}^T \mathbf{u} + \nabla_X{}^T \mathbf{u} \cdot \nabla_X \mathbf{u}\right) \; ; \; \Delta_{ij} = \frac{1}{2}\left(\frac{\partial u_i}{\partial X_j} + \frac{\partial u_j}{\partial X_i} + \frac{\partial u_k}{\partial X_i}\frac{\partial u_k}{\partial X_j}\right) \tag{2.13}$$

In some problems, one can use a first order approximation, as long as the condition $\|\nabla \mathbf{u}\| \ll 1$ of infinitesimal transformation is respected. Thus, the Green-Lagrange tensor is reduced to the linear strain deformation $\boldsymbol{\varepsilon}$:

$$\boldsymbol{\Delta} \simeq \boldsymbol{\varepsilon} = \frac{1}{2}\left(\nabla_X \mathbf{u} + \nabla_X{}^T \mathbf{u}\right) \; ; \; \varepsilon_{ij} = \frac{1}{2}\left(\frac{\partial u_i}{\partial X_j} + \frac{\partial u_j}{\partial X_i}\right) \tag{2.14}$$

Since tensor $\boldsymbol{\Delta}$ has the same order as $\nabla_X \mathbf{u}$, the condition of infinitesimal transformation implies infinitesimal strains, expressed by $\|\boldsymbol{\Delta}\| \ll 1$. Note that the application of linear measure of strain results in some limitations. As for example, in a rigid body rotation, $\boldsymbol{\Delta}$ is null, while $\nabla_X \mathbf{u}$ can take any different order of magnitude.

Under the condition of infinitesimal transformation, the determinant of the deformation gradient, also called the Jacobian operator, is written as:

$$\left(J = \det \mathbf{F}\right) \simeq 1 + \nabla \cdot \mathbf{u} \; ; \; J = 1 + \frac{\partial u_i}{\partial x_i} = 1 + \varepsilon_{ii} \tag{2.15}$$

In infinitesimal transformations, the trace of the linear deformation tensor ε_{ii}, represents the volumetric expansion of the porous medium, which is now defined by:

$$\epsilon = \varepsilon_{ii} = \nabla \cdot \mathbf{u} \tag{2.16}$$

The transformation of the initial volume $d\Omega_0$ in $d\Omega_t$ is performed through the Jacobian operator by $d\Omega_t = J\, d\Omega_0$. Based on (2.15) and (2.16) we arrive at:

$$d\Omega_t \simeq \left(1+\epsilon\right) d\Omega_0 \tag{2.17}$$

The dilation observed in the porous medium is due to variations in the connected pore space, and the volumetric expansion ϵ_s experienced by the solid matrix. Analogously to (2.17), from ϵ_s the relationship is defined as:

$$d\Omega_t^s = \left(1+\epsilon_s\right) d\Omega_0^s \tag{2.18}$$

Based on the concepts of Eulerian and Lagrangian porosity, the volume occupied by the solid matrix with the total volume can be related in the initial time ($t=0$) and current time ($t=t$), as follows:

$$\begin{aligned} d\Omega_t^s &= \left(1-n\right) d\Omega_t = d\Omega_t - \phi d\Omega_0 \\ d\Omega_0^s &= \left(1-\phi_0\right) d\Omega_0 \end{aligned} \tag{2.19}$$

The balance of the total volume can now be solved,

$$\epsilon = (1-\phi_0)\,\epsilon_s + \phi - \phi_0 \tag{2.20}$$

2.4. BEHAVIOR OF THE FLUID PHASE

In the development of constitutive equations for a porous medium, the description of the fluid motion in relation to the initial configuration of the skeleton is necessary.

2.4.1. Particle Derivative

As aforementioned in the previous section, the description of the skeleton's deformation can be done as a function of time t and the position vector X, both referenced in the initial configuration of the particle. In this Lagrangian description, the skeleton's strain kinematics is formulated by the derivatives in total time.

In some cases, it may be of interest to formulate the problem according to an Eulerian description, taking into account only the current configuration of the skeleton at a given time instant. In this type of approximation, it is necessary to define a velocity field $\mathbf{V}^{\pi}(\mathbf{x},t)$ of the particle, which can be either a fluid particle or a skeleton particle (indicated by $\pi = f$ or $\pi = s$, respectively). The particle derivative concept is shown below.

In a multiphase domain, the derivatives of any field defined for any domain can be taken in relation to one of the phases, separately. In the case of a porous medium, derivatives can be taken with respect to the skeleton or the fluid. $\mathrm{d}^{\pi}\varsigma/\mathrm{dt}$ is defined as a particle time derivative of the field ς related to the particle π ($=\mathrm{s}$ or f).

For example, we can write the velocity for particle π localized by $\mathbf{x}$:

$$\mathbf{V}^{\pi}(\mathbf{x},\mathrm{t})=\frac{\mathrm{d}^{\pi}\mathbf{x}}{\mathrm{dt}}\ ;\ \pi=\mathrm{s}\ \text{ou}\ \mathrm{f} \tag{2.21}$$

The particle derivative of a material vector $\mathrm{d}\mathbf{x}$ is calculated as:

$$\frac{\mathrm{d}^{\pi}}{\mathrm{dt}}\left(\mathrm{d}\mathbf{x}\right)=\frac{\mathrm{d}^{\pi}}{\mathrm{dt}}\left[\left(\mathbf{x}+\mathrm{d}\mathbf{x}\right)-\mathbf{x}\right]=\mathbf{V}^{\pi}(\mathbf{x}+\mathrm{d}\mathbf{x},\mathrm{t})-\mathbf{V}^{\pi}(\mathbf{x},\mathrm{t}) \tag{2.22}$$

$$\frac{\mathrm{d}^{\pi}}{\mathrm{dt}}\left(\mathrm{d}\mathbf{x}\right)=\nabla_{\mathrm{x}}\mathbf{V}^{\pi}\cdot\mathrm{d}\mathbf{x}\ ;\ \left(\nabla_{\mathrm{x}}\mathbf{V}^{\pi}\right)_{\mathrm{ij}}=\frac{\partial \mathrm{V}_{\mathrm{i}}^{\pi}}{\partial \mathrm{x}_{\mathrm{j}}} \tag{2.23}$$

For an arbitrary field $\varsigma(\mathbf{x},\mathrm{t})$, we write the particle derivative considering that $\mathbf{x}$ assumes successive positions $\mathbf{x}^{\pi}(\mathrm{t})$ occupied by the particle:

$$\frac{\mathrm{d}^{\pi}\varsigma}{\mathrm{dt}}=\frac{\mathrm{d}\varsigma}{\mathrm{dt}}+\left(\nabla_{\mathrm{x}}\varsigma\right)\cdot\mathbf{V}^{\pi} \tag{2.24}$$

The acceleration of a particle $\boldsymbol{\gamma}^{\pi}$ can be obtained, for example:

$$\boldsymbol{\gamma}^{\pi}=\frac{\mathrm{d}^{\pi}\mathbf{V}^{\pi}}{\mathrm{dt}}=\frac{\mathrm{d}\mathbf{V}^{\pi}}{\mathrm{dt}}+\left(\nabla_{\mathrm{x}}\mathbf{V}^{\pi}\right)\cdot\mathbf{V}^{\pi}\ ;\ \gamma_{\mathrm{i}}^{\pi}=\frac{\mathrm{dV}_{\mathrm{i}}^{\pi}}{\mathrm{dt}}=\frac{\mathrm{dV}_{\mathrm{i}}^{\pi}}{\mathrm{dx}_{\mathrm{j}}}\mathrm{V}_{\mathrm{j}}^{\pi} \tag{2.25}$$

Taking the integral over the volume $\mathrm{d}\Omega_{\mathrm{t}}$ of any given variable ς, its particle derivative is

$$\frac{\mathrm{d}^{\pi}}{\mathrm{dt}}\int_{\Omega_{\mathrm{t}}}\varsigma\mathrm{d}\Omega_{\mathrm{t}}=\int_{\Omega_{\mathrm{t}}}\frac{\mathrm{d}^{\pi}}{\mathrm{dt}}\left(\varsigma\mathrm{d}\Omega_{\mathrm{t}}\right) \tag{2.26}$$

which can be rewritten as follows, according to (2.24):

$$\frac{\mathrm{d}^{\pi}}{\mathrm{dt}}\int_{\Omega_{\mathrm{t}}}\varsigma\mathrm{d}\Omega_{\mathrm{t}}=\int_{\Omega_{\mathrm{t}}}\left(\frac{\mathrm{d}\varsigma}{\mathrm{dt}}+\varsigma\nabla_{\mathrm{x}}\cdot\mathbf{V}^{\pi}\right)\mathrm{d}\Omega_{\mathrm{t}} \tag{2.27}$$

or, equivalently:

$$\frac{\mathrm{d}^{\pi}}{\mathrm{dt}}\int_{\Omega_t}\varsigma\,\mathrm{d}\Omega_t=\int_{\Omega_t}\left(\frac{\mathrm{d}\varsigma}{\mathrm{dt}}+\nabla_x\cdot\left(\varsigma\mathbf{V}^{\pi}\right)\right)\mathrm{d}\Omega_t \tag{2.28}$$

Also of interest is the definition of a particle derivative of any material volume $\mathrm{d}\Omega_t$:

$$\frac{\mathrm{d}^{\pi}}{\mathrm{dt}}\left(\mathrm{d}\Omega_t\right)=\left(\nabla_x\cdot\mathbf{V}^{\pi}\right)\mathrm{d}\Omega_t \tag{2.29}$$

2.4.2. Relative Flow Vector of a Fluid Mass. Filtration Vector. Fluid Mass Content

Let the mass that flows in the interval between t and $t+\mathrm{dt}$, through the surface da according to the normal direction $\mathbf{n}$, be defined by $J_f\ \mathrm{da}$ (Figure 2.3). One can write

$$J_f\ \mathrm{da}=\mathbf{w}\cdot\mathbf{n}\mathrm{da} \tag{2.30}$$

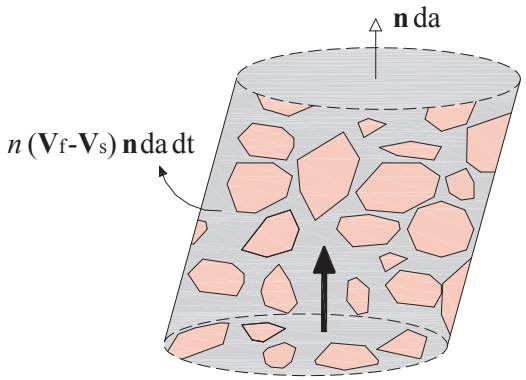

Figure 2.3 - Infinitesimal volume flowing through a surface da in the interval dt

with $\mathbf{w}(\mathbf{x},t)$ the Eulerian relative flow vector, defined in the material point considered. In the increment dt, the volume that flows through the surface da is $n(\mathbf{V}^f-\mathbf{V}^s)\cdot\mathbf{n}\ \mathrm{da}\ \mathrm{dt}$. Then, we define the relative flow as a function of the filtration vector ν:

$$\mathbf{w}=\rho_f\boldsymbol{\nu}\ ;\ \boldsymbol{\nu}=n(\mathbf{V}^f-\mathbf{V}^s) \tag{2.31}$$

2.5. MASS BALANCE

2.5.1. Eulerian Continuity Equations

Let ρ_s and ρ_f be the mass density of the solid matrix and fluid, respectively. Thus, an infinitesimal volume $\mathrm{d}\Omega_t$ contains $\rho_s(1-n)\,\mathrm{d}\Omega_t$ of skeleton mass and a fluid mass

equivalent to $\rho_f n \, d\Omega_t$. As long as there is no mass exchange, one can express the mass balance for the two continuous media considered, as follows.

$$\begin{aligned} &\frac{d^s}{dt}\int_{\Omega_t} \rho_s (1-n)\, d\Omega_t = 0 \\ &\frac{d^f}{dt}\int_{\Omega_t} \rho_f n \, d\Omega_t = 0 \end{aligned} \tag{2.32}$$

Applying equation (2.26), the differential operators above can be included in the kernels of their integrals, which imposes the nullities:

$$\frac{d^s}{dt}\left(\rho_s (1-n)\, d\Omega_t\right) = 0 \tag{2.33}$$

$$\frac{d^f}{dt}\left(\rho_f n \, d\Omega_t\right) = 0 \tag{2.34}$$

Finally, the Eulerian continuity equations for the fluid and solid phases are written, using (2.28) as follows:

$$\frac{\partial\left(\rho_s (1-n)\right)}{\partial t} + \nabla_x \cdot \left(\rho_s (1-n)\mathbf{V}^s\right) = 0 \tag{2.35}$$

$$\frac{\partial\left(\rho_f n\right)}{\partial t} + \nabla_x \cdot \left(\rho_f n \mathbf{V}^f\right) = 0 \tag{2.36}$$

Resorting to equation (2.31), we can rewrite the fluid continuity equation (2.36), in order to relate the motions of the fluid and of the skeleton.

$$\frac{d^s\left(\rho_f n\right)}{dt} + \rho_f n \nabla_x \cdot \mathbf{V}^s + \nabla_x \cdot \mathbf{w} = 0 \tag{2.37}$$

2.5.2. Lagrangian Continuity Equations

The representation of the fluid mass balance for a Lagrangian description is now described. We define the Lagrangian fluid mass m_f per unit volume content $d\Omega_0$. Its relationship with the Eulerian fluid mass content $\rho_f n$, per unit volume $d\Omega_t$, is written as:

$$\rho_f n \, d\Omega_t = m_f \, d\Omega_0 \tag{2.38}$$

Applying equation (2.7), $m_f = \rho_f \phi$ is obtained, with ϕ the Lagrangian porosity, defined in section 2.3.2.

Take a Lagrangian vector $\mathbf{M}(\mathbf{X}, t)$, which is related to the Eulerian vector by $\mathbf{w}(\mathbf{x}, t)$:

$$\mathbf{w} \cdot \mathbf{n}\, da = \mathbf{M} \cdot \mathbf{N}\, dA \tag{2.39}$$

With dA as the surface defined by normal $\mathbf{N}$, in the initial configuration, which corresponds to the surface da in the deformed state. Assuming that the flow of $\mathbf{w}$ through da is equivalent to the flow of $\mathbf{M}$ through dA, we can write:

$$\begin{aligned} &\mathbf{M} = J\mathbf{F}^{-1} \cdot \mathbf{w} \;;\; M_i = J \frac{\partial X_i}{\partial x_j} w_j \\ &\nabla_x \cdot \mathbf{w}\, d\Omega_t = \nabla_X \cdot \mathbf{M}\, d\Omega_0 \;;\; J \frac{\partial w_i}{\partial x_i} = \frac{\partial M_i}{\partial X_i} \end{aligned} \tag{2.40}$$

The application of (2.38) and (2.40), and the use of the particle derivative of the volume $d\Omega_t$, given in (2.29), allows writing the fluid continuity equation (2.37) for a Lagrangian description:

$$\frac{dm_f}{dt} + \nabla_x \cdot \mathbf{M} = 0 \;;\; \frac{\partial m_f(X_i, t)}{\partial t} + \frac{\partial M_i}{\partial X_i} = 0 \tag{2.41}$$

Similarly, we write the equation of skeleton mass balance, integrating (2.33) as:

$$\rho_s (1-n)\, d\Omega_t = \rho_s^0 (1-n_0)\, d\Omega_0 \tag{2.42}$$

with ρ_s^0 as the density of the initial mass of the solid matrix, and $n_0 = \phi_0$ the initial porosity of the medium. Knowing that $d\Omega_t = J\, d\Omega_0$, we arrive at:

$$m_s = m_s^0 = \rho_s^0 (1 - \phi_0) \tag{2.43}$$

where $m_s = J\rho_s(1-n)$ is the solid mass content, in relation to the original volume $d\Omega_0$. The equation shows that the mass remains constant and equal to its value in the initial configuration.

Equations (2.41) and (2.43) are the Lagrangian formulation, alternatives to the Eulerian equations of continuity, given in (2.35) and (2.36).

2.6. MOMENTUM BALANCE

Now we formulate the momentum balance for a porous medium, still according to the hypothesis adopted in the preceding paragraphs, which is treated as a superposition of two continuous media, interacting with each other. The momentum balance concept is important to obtain the total stress tensors.

2.6.1. The Hypothesis of Local Forces

Any material domain Ω_t can be subject to two types of external forces: the body forces and the surface forces. Generally, the body forces solicit the skeleton and the fluid in the same way. This is the case, for example, of forces due to gravity. An infinitesimal force $\delta\mathbf{f}$ acting on the elementary volume $d\Omega_t$ is defined by a volume force density per unit mass $\mathbf{f}$:

$$\delta\mathbf{f} = \rho\,\mathbf{f}(\mathbf{x}, t)d\Omega_t \tag{2.44}$$

The density of the porous medium ρ, which includes the matrix and fluid phase, is given by:

$$\rho = \rho_s(1-n) + \rho_f n \tag{2.45}$$

It is assumed that the body force density $\mathbf{f}$ depends only on the current position of particle $\mathbf{x}$, and time t. Then, the effects caused by the external body forces are assimilated the same way by infinitesimal and total domains $d\Omega_t$ and Ω_t. These body forces are local forces. Here the non-local body forces, the ones depending on the distance between particles, for instance, are not considered.

The surface forces act on the boundary $\partial\Omega_t$ of the domain Ω_t. Similarly to what was described for the volume forces, we can define an infinitesimal surface force $\delta\mathbf{T}$ through its density $\mathbf{T}$, as follows:

$$\delta\mathbf{T} = \mathbf{T}(\mathbf{x}, t, \mathbf{n})da \tag{2.46}$$

Note that $\mathbf{T}$ also depends on $\mathbf{n}$, the outward unit normal to the surface da, at the point defined by $\mathbf{x}$. It is assumed that the effects of surface forces acting on an infinitesimal region of $\partial\Omega_t$ are noticeable in the vicinity of this restricted area. The hypothesis that surface forces have a local nature is known as Cauchy's hypothesis.

2.6.2. Momentum Balance

In a given porous domain Ω_t, it follows that the result of all forces must equal to the rate of change of the linear momentum balance, that is:

$$\frac{d^s}{dt}\int_{\Omega_t}\rho_s(1-n)\mathbf{V}^s\,d\Omega_t+\frac{d^f}{dt}\int_{\Omega_t}\rho_f n\mathbf{V}^f\,d\Omega_t=\int_{\Omega_t}\rho\mathbf{f}(\mathbf{x},t)\,d\Omega_t+\int_{\partial\Omega_t}\mathbf{T}(\mathbf{x},t,\mathbf{n})\,da \tag{2.47}$$

The terms $\rho_s(1-n)\mathbf{V}^s\,d\Omega_t$ and $\rho_f n\mathbf{V}^f\,d\Omega_t$ represent the amount of linear momentum balance respectively related to the particles of the skeleton and the fluid contained in $d\Omega_t$. It is considered that the external forces act on all the matter contained in Ω_t, without any distinction between fluid and skeleton. Note the role of particle derivatives d^{π}/dt, which incorporate the effects of the different motions of the solid and fluid particles in the change of the global momentum balance.

Similarly, we can write the angular momentum balance:

$$\begin{aligned}&\frac{d^s}{dt}\int_{\Omega_t}\mathbf{x}\times\rho_s(1-n)\mathbf{V}^s\,d\Omega_t+\frac{d^f}{dt}\int_{\Omega_t}\mathbf{x}\times\rho_f n\mathbf{V}^f\,d\Omega_t\\&=\int_{\Omega_t}\mathbf{x}\times\rho\mathbf{f}(\mathbf{x},t)\,d\Omega_t+\int_{\partial\Omega_t}\mathbf{x}\times\mathbf{T}(\mathbf{x},t,\mathbf{n})\,da\end{aligned} \tag{2.48}$$

2.6.3. The Dynamic Theorem

The inertial forces generated in the volume $d\Omega_t$ may be related to the external forces $\delta\mathbf{f}$ and $\delta\mathbf{T}$, acting in them. Taking the particle derivatives in (2.47), and using the definitions (2.21), (2.25), (2.33) and (2.34), the following is written:

$$\int_{\Omega_t}\left(\rho_s(1-n)\boldsymbol{\gamma}^s+\rho_f n\boldsymbol{\gamma}^f\right)d\Omega_t=\int_{\Omega_t}\rho\mathbf{f}(\mathbf{x},t)\,d\Omega_t+\int_{\partial\Omega_t}\mathbf{T}(\mathbf{x},t,\mathbf{n})\,da \tag{2.49}$$

The integrand on the left represents the inertial force related to the material contained in $d\Omega_t$ in a current time t.

The expression (2.49), also called theorem of the dynamic resultant, is valid for any domain Ω_t, considering the hypothesis of local forces, which ensures that a body force $\mathbf{f}(\mathbf{x},t)$ acting on volume $d\Omega_t$ is independent of choosing domain Ω_t, which contains it.

The moments due to inertial forces also correspond with the moments of external forces, so that we can equate a theorem similar to (2.49), starting from equation (2.48):

$$\int_{\Omega_t} \mathbf{x}\times\left(\rho_s(1-n)\boldsymbol{\gamma}^s + \rho_f n\boldsymbol{\gamma}^f\right)d\Omega_t = \int_{\Omega_t} \mathbf{x}\times\rho\mathbf{f}\left(\mathbf{x},t\right)\,d\Omega_t + \int_{\partial\Omega_t} \mathbf{x}\times\mathbf{T}(\mathbf{x},t,\mathbf{n})\,da \tag{2.50}$$

2.7. STRESS TENSOR

Based on the momentum balance, one can arrive at a definition of the stress tensor $\boldsymbol{\sigma}$. Let us assume an infinitesimal tetrahedron (Figure 2.4), whose three sides dS_j are parallel to the plans coordinated and guided by $-\mathbf{e}_j$. The surfaces dS_j are related to the surface base area dS of the normal $\mathbf{n}$:

$$dS_j = dS\mathbf{n}\cdot e_j = dSn_j \tag{2.51}$$

Applying the theorem (2.49) to the tetrahedron, the following is obtained:

$$\frac{hS}{3}O\left(\rho_s(1-n)\boldsymbol{\gamma}^s + \rho_f n\boldsymbol{\gamma}^f - \rho\mathbf{f}\right) \simeq \mathbf{T}(\mathbf{n})dS + \sum_{i=1\ldots3}\mathbf{T}(-e_j)dS_j \tag{2.52}$$

with h as the height of the tetrahedron, its volume is $hS/3$. $O(\varsigma)$ represents the order of magnitude of the field ς. Assuming the action-reaction principle $\mathbf{T}(-\mathbf{n}) = -\mathbf{T}(\mathbf{n})$, and replacing (2.51) in (2.52):

$$\frac{hS}{3}O\left(\rho_s(1-n)\boldsymbol{\gamma}^s + \rho_f n\boldsymbol{\gamma}^f - \rho\mathbf{f}\right) \simeq \mathbf{T}(\mathbf{n}) - \sum_{i=1\ldots3}\mathbf{T}(e_j)n_j \tag{2.53}$$

Letting $h\to 0$, the tetrahedron is degenerated at a point, canceling the term to the left of equation (2.53).

$$\mathbf{T}(\mathbf{n}) = \sum_{i=1\ldots3}\mathbf{T}(e_j)n_j \tag{2.54}$$

Equation (2.54) defines a linear operator that relates $\mathbf{T}(\mathbf{x},t,\mathbf{n})$ to normal $\mathbf{n}$, known as the Cauchy stress tensor $\boldsymbol{\sigma} = \boldsymbol{\sigma}(\mathbf{x},t)$, with components σ_{ij}. This relates to the stress vector $\mathbf{T}(\mathbf{x},t,\mathbf{n})$ as:

$$\mathbf{T}(\mathbf{x},t,\mathbf{n} = \mathbf{n}_j e_j) = \boldsymbol{\sigma}\cdot\mathbf{n} = \sigma_{ij}n_j e_i \tag{2.55}$$

The tensorial nature of tensor $\boldsymbol{\sigma}$ is a direct consequence of the hypothesis of local contact forces, in item 2.6.1, expressed by $\mathbf{T} = \mathbf{T}(\mathbf{x},t,\mathbf{n})$.

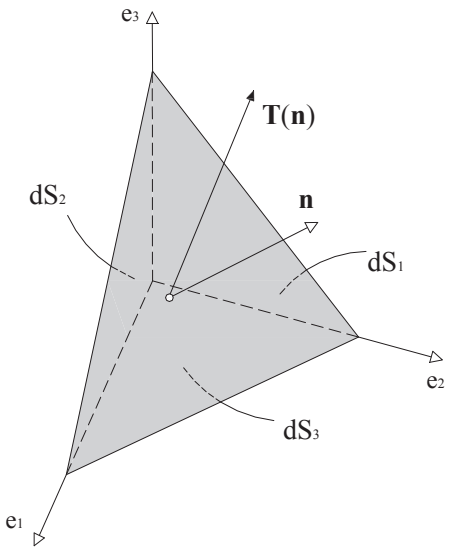

Figure 2.4 - Infinitesimal tetrahedron to define the stress tensor

2.8. EQUILIBRIUM EQUATION

The equation of motion of the elementary volume $d\Omega_t$ can be obtained from the theorem (2.49), in which the definition given in (2.55) is introduced, obtaining:

$$\int_{\Omega_t} \left(\rho \mathbf{f} - \rho_s (1-n) \boldsymbol{\gamma}^s - \rho_f n \boldsymbol{\gamma}^f \right) d\Omega_t + \int_{\partial\Omega_t} \boldsymbol{\sigma} \cdot \mathbf{n} \, da = 0 \tag{2.56}$$

The application of the divergence theorem to the surface integral given above allows to rewrite the equation as:

$$\int_{\Omega_t} \left(\nabla_x \cdot \boldsymbol{\sigma} + \rho \mathbf{f} - \rho_s (1-n) \boldsymbol{\gamma}^s - \rho_f n \boldsymbol{\gamma}^f \right) d\Omega_t = 0 \tag{2.57}$$

The dynamic theorem, written above, should also be valid for any domain Ω_t. Then we arrive to the local equation of equilibrium:

$$\begin{aligned} &\nabla_x \cdot \boldsymbol{\sigma} + \rho_s (1-n) \left(\mathbf{f} - \boldsymbol{\gamma}^s \right) - \rho_f n \left(\mathbf{f} - \boldsymbol{\gamma}^f \right) = 0 \; ; \\ &\frac{\partial \sigma_{ij}}{\partial x_j} + \rho_s (1-n) \left(f_i - \gamma_i^s \right) - \rho_f n \left(f_i - \gamma_i^f \right) = 0 \end{aligned} \tag{2.58}$$

Similarly, we can rewrite the dynamic moment theorem (2.50), as follows.

$$\int_{\Omega_t} \mathbf{x} \times \left(\rho \mathbf{f} - \rho_s (1-n) \boldsymbol{\gamma}^s - \rho_f n \boldsymbol{\gamma}^f \right) d\Omega_t + \int_{\partial\Omega_t} \mathbf{x} \times \boldsymbol{\sigma} \cdot \mathbf{n} \, da = 0 \tag{2.59}$$

Based on the divergence theorem, we have:

$$\int_{\partial\Omega_t} \mathbf{x}\times\boldsymbol{\sigma}\cdot\mathbf{n}\ \mathrm{da} = \int_{\Omega_t} \left(\mathbf{x}\times\nabla_x\cdot\boldsymbol{\sigma} + 2\boldsymbol{\sigma}^{as}\right)\mathrm{d}\Omega_t \tag{2.60}$$

where $\boldsymbol{\sigma}^{as}$ is the anti-symmetric portion of the stress tensor, defined below in Cartesian coordinates.

$$2\boldsymbol{\sigma}^{as} = (\sigma_{23}-\sigma_{32})\mathrm{e}_1 + (\sigma_{13}-\sigma_{31})\mathrm{e}_2 + (\sigma_{12}-\sigma_{21})\mathrm{e}_3 \tag{2.61}$$

Then, equation (2.59) is:

$$\int_{\Omega_t} \left[\mathbf{x}\times\left(\rho\mathbf{f} - \rho_s(1-n)\boldsymbol{\gamma}^s - \rho_f n\boldsymbol{\gamma}^f + \nabla_x\cdot\boldsymbol{\sigma}\right) + 2\boldsymbol{\sigma}^{as}\right]\mathrm{d}\Omega_t = 0 \tag{2.62}$$

The observation of the nullity in the equilibrium equation (2.58) allows to write:

$$\int_{\Omega_t} \boldsymbol{\sigma}^{as}\mathrm{d}\Omega_t = 0 \tag{2.63}$$

Equation (2.63) is valid for any volume Ω_t, which implies $\boldsymbol{\sigma}^{as} = 0$. Then, based on (2.61), the symmetry of the stress tensor is verified.

$$\boldsymbol{\sigma} = \boldsymbol{\sigma}^T\ ;\ \sigma_{ij} = \sigma_{ji} \tag{2.64}$$

The symmetry is valid in the absence of external moments distributed in volume Ω_t.

2.9. PARTIAL STRESS TENSOR

The tensor $\boldsymbol{\sigma}$ includes the stress related to the skeleton and the fluid, without any distinction. In order to identify their respective contributions, the hypothesis of local contact forces (2.46) for each phase is written, such as:

$$\delta\mathbf{T}^s = \mathbf{T}^s(\mathbf{x},\mathrm{t},\mathbf{n})\mathrm{da}\ ;\ \delta\mathbf{T}^f = \mathbf{T}^f(\mathbf{x},\mathrm{t},\mathbf{n})\mathrm{da} \tag{2.65}$$

Equating the momentum balance separately, for the skeleton and for the fluid, one can define the partial stress tensors $\boldsymbol{\sigma}^s$ and $\boldsymbol{\sigma}^f$, respectively.

$$\mathbf{T}^s(\mathbf{x},\mathrm{t},\mathbf{n}) = (1-n)\boldsymbol{\sigma}^s\cdot\mathbf{n}\ ;\ \mathbf{T}^f(\mathbf{x},\mathrm{t},\mathbf{n}) = n\boldsymbol{\sigma}^f\cdot\mathbf{n}$$

The symmetry defined in (2.64) should also be seen in the partial tensors, as well as satisfying the equilibrium equation, as follows:

$$\begin{aligned}&\nabla_x \cdot \left[(1-n)\boldsymbol{\sigma}^s \right] + \rho_s (1-n)\left(\mathbf{f} - \boldsymbol{\gamma}^s \right) + \mathbf{f}_{int}^{\rightarrow s} = 0 \\ &\nabla_x \cdot \left[n\boldsymbol{\sigma}^f \right] + \rho_f n\left(\mathbf{f} - \boldsymbol{\gamma}^f \right) + \mathbf{f}_{int}^{\rightarrow f} = 0\end{aligned} \tag{2.66}$$

The volume strength $\mathbf{f}_{int}^{\rightarrow \pi}$ represents the interaction force experienced by the medium π, due to the other medium. The action and reaction principle foresees the balance of the interaction forces, that is; $\mathbf{f}_{int}^{\rightarrow s} + \mathbf{f}_{int}^{\rightarrow f} = 0$.

The balance can be restored in its original form (2.58), from the sum of equations (2.66), resulting in:

$$\mathbf{T} = \mathbf{T}^s + \mathbf{T}^f \; ; \boldsymbol{\sigma} = (1-n)\boldsymbol{\sigma}^s + n\boldsymbol{\sigma}^f \tag{2.67}$$

At a mesoscopic scale, the partial tensors can be interpreted as the tensors which contain the average stress values, in each phase. For the fluid, it is reasonable to approximate the stresses through a spherical tensor, defined as a function of pore pressure to which the fluid is subject to.

$$\boldsymbol{\sigma}^f = -p\boldsymbol{I} \tag{2.68}$$

then the stress partition (2.67) results in:

$$\boldsymbol{\sigma} = (1-n)\boldsymbol{\sigma}^s + np\boldsymbol{I} \tag{2.69}$$

and the equilibrium equation of the fluid in (2.66) can be rewritten as:

$$-\nabla_x (np) + \rho_f n\left(\mathbf{f} - \boldsymbol{\gamma}^f \right) + \mathbf{f}_{int}^{\rightarrow f} = 0 \tag{2.70}$$

2.10. ASPECTS ON THE CONTINUUM DAMAGE MECHANICS

The rupture process of a body is progressive, starting with a microcracking state that localizes and develops into a state of effective opening of cracks, which can in fact induce to rupture. The phenomenon identified between the onset of micro-cracking and cracking is called damage.

Thus, the damage theory is no longer valid to the effective crack opening, a state described by fracture mechanics. According to Janson and Hult (1977) *apud* Proença (2001), one can differentiate the two theories as follows:

- In damage mechanics the strength of a loaded structure is determined by the evolution of a defects field (microcracks or microvoids) considered continuously distributed;

- In the fracture mechanics, the strength of a loaded structure is determined by the evolution of a single defect, such as a pre-defined oriented crack in a sound medium.

In the continuum damage mechanics, the damage assessment is conducted by checking the strength or stiffness decrease in the solid. This is because one cannot directly quantify the damage, but can measure the damage undergone by their overall mechanical properties.

2.10.1. Damage Variable and Effective Stress

Consider a damaged solid body, from which an infinitesimal volume is isolated. Let dA be the surface area of this volume defined by the normal $\mathbf{n}$. The microcracks and voids in this section occupy an area dA^d. Then, the effective resistant area is $d\bar{A} = dA - dA^d$. The representative damage variable is defined by:

$$\mathbf{D}_n = \frac{dA^d}{dA} \tag{2.71}$$

From a physical point of view, the damage variable $\mathbf{D}_n$ is the relative value of the damaged section area, cut by a plane normal to $\mathbf{n}$.

Note that by assuming isotropy, the variable has a scalar nature D.

Let σ be the stress normal to the surface dA in the presence of any normal force applied. The resistant area of the section can be written as

$$d\bar{A} = dA - dA^d = dA(1-D) \tag{2.72}$$

which allows to define the effective portion of the stress:

$$\sigma^{ef} = \sigma\frac{dA}{d\bar{A}} = \frac{\sigma}{1-D} \tag{2.73}$$

In the case of isotropic damage, the effective stress concept can be extended to two-dimensional and three-dimensional problems, where it is valid to write the tensor $\boldsymbol{\sigma}^{ef}$.

The effective stress concept is common to both the study of porous media and the study of damaged solid media. It represents the stress portion that effectively acts on the solid skeleton, excluding the stress portions associated with the fluid pore pressure (2.68), and with the dissipative damage process. This partition of the total stress tensor will become clearer in the presentation of the constitutive equations of the coupled problem, in the following chapter.

2.10.2. Isotropic Local Damage Model (Marigo, 1981)

Let us assume the free energy associated with a solid, written as:

$$\rho\psi(\varepsilon_{jk}, D) = \frac{1}{2}(1-D)\,E_{jklm}\varepsilon_{jk}\varepsilon_{lm} \tag{2.74}$$

with ε_{jk} and E_{jklm} the elastic and strain tensors of the intact material, respectively. The mass density is indicated by ρ. Let D be the only internal scalar damage variable. It is understood that D assesses the state of degradation of the material, taking values between zero and one. The variable D that is null indicates intact material, while the unit value is associated with complete degradation.

One should note the correspondence between this energy expression and equation (3.1), which represents the free energy potential associated with the saturated porous medium. Equation (2.74) shows only the dissipation portion related to the strain tensor in a solid, penalized by the damage variable.

The derivatives of the energy potential with respect to the state variables ε_{jk} and D lead to define the associated variables, which are the total stress

$$\sigma_{jk} = \rho\frac{\partial\psi}{\partial\varepsilon_{jk}} = \frac{1}{2}(1-D)\,E_{jklm}\varepsilon_{lm} \tag{2.75}$$

and the thermodynamic force Y conjugated to damage:

$$Y = -\rho\frac{\partial\psi}{\partial D} = \frac{1}{2}E_{jklm}\varepsilon_{jk}\varepsilon_{lm} \tag{2.76}$$

In addition to the state laws given above, it is necessary to define a damage criterion. In this model, it takes the form:

$$F(Y, D) = Y - \kappa(D) \tag{2.77}$$

The term $\kappa(D)$ stores the maximum value reached during the loading history, adopted in its linear form $\kappa(D) = Y_0 + AD$, where Y_0 and A are material dependent. The damage evolution becomes from the consistency condition $\dot{F}(Y, D) = 0$, resulting in

$$\dot{D} = \dot{Y}/A \tag{2.78}$$

2.10.3 Comments on Strain Localization

Brittle or quasi-brittle materials – bones and rocks, for example – in some parts of its deformation process, may show a progressive loss of strength, in a behaviour called softening. This is induced by the damage process. Depending on the material's constitutive model, this softening can also cause a loss of stiffness in the system. This is the case of the continuous damage models.

The localization phenomenon occurs in materials that undergo softening, and is characterized by large discontinuities in the strain field. Small localized regions of the body dissipate more energy, hence showing much greater strain values than those measured in other parts of the body. The onset of localization can be caused by geometric imperfections, by the presence of heterogeneities of the material, by boundary conditions or by loading conditions.

Mathematically, the ellipticity loss of the local equilibrium equations indicates the occurrence of strain localization. Thus, the boundary value problem becomes ill-posed, leading to the loss of solution uniqueness.

To avoid this problem, one can resort to the concept of the material's characteristic length. Some non-local damage theories take this concept into account. One of them is briefly described here.

The strategy presented here is based on the concept of non-local integral proposed by Pijaudier-Cabot and Bazant (1987), which consists in considering a non-local thermodynamic force $\overline{Y}$. The value of the force Y is weighted with a function defined over the whole domain Ω or in part of it, evaluated in the neighbourhood of the point of interest. This function φ_Y has a radial character, depending on the distance between the base point s and the mapped point q. The non-local force is defined by the integral:

$$\overline{Y}(\mathrm{s}) = \frac{1}{V(\mathrm{s})} \int_{\Omega} \varphi_Y \left(\left\| \mathrm{s} - \mathrm{q} \right\| \right) Y(\mathrm{q}) \, \mathrm{dq} \tag{2.79}$$

where $V(\mathrm{s})$ is

$$V(\mathrm{s}) = \int_{\Omega} \varphi_Y \left(\left\| \mathrm{s} - \mathrm{q} \right\| \right) \, \mathrm{dq} \tag{2.80}$$

The following weight function is chosen, for example:

$$\varphi_Y \left(\left\| \mathrm{s} - \mathrm{q} \right\| \right) = \exp\left(\frac{\left\| \mathrm{s} - \mathrm{q} \right\|^2}{2l^2} \right) \tag{2.81}$$

With l as the characteristic length of the material. It is seen that, in the condition $l \to 0$ the weight function tends to the Dirac distribution $\delta(\mathrm{s}-\mathrm{q})$, which refers to the local model. The function takes higher values as the points s and q approximate each other, and tends to lower values for points further away from each other.

The damage criterion is rewritten as $\overline{F}(\overline{Y},\mathrm{D}) = \overline{Y} - \kappa(\mathrm{D})$, and the evolution law results:

$$\dot{\mathrm{D}} = \frac{\dot{\overline{Y}}}{A} \tag{2.82}$$

Note that the stresses are still calculated locally, according to (2.75). The non-local thermodynamic variable is responsible for the evolution of the damage process, that is, there is the contribution of values $\mathrm{Y}(\mathrm{q})$ from the whole domain.

Chapter 3

Poro-damage Formulation and BEM Implementation

3.1. OVERALL CONSIDERATIONS

The concepts of poromechanics and continuum damage mechanics presented herein enable developing a formulation for poroelasticity taking into account damage in the solid matrix, a behavior that from this point of the text will be identified as poro-damage. The coupled problem is defined from the free energy potential in the system, from which the constitutive equations are obtained. The field equations, which complement the formulation, are those already defined in the previous chapter.

The damage process of the skeleton induces changes in the mechanical properties of the porous material. This chapter presents the expressions for the evolution of these parameters according to the deterioration level on the skeleton.

Given the difficulties in obtaining analytical solutions for modeling problems in general, the so-called numerical methods emerge, based on approximate solutions calculated at discrete points in the domain under analysis. Among the known methods, the boundary element method appears as a good alternative to obtain numerical answers to several problems.

The integral formulation of the coupled model is written, and the corresponding nonlinear BEM formulation is then developed, enabling the computational implementation of the referred model.

3.2. PORO-DAMAGE FORMULATION

Let us assume a poroelastic system, under quasi-static linear regime. The description of the mechanical behavior of this system requires the following set of equations:

- Constitutive laws for porous solid and for the fluid
- Balance equation of the porous medium
- Fluid continuity equation
- Fluid transport law

The consideration of the damage process in the poroelastic system incurs changes at two points of the aforementioned equations. The constitutive law that governs the solid considers the gradual degradation undergone by the material, through the stress part associated with the damage, which leads to changes in the porous medium equilibrium.

3.2.1. Constitutive Laws

Let us assume the free energy potential per unit volume of a saturated porous medium subject to damage, written as:

$$\rho\psi(\varepsilon_{kj},\phi-\phi_0,\mathrm{D})=\frac{1}{2}(1-\mathrm{D})\varepsilon_{kj}:\mathrm{E}^{d}_{kjlm}:\varepsilon_{lm}+\frac{1}{2}b^2M\left[\mathrm{Tr}\left(\varepsilon_{kj}\right)\right]^2$$
$$+\frac{1}{2}M\left(\phi-\phi_0\right)^2-bM\left(\phi-\phi_0\right)\mathrm{Tr}\left(\varepsilon_{kj}\right) \tag{3.1}$$

in which the constants M and b represent the Biot modulus and the Biot coefficient of the effective stress, respectively. In saturated condition, the Lagrangian porosity ϕ measures the variation of fluid content, that is, the variation of fluid volume per unit volume of porous medium. The mass density of the porous medium is described by ρ. The tensor ε_{kj} contains the solid skeleton strains. The internal damage variable, represented by D, assesses the deterioration state of the material, taking values between zero and one. The null variable D indicates sound material, while the unit value is associated with complete degradation.

E^{d}_{kjlm} represents the isotropic elastic tensor of the material under drained conditions, defined by:

$$\mathrm{E}^{d}_{kjlm}=\left(\mathrm{K}^{d}-\frac{2\mathrm{G}}{3}\right)\delta_{kj}\delta_{lm}+2\mathrm{G}I_{kjlm} \tag{3.2}$$

The bulk modulus K^{d} and the shear modulus G refer to the drained material and can be obtained experimentally. The fourth order identity tensor is represented by I_{kjlm}. It can be observed that one of the possible sets of parameters for the characterization of porous material is formed by M, b, K^{d} and G.

The derivatives of the energy potential (3.1) with respect to the internal variables of the system, ε_{kj}, ϕ and D give rise to its conjugate pairs, in other words, they define the associated variables, which are the total stress σ_{kj}, pore pressure p and the thermodynamic force associated with damage Y:

$$\sigma_{kj}=\rho\frac{\partial\psi}{\partial\varepsilon_{kj}}=(1-\mathrm{D})\mathrm{E}^{d}_{kjlm}\varepsilon_{lm}+bM\left[b\mathrm{Tr}\left(\varepsilon_{kj}\right)-\left(\phi-\phi_0\right)\right]\delta_{kj} \tag{3.3}$$

$$\left(\mathrm{p}-\mathrm{p}_0\right)=\rho\frac{\partial\psi}{\partial\left(\phi-\phi_0\right)}=M\left[\left(\phi-\phi_0\right)-b\mathrm{Tr}\left(\varepsilon_{kj}\right)\right] \tag{3.4}$$

$$Y=-\rho\frac{\partial\psi}{\partial\mathrm{D}}=\frac{1}{2}\varepsilon_{kj}\mathrm{E}^{d}_{kjlm}\varepsilon_{lm} \tag{3.5}$$

Considering $(\phi - \phi_0)$ and $(\mathrm{p} - \mathrm{p}_0)$ allows to observe the presence of initial fields of pore pressure and porosity, better defining the boundary value problem. Thus, the terms in brackets can be interpreted as the evolution of the variable along the loading process. Substituting (3.4) in (3.3), we arrive at the following expression:

$$\sigma_{kj} = \mathrm{E}^{d}_{kjlm}\varepsilon_{lm} - \mathrm{D}\mathrm{E}^{d}_{kjlm}\varepsilon_{lm} - b(\mathrm{p} - \mathrm{p}_0)\delta_{kj} \tag{3.6}$$

in which it can be seen that the total stress tensor is composed of three parts. The first one depends on the elastic properties of the solid phase, called effective stress. The second, also related to the solid, includes the non-linear effects of the damage process. The last part is related to pore pressure p. Note that the p values are taken with a positive value, by convention. Then, equation (3.6) can be expressed as:

$$\sigma_{kj} = \sigma^{ef}_{kj} - \sigma^{d}_{kj} - b(\mathrm{p} - \mathrm{p}_0)\delta_{kj} \tag{3.7}$$

with σ^{d}_{kj} as the stress part associated with damage.

It can be seen that the pore pressure affects only the hydrostatic components of the total stress. It is known that at any point of a fluid, the pressure measured has a normal component, with the same value in all directions, and a tangential component, related to viscosity. For non-viscous fluid, an accepted condition in this work, that tangential part is neglected.

With the stress and strain tensors, the material parameters under undrained condition, expressed by $\phi = 0$, are also defined. The undrained bulk modulus K^{u} and the Skempton coefficient B are:

$$\mathrm{K}^{u} = -\frac{1}{3}\left.\frac{\partial \mathrm{Tr}(\sigma_{kj})}{\partial \mathrm{Tr}(\varepsilon_{kj})}\right|_{\phi=0}$$
$$B = -3\left.\frac{\partial \mathrm{p}}{\partial \mathrm{Tr}(\sigma_{kj})}\right|_{\phi=0} \tag{3.8}$$

It is found that K^{u} relates the volumetric strain with the hydrostatic stress, while B relates this stress to the pore pressure p.

These parameters can be related to the ones defined in drained condition, as follows:

$$b = \frac{\mathrm{K}^{\mathrm{u}} - \mathrm{K}^{\mathrm{d}}}{B\mathrm{K}^{\mathrm{u}}}$$
$$M = \frac{B^2\left(\mathrm{K}^{\mathrm{u}}\right)^2}{\mathrm{K}^{\mathrm{u}} - \mathrm{K}^{\mathrm{d}}} \tag{3.9}$$

3.2.2. Fluid Transport Law

The transport of a fluid in an interstitial space is described by a flow law, derived from the fluid dissipation equation. Let us consider the dissipation equation below:

$$\wp_{\mathrm{f}} = \left[-\nabla_{\mathrm{x}}\mathrm{p} + \rho_{\mathrm{f}}\left(\mathbf{f} - \boldsymbol{\gamma}_{\mathrm{f}}\right)\right]\cdot\boldsymbol{\nu} \tag{3.10}$$

Overall, it is written as:

$$\wp_{\mathrm{f}} = \boldsymbol{\iota}\cdot\boldsymbol{\nu} \tag{3.11}$$

$$\boldsymbol{\nu} = n(\mathbf{V}^{\mathrm{f}} - \mathbf{V}^{\mathrm{s}})\ ;\ \boldsymbol{\iota} = -\nabla_{\mathrm{x}}\mathrm{p} + \rho_{\mathrm{f}}\left(\mathbf{f} - \boldsymbol{\gamma}_{\mathrm{f}}\right) \tag{3.12}$$

with ν as the vector that represents the filtration - as defined in 2.4.2 – and ι the force that induces the filtration. Assuming a laminar flow of the fluid through the porous space, a linear relationship between the two quantities can be considered. Darcy's Law, in its linear classic version, uses the permeability tensor $\mathbf{k}$:

$$n(\mathbf{V}^{\mathrm{f}} - \mathbf{V}^{\mathrm{s}}) = \mathbf{k}\left[-\nabla_{\mathrm{x}}\mathrm{p} + \rho_{\mathrm{f}}\left(\mathbf{f} - \boldsymbol{\gamma}_{\mathrm{f}}\right)\right] \tag{3.13}$$

which is defined by

$$\mathbf{k} = \frac{\boldsymbol{k}}{\mu} \tag{3.14}$$

due to the intrinsic permeability of the skeleton $\boldsymbol{k}$ and to the fluid viscosity μ. In the case of partially saturated domains, there is also the influence of relative permeability corresponding to each fluid phase in this value. Note that this coefficient is taken as the scale $\mathbf{k} = \mathrm{k}$ in this study, on account of the admitted isotropy. In a more general law, it is necessary to use the anisotropic permeability tensor.

In this work, we will use a Lagrangian description of the variables. In the Lagrangian description, the flow and filtration vectors result as:

$$\mathbf{M} = \rho_{\mathrm{f}}\boldsymbol{\nu}_{lag}\ ;\ \boldsymbol{\nu}_{lag} = \boldsymbol{\nu} = \phi(\mathbf{V}^{\mathrm{f}} - \mathbf{V}^{\mathrm{s}}) \tag{3.15}$$

Darcy's linear Law, which relates the pore-pressure gradient and relative velocity of the fluid in relation to the skeleton, is written as:

$$\phi(\mathbf{V}^{\mathrm{f}} - \mathbf{V}^{\mathrm{s}}) = \mathrm{k}\left[-\nabla_{\mathrm{x}}\mathrm{p} + \rho_{\mathrm{f}}\left(\mathbf{f} - \boldsymbol{\gamma}_{\mathrm{f}}\right)\right] \tag{3.16}$$

From this point of the text, the total force over the fluid, including its acceleration, will be represented by $\boldsymbol{f} = \rho_{\mathrm{f}}\left(\mathbf{f} - \boldsymbol{\gamma}_{\mathrm{f}}\right)$.

$$\boldsymbol{\nu} = \mathrm{k}\left(-\nabla_{\mathrm{x}}\mathrm{p} + \boldsymbol{f}\right) \; ; \; \nu_{\mathrm{k}} = \mathrm{k}\left(-\mathrm{p}_{,\mathrm{k}} + f_{\mathrm{k}}\right) \tag{3.17}$$

3.2.3. Fluid Continuity Equation

The lagrangian fluid continuity equation, neglecting a possible source of fluid is written as:

$$\frac{\mathrm{d}m_{\mathrm{f}}}{\mathrm{dt}} + \nabla_{\mathrm{x}} \cdot \mathbf{M} = 0 \tag{3.18}$$

Applying the definition $m_{\mathrm{f}} = \rho_{\mathrm{f}}\phi$ and equation (3.15), another form is admitted for equation (3.18):

$$\frac{\mathrm{d}\left(\rho_{\mathrm{f}}\phi\right)}{\mathrm{dt}} + \left(\rho_{\mathrm{f}}\nu_{\mathrm{k}}\right)_{,\mathrm{k}} = 0 \tag{3.19}$$

The fluid mass density depends on the pressure and temperature. Considering an isothermal process, there is only the influence of pressure, which can be represented by $\frac{\partial\rho_{\mathrm{f}}}{\partial\mathrm{p}} = \rho_{\mathrm{f}}\mathrm{K}_{\mathrm{f}}$, with the bulk modulus of the fluid represented by K^{f}. The derivatives in (3.19) lead to the equation:

$$\nu_{\mathrm{k,k}} = -\dot{\phi} - \mathrm{K}^{\mathrm{f}}\left(\phi\dot{\mathrm{p}} + \nu_{\mathrm{k}}\mathrm{p}_{,\mathrm{k}}\right) \tag{3.20}$$

Inserting Darcy's Law definition into equation (3.20), an function in terms of pore-pressure p is obtained:

$$\nu_{\mathrm{k,k}} = -\dot{\phi} - \mathrm{K}^{\mathrm{f}}\left[\phi\dot{\mathrm{p}} + \mathrm{k}\left(-\mathrm{p}_{,\mathrm{k}}{}^{2} + f_{\mathrm{k}}\mathrm{p}_{,\mathrm{k}}\right)\right] \tag{3.21}$$

The consideration of K^{f} introduces a nonlinearity into the problem, associated with the term $\mathrm{p}_{,\mathrm{k}}{}^{2}$. In the equation (3.21) this parameter is not taken into account. However, the fluid compressibility is implicitly (or partially) considered, using K^{f} in the calculation for the mechanical properties of the material.

3.2.4. Equilibrium Equation

As presented in 2.8, the local equilibrium for the porous medium can be written as follows:

$$\nabla_x \cdot \boldsymbol{\sigma} + \rho_s (1-n)\left(\mathbf{f} - \boldsymbol{\gamma}^s\right) - \rho_f n\left(\mathbf{f} - \boldsymbol{\gamma}^f\right) = 0 \tag{3.22}$$

From this point of the text, a simple notation will be used to represent the volume forces acting on the porous medium, with no distinction between forces in the fluid or solid phase. This is to achieve greater clarity in the exposition of the integral formulations of the problem. Therefore, we have the equilibrium written due to tensor $\mathbf{b}$, as follows.

$$\nabla_x \cdot \boldsymbol{\sigma} + \mathbf{b} = 0 \; ; \; \sigma_{kj,j} + b_k = 0 \tag{3.23}$$

Equations (3.7), (3.17), (3.21) and (3.23), complemented by the strain-displacement relation

$$\boldsymbol{\varepsilon} = \frac{1}{2}\left(\nabla_X \mathbf{u} + \nabla_X{}^T \mathbf{u}\right) \; ; \; \varepsilon_{kj} = \frac{1}{2}\left(u_{k,j} + u_{j,k}\right) \tag{3.24}$$

define the poro-damage problem, in a quasi-static regime.

3.2.5. Rates of the Variables

Given the transient nature of the problem, the following rates of the variables should be defined:

$$\dot{\sigma}_{kj} = \frac{1}{2}(1-D)E^d_{kjlm}\dot{\varepsilon}_{lm} - \dot{D}\varepsilon_{lm} - b\dot{p}\delta_{kj} \tag{3.25}$$

$$\dot{\phi} = b\,\mathrm{Tr}(\dot{\varepsilon}_{kj}) + \frac{1}{M}\dot{p} \tag{3.26}$$

$$\dot{p} = M\left[\dot{\phi} - b\,\mathrm{Tr}(\dot{\varepsilon}_{kj})\right] \tag{3.27}$$

3.3. INFLUENCE OF DAMAGE ON THE POROELASTIC PARAMETERS

The damage process evolution can be measured through the gradual deterioration in the mechanical properties of the solid skeleton. Thus, the mechanical parameters of the porous material, dependent on the parameters of the solid matrix, also undergo the influence of the damage. The Biot coefficient of the effective stress is defined by

$$b = 1 - \frac{K^d}{K_s} \tag{3.28}$$

with K_s as the bulk modulus of the solid constituent, with a value that is higher than the modulus K^d. This latter is calculated with the values of modulus G and Poisson's ratio υ measured under a drained condition:

$$K^d = \frac{2G(1+\upsilon)}{3(1-2\upsilon)} \tag{3.29}$$

Introducing the damage effect directly on the drained modulus, one obtains

$$K^d(D) = (1-D)\frac{2G(1+\upsilon)}{3(1-2\upsilon)} = (1-D)K^d \tag{3.30}$$

which can be applied over time in expression (3.28). The Biot modulus M is calculated using the expression:

$$M = \frac{K^u - K^d}{b^2} \tag{3.31}$$

which can also be written with the damaged values. An expression to calculate the undrained modulus can be defined based on its drained equivalent (Detournay and Cheng, 1993):

$$K^u = \frac{2G(1+\upsilon^u)}{3(1-2\upsilon^u)} \tag{3.32}$$

in which Poisson's undrained ratio υ^u is determined experimentally.

3.4. ASPECTS ON THE BOUNDARY ELEMENT METHOD

The numerical methods are alternatives for the mathematical solutions to study engineering problems. The latter are usually limited by difficulties in obtaining analytical solutions to more or less complex problems that include general geometries and non-linear behaviors.

One of the areas in engineering research is the development of suitable numerical methods to solve these problems. In the case of this work, the numerical method to be used is the boundary element method. This method applies, as the weighting function, an analytical solution of a problem that is similar to that which is sought to be resolved, but with particular boundary conditions. This function is called a fundamental solution.

When the physical properties of the domain, for which the fundamental solution was calculated, correspond exactly to the properties of the domain analyzed, it is not necessary to use any domain discretization. This usually occurs for linear problems. However, when

there is some limitation in the fundamental solution, the domain discretization to consider the residual quantities is then necessary.

Nevertheless, the fact that many of the unknown variables, usually the most important, belong exclusively to the boundary, the mesh density used in the domain is considerably reduced when compared to the domain methods, as for instance the finite element method.

This section provides, in general, some principles of the method. The symbols used herein do not retain any correspondence with the variables already defined in previous chapters.

3.4.1. Boundary Elements and Discretization

Considering the integral formulation of a problem, written for the boundary points, its treatment depends on the clear description of this boundary. The main objective of BEM is, based on the integral formulation, the assembly of an algebraic system, which allows to directly determine the approximate boundary values and, from these, the other values of interest for the analysis. Clearly, there are endless possible equations to be written, since the integral formulation can be applied to the infinite points of the boundary of the domain or to the external points.

The equivalent representation of the boundary, in a finite dimension, is done by defining the nodes that delimit the so-called boundary elements. This boundary parametrization can result as exact or approximate, depending on the domain geometry under analysis and the type of parameterization used. Figure 3.1 illustrates the two situations, using linear elements.

Besides the geometric characterization of the element, the variables of interest to the problem must be evaluated from a finite number of values associated with the discretization nodes. It is common to use polynomial functions to interpolate the variables along the boundary elements, that is, between the discretization nodes.

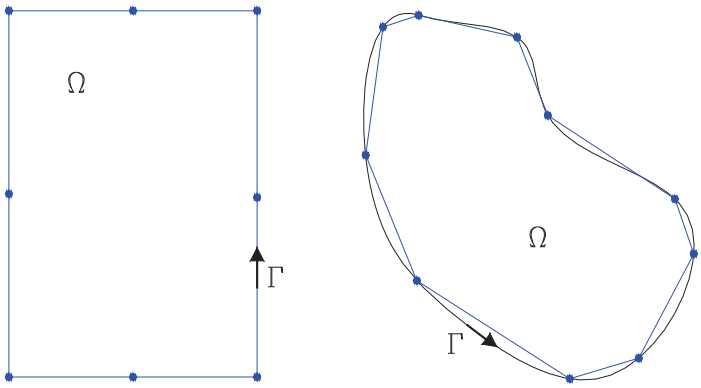

Figure 3.1 – Exact and Approximate Boundary Discretizations

The shape functions to approximate the boundary geometry and the variables involved can be chosen freely, depending on the type of problem studied and the required accuracy of the results. The combination of two equal interpolation functions gives rise to the isoparametric element. In this study, the linear isoparametric element is used, as illustrated below.

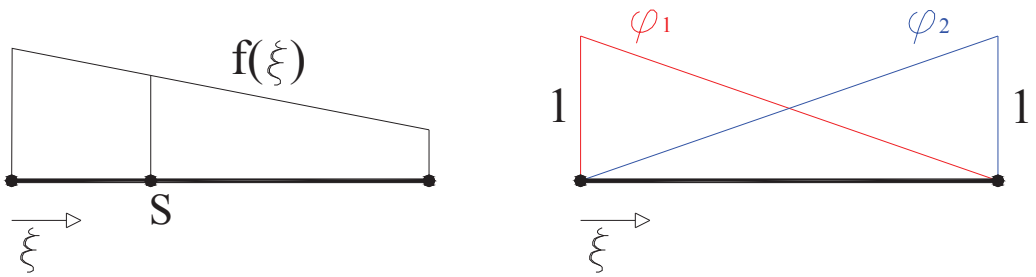

Figure 3.2 – Linear Isoparametric Element

In which φ_1 and φ_2 are the functions that compose the linear distribution $f(\xi)$, defined on the local dimensionless coordinate $\xi = [0,1]$. Then, the coordinates of a point S or an unknown evaluated at this point can be written according to the same approximate form, respectively

$$x_m(S) = \varphi_n(S) x_m^n \tag{3.33}$$

$$a_m(S) = \varphi_n(S) a_m^n \tag{3.34}$$

The subscript m refers to the direction and n to the node considered in the element.

Based on equation (3.34), displacements and tractions on a generic element can be represented in a matrix form. For a two-dimensional problem, we have:

$$\mathbf{u} = \begin{Bmatrix} u_1 \\ u_2 \end{Bmatrix} = \begin{bmatrix} \varphi_1 & 0 & \varphi_2 & 0 \\ 0 & \varphi_1 & 0 & \varphi_2 \end{bmatrix} \begin{Bmatrix} u_1^1 \\ u_2^1 \\ u_1^2 \\ u_2^2 \end{Bmatrix} \tag{3.35}$$

$$\mathbf{t} = \begin{Bmatrix} t_1 \\ t_2 \end{Bmatrix} = \begin{bmatrix} \varphi_1 & 0 & \varphi_2 & 0 \\ 0 & \varphi_1 & 0 & \varphi_2 \end{bmatrix} \begin{Bmatrix} t_1^1 \\ t_2^1 \\ t_1^2 \\ t_2^2 \end{Bmatrix} \tag{3.36}$$

Similarly for the coordinates:

$$\mathbf{x} = \begin{Bmatrix} x_1 \\ x_2 \end{Bmatrix} = \begin{bmatrix} \varphi_1 & 0 & \varphi_2 & 0 \\ 0 & \varphi_1 & 0 & \varphi_2 \end{bmatrix} \begin{Bmatrix} x_1^1 \\ x_2^1 \\ x_1^2 \\ x_2^2 \end{Bmatrix} \tag{3.37}$$

In some problems it is necessary to represent discontinuities on boundary conditions between adjacent elements. In such cases, one can apply the discontinuous element concept (Figure 3.3), together with the definition of double nodes, which are nodes with the same coordinates, but with different associated values. In order to write two different equations for these nodes, the collocation point is moved along the element axis, at a distance corresponding to 1/4 of its length, as suggested in Venturini (1988).

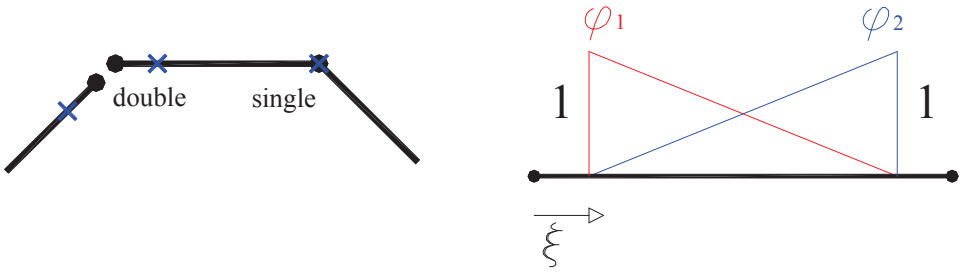

Figure 3.3 – Discontinuous adjacent elements, with double node; Interpolation functions in a discontinuous element

3.4.2. Domain Discretization

As will be seen in this section, the integrals over the domain, which are in the proposed formulation, can be subdivided into two basic classes. In the first one, the kernel, which consists of a fundamental solution or its derivatives, multiplies a term of known value over the domain (3.38), as in the case of body force integrals. Another situation is that in which the term multiplied is a system unknown, as in equation (3.39). In this section, the notations X^* and T are used to represent a generic fundamental solution and any given variable, respectively. When the variable has its value known, a bar on its representation is used.

$$\int_\Omega \mathbf{X}^* \overline{\mathbf{T}} \, d\Omega \tag{3.38}$$

$$\int_\Omega \mathbf{X}^* \mathbf{T} \, d\Omega \tag{3.39}$$

In the case of integrals (3.38), the objective is to transfer the domain integral to the boundary, so that it can be evaluated in the usual way, as well as the other terms over the boundary.

Let us assume the existence of a primitive of the fundamental solution:

$$\nabla^2 \mathbf{L} = \mathbf{X}^* \tag{3.40}$$

The integral can then be rewritten as:

$$\int_\Omega \mathbf{X}^* \overline{\mathbf{T}}\, d\Omega = \int_\Omega \nabla^2 \mathbf{L}\, \overline{\mathbf{T}}\, d\Omega = \int_\Omega \left(\frac{\partial^2 \mathbf{L}}{\partial x_1^2} + \frac{\partial^2 \mathbf{L}}{\partial x_2^2} \right) \overline{\mathbf{T}}\, d\Omega \tag{3.41}$$

Making an integration by parts, we have:

$$\int_\Omega \left(\frac{\partial^2 \mathbf{L}}{\partial x_1^2} + \frac{\partial^2 \mathbf{L}}{\partial x_2^2} \right) \overline{\mathbf{T}}\, d\Omega = \int_\Gamma \left(\frac{\partial \mathbf{L}}{\partial x_1} \eta_1 + \frac{\partial \mathbf{L}}{\partial x_2} \eta_2 \right) \overline{\mathbf{T}}\, d\Gamma - \int_\Omega \left(\frac{\partial \mathbf{L}}{\partial x_1} \frac{\partial \overline{\mathbf{T}}}{\partial x_1} + \frac{\partial \mathbf{L}}{\partial x_2} \frac{\partial \overline{\mathbf{T}}}{\partial x_2} \right) d\Omega \tag{3.42}$$

A second integration by parts leads to

$$\int_\Gamma \left(\frac{\partial \mathbf{L}}{\partial x_1} \eta_1 + \frac{\partial \mathbf{L}}{\partial x_2} \eta_2 \right) \overline{\mathbf{T}}\, d\Gamma - \int_\Gamma \left(\frac{\partial \overline{\mathbf{T}}}{\partial x_1} \eta_1 + \frac{\partial \overline{\mathbf{T}}}{\partial x_2} \eta_2 \right) \mathbf{L}\, d\Gamma + \int_\Omega \left(\frac{\partial^2 \overline{\mathbf{T}}}{\partial x_1^2} + \frac{\partial^2 \overline{\mathbf{T}}}{\partial x_2^2} \right) \mathbf{L}\, d\Omega \tag{3.43}$$

Finally, the original integral in the domain results as:

$$\int_\Omega \nabla^2 \mathbf{L} \cdot \overline{\mathbf{T}}\, d\Omega = \int_\Gamma \left(\frac{\partial \mathbf{L}}{\partial \eta} \right) \overline{\mathbf{T}}\, d\Gamma - \int_\Gamma \left(\frac{\partial \overline{\mathbf{T}}}{\partial \eta} \right) \mathbf{L}\, d\Gamma + \int_\Omega \nabla^2 \overline{\mathbf{T}} \cdot \mathbf{L}\, d\Omega \tag{3.44}$$

Note that successive integrations can be made in order to cancel the remaining integral domain in the last term of the evolution. After two integrations, as shown above, it is possible to treat integrals whose term $\overline{\mathbf{T}}$ has a constant or linear distribution, since its Laplacian is zero. This technique is known as multiple reciprocity.

One may use different methodologies to treat the type of domain terms (3.39). A semi-analytical procedure to calculate these integrals is shown herein, from the definition of the variable of interest in discrete regions of the domain.

Consider a portion of the domain Ω, discretized in cells Ω_m, as illustrated below.

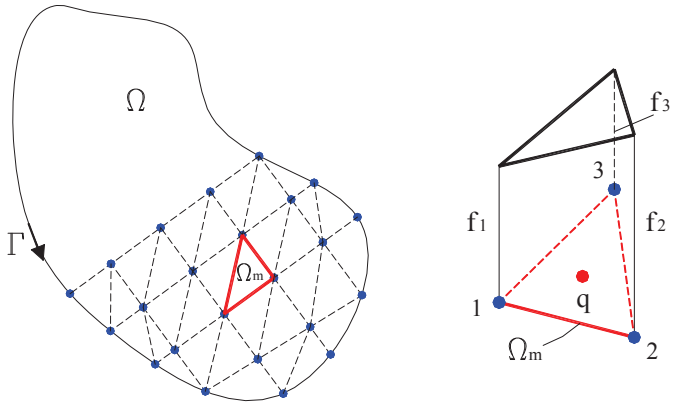

Figure 3.4 – Division of the domain into cells; linear approximation of variables in the cell

Approximating the value of $f(q)$ in each cell Ω_m by a function $\varphi_l(q)$, we have:

$$f^m(q) = \varphi_l(q) f_l^m \tag{3.45}$$

Thus, an integral containing the term in $f(q)$ can be written as a sum of the integrals in each cell, for example:

$$\int_\Omega u^*(S,q) f(q) d\Omega = \sum_{m=1}^{N_{cel}} \int_{\Omega_m} u^*(S,q) \varphi_l(q) d\Omega_m f_l^m \tag{3.46}$$

The integration of a domain term in the cells results in a matrix of coefficients, which represents the influence of the nodal values f_l.

In this work, triangular cells with linear approximation are used for the variables. For the cells whose nodes belong to the boundary, a procedure to move the collocation point into the cell, along the corresponding bisector, is adopted.

The linear shape function is given by:

$$\varphi_l = \frac{1}{2A_c}\left(\alpha_0 + \beta_0 x + \gamma_0 y\right) \tag{3.47}$$

With A_c as the cell area, and the terms α_0, β_0 and γ_0 defined by cyclic notation, with $i, j, k = 1 \ldots 3$, as follows:

$$\begin{aligned} \alpha_0 &= x_j y_k - x_k y_j \\ \beta_0 &= y_j - y_k \\ \gamma_0 &= x_k - x_j \end{aligned} \tag{3.48}$$

The approximations of the variables over the cell are integrated according to a semi-analytical procedure, which can be found in Botta (2003) and which is briefly described below. First, let us assume an integral domain, written as a sum of integrals over the cells:

$$\int_\Omega u^* f \, d\Omega = \sum_{m=1}^{N_{cel}} \int_{\Omega_m} u^* \varphi_l \, d\Omega_m \, f_l^m \tag{3.49}$$

the summation is written in polar coordinates, obtaining:

$$\sum_{m=1}^{N_{cel}} \int_\theta \int_r u^* \varphi_l \, r \, dr \, d\theta \, f_l^m \tag{3.50}$$

Performing an analytical integration with respect to r, we arrive at the expression below.

$$\sum_{m=1}^{N_{cel}} \int_{\theta} \Psi \; d\theta \; f_l^m \tag{3.51}$$

An equivalent expression, represented over the boundary of a cell Γ_m is:

$$\sum_{m=1}^{N_{cel}} \int_{\Gamma_m} \Psi \left(\frac{1}{r} \frac{\partial r}{\partial n} d\Gamma_m \right) f_l^m \tag{3.52}$$

Depending on the natural coordinates of the cell boundary, we obtain

$$\sum_{m=1}^{N_{cel}} \int_{\Gamma_m} \left| J_p \right| \Psi \; \frac{1}{r} \frac{\partial r}{\partial n} d\xi_m \; f_l^m \tag{3.53}$$

this expression can be integrated by any given numerical procedure.

3.5. BEM FORMULATION

Using the boundary element method requires developing the integral formulation of the problem in question. Also, it is necessary to define the fundamental solutions for the variables involved.

As already stated, the poroelastic system can be described by superposition of the fluid and solid phases. Thus, in the formulation there are equations related to the fluid pore-pressure, as well as the ones from elasto-damage problem, to which terms that reflect the effect of pore-pressures are incorporated. Thus, there is a set of integral equations that represent the coupling between the mechanical behaviors of the phases.

We seek herein to present the integral equations for both the solid and fluid phases.

3.5.1. Integral Formulation for the Solid Phase

Fundamental Solutions. To characterize the fundamental problem, an infinite domain Ω^* is considered subject to a unit force acting at point s (source point), in the direction i. The point where the effects due to that force are measured is called the field point and is represented by q. In order to represent the unit force of the fundamental problem, we consider the term $\bar{b}_k(q)$, from the equilibrium equation of elastostatics $\sigma^{ef}_{kj,j} + \bar{b}_k = 0$, as a Dirac delta distribution, weighted by a Kronnecker delta that establishes the directions i and k, as follows:

$$\bar{b}_{ik}(q) = \delta(s,q)\delta_{ik} \tag{3.54}$$

The Dirac distribution, commonly used in the representation of concentrated loads in elasticity, assumes zero values or tends to infinite, as follows:

$$\delta(s,q)=\begin{cases}\infty, s=q\\ 0, s\neq q\end{cases} \tag{3.55}$$

An important property of this function is the following:

$$\int_{\Omega}\mathbf{f}(y)\delta(x,y)d\Omega(y)=\mathbf{f}(x) \tag{3.56}$$

The equilibrium equation of elastostatics, for the purpose of a fundamental solution, can then be written as:

$$\sigma^{ef*}_{ikj,j}(s,q)+\delta(s,q)\delta_{ik}=0 \tag{3.57}$$

In which σ^{ef*}_{ikj} is the effective stress tensor in the fundamental state. All the quantities in the text referring to the fundamental state are indicated with an asterisk (*).

Hooke's Law, which is the constitutive relationship for only the solid phase, relates the strain tensor with the effective stress, as follows:

$$\sigma^{ef}_{kj}(q)=E_{kjlm}\varepsilon_{lm}(q)=\frac{2G\upsilon}{(1-2\upsilon)}\delta_{kj}\varepsilon_{mm}(q)+2G\varepsilon_{kj}(q) \tag{3.58}$$

From the strain-displacement relation, Hooke's Law is written in terms of displacements. Differentiating it with respect to x_j, we obtain the first term of the equilibrium equation (3.57), which results as:

$$\frac{1}{1-2\upsilon}u^{*}_{ij,kj}(s,q)+u^{*}_{ik,jj}(s,q)+\frac{1}{G}\delta(s,q)\delta_{ik}=0 \tag{3.59}$$

in which $u^{*}(s,q)$ represents the displacement field in the fundamental state.

The solution to equation (3.59), for the two-dimensional case is

$$u^{*}_{ik}(s,q)=\frac{1}{8\pi(1-\upsilon)G}\left[-(3-4\upsilon)\ln(r)\delta_{ik}+r_i r_{,k}\right] \tag{3.60}$$

with r as the distance between the source and field points s and q, respectively.

Differentiating equation (3.60) with respect to x_j, and using the strain-displacement relation, we obtain the strain tensor in the fundamental problem:

$$\varepsilon^{*}_{ijk}(s,q) = -\frac{1}{8\pi(1-\upsilon)Gr}\Big[(1-2\upsilon)(r_{,k}\delta_{ij} + r_{,j}\delta_{ik}) - r_{,i}\delta_{jk} + 2r_{,i}r_{,j}r_{,k}\Big] \tag{3.61}$$

From Hooke's law, the fundamentals effective stresses can be written as follows:

$$\sigma^{ef*}_{ijk}(s,q) = -\frac{1}{4\pi(1-\upsilon)r}\Big[(1-2\upsilon)(r_{,k}\delta_{ij} + r_{,j}\delta_{ik} - r_{,i}\delta_{jk}) + 2r_{,i}r_{,j}r_{,k}\Big] \tag{3.62}$$

Also of interest is the fundamental solution for a Traction defined by the normal η, on a point Q of the boundary. From expression (3.62), and using Cauchy's formula

$$t_k(Q) = \sigma^{ef}_{jk}(Q)\eta_j \tag{3.63}$$

we arrive at

$$t^{*}_{ik}(s,q) = -\frac{1}{4\pi(1-\upsilon)r}\Big\{\Big[(1-2\upsilon)\delta_{ik} + 2r_{,i}r_{,k}\Big]r_{,\eta} - (1-2\upsilon)(r_{,i}\eta_k - r_{,k}\eta_i)\Big\} \tag{3.64}$$

Boundary Integral Equations. First, the equilibrium equation (3.23) is written in its expanded form, containing the nonlinear and pore-pressure terms at the source point s, as follows:

$$\sigma_{kj,j}(s) + b_k(s) = \sigma^{ef}_{kj,j}(s) - \sigma^{d}_{kj,j}(s) - b\delta_{kj}p_{,j}(s) + b_k(s) = 0 \tag{3.65}$$

The tractions at point S of boundary Γ, are given by:

$$T_k(S) = \sigma_{kj}(S)\eta_j = \Big[\sigma^{ef}_{kj}(S) - \sigma^{d}_{kj,j}(s) - b\delta_{kj}p(S)\Big]\eta_j \tag{3.66}$$

The total stress equation is written as

$$\sigma_{kj}(s) = \frac{2G\upsilon}{(1-2\upsilon)}\delta_{kj}\Big[\varepsilon_{mm}(s) - \varepsilon^{d}_{ll}(s)\Big] + 2G\Big[\varepsilon_{kj}(s) - \varepsilon^{d}_{kj}(s)\Big] - b\delta_{kj}p(s) \tag{3.67}$$

which can be written in terms of displacements:

$$\begin{aligned}\sigma_{kj}(s) &= \frac{2G\upsilon}{(1-2\upsilon)}\delta_{kj}u_{m,m}(s) + G\Big[u_{k,j}(s) + u_{j,k}(s)\Big] \\ &-\frac{2G\upsilon}{(1-2\upsilon)}\delta_{kj}\varepsilon^{d}_{ll}(s) - 2G\varepsilon^{d}_{kj}(s) - b\delta_{kj}p(s)\end{aligned} \tag{3.68}$$

Applying the boundary element method to a particular body requires its equilibrium representation in the integral form, which can be obtained from weighted residual methods, defining as weighting function the fundamental solution to the basic variable of the problem.

Although the procedure via weighted residuals is well established, an alternative approach, proposed by Somigliana (1886), is used herein, based on Betti reciprocal theorem. The theorem is based on the principle of energy conservation and defines that for a solid volume V between any two states, exists the relationship:

$$\int_V \sigma_1(q)\varepsilon_2(q)dV = \int_V \varepsilon_1(q)\sigma_2(q)dV \tag{3.69}$$

It should be noted that for applying the principles of reciprocity, such as Betti's one, it is necessary that the two fields involved keep a linear and proportional relationship between them. Therefore, the theorem will be written in terms of effective stress, which is linear and proportional to the strain tensor.

Thus, let us assume a finite domain Ω, delimited by the boundary Γ, which represents the body under analysis, inserted in an infinite medium Ω^*. Consider the existence of two loads, with one of them acting in region Ω, corresponding to the real problem. The second one, related to the fundamental problem, acts on the infinite domain Ω^*. Based on the aforementioned theorem, it is possible to write

$$\int_\Omega \sigma_{kj}^{ef}(q)\varepsilon_{ijk}^*(s,q)d\Omega = \int_\Omega \varepsilon_{kj}(q)\sigma_{ijk}^*(s,q)d\Omega \tag{3.70}$$

in which the definition of effective stresses can be inserted:

$$\int_\Omega \left(\sigma_{kj}(q) + \sigma_{kj}^d(q) + b\delta_{kj}p(q)\right)\varepsilon_{ijk}^*(s,q)d\Omega = \int_\Omega \varepsilon_{kj}(q)\sigma_{ijk}^*(s,q)d\Omega \tag{3.71}$$

From the strain-displacement relation, the expression (3.71) takes the form of

$$\int_\Omega \left(\sigma_{kj}(q) + \sigma_{kj}^d(q) + b\delta_{kj}p(q)\right)u_{ik,j}^*(s,q)d\Omega = \int_\Omega u_{k,j}(q)\sigma_{ijk}^*(s,q)d\Omega \tag{3.72}$$

Integrating it by parts, we get:

$$\begin{aligned}&\int_\Gamma \sigma_{kj}(Q)u_{ik}^*(s,Q)\eta_j d\Gamma - \int_\Omega \sigma_{kj,j}(q)u_{ik}^*(s,q)d\Omega + \int_\Omega \sigma_{kj}^d(q)\varepsilon_{ijk}^*(s,q)d\Omega \\ &+ \int_\Omega \delta_{kj}bp(q)\varepsilon_{ijk}^*(s,q)d\Omega = \int_\Gamma \sigma_{ijk}^*(Q)u_k(Q)\eta_j d\Gamma - \int_\Omega \sigma_{ijk,j}^*(q)u_k(s,q)d\Omega\end{aligned} \tag{3.73}$$

Based on Cauchy's formula, we can write

$$\int_{\Gamma} T_k u_{ik}^*(s,Q)d\Gamma - \int_{\Omega} \sigma_{kj,j}(q)u_{ik}^*(s,q)d\Omega + \int_{\Omega} b\delta_{kj}p(q)\varepsilon_{ijk}^*(s,q)d\Omega$$
$$+\int_{\Omega} \sigma_{kj}^d(q)\varepsilon_{ijk}^*(s,q)d\Omega = \int_{\Gamma} T_{ik}^* u_k(Q)d\Gamma - \int_{\Omega} \sigma_{ijk,j}^*(q)u_k(q)d\Omega \quad (3.74)$$

The derivatives of the stresses that appear in the domain integrals can be replaced by the corresponding load values, according to equations (3.57) and (3.65), leading to:

$$\int_{\Gamma} T_k u_{ik}^*(s,Q)d\Gamma + \int_{\Omega} b_k(q)u_{ik}^*(s,q)d\Omega + \int_{\Omega} b\delta_{kj}p(q)\varepsilon_{ijk}^*(s,q)d\Omega$$
$$+\int_{\Omega} \sigma_{kj}^d(q)\varepsilon_{ijk}^*(s,q)d\Omega = \int_{\Gamma} T_{ik}^* u_k(Q)d\Gamma - \int_{\Omega} \delta(s,q)\delta_{ik}u_k(q)d\Omega \quad (3.75)$$

Using the Dirac delta property shown in equation (3.56), the equation above is organized as follows:

$$u_i(s) = \int_{\Gamma} T_k(Q)u_{ik}^*(s,Q)d\Gamma - \int_{\Gamma} T_{ik}^*(s,Q)u_k(Q)d\Gamma + \int_{\Omega} \delta_{kj}p(q)\varepsilon_{ijk}^*(s,q)d\Omega$$
$$+\int_{\Omega} \sigma_{kj}^d(q)\varepsilon_{ijk}^*(s,q)d\Omega + \int_{\Omega} b_k(q)u_{ik}^*(s,q)d\Omega \quad (3.76)$$

Equation (3.76) defines the displacement field for any source point s within the domain, from the displacements and forces measured in the boundary points.

In order to use BEM, it is necessary to represent the displacement field for the points on the boundary. In this way, it is introduced a semi-circular complementary region, with radius ω, around the placing point S (Figure 3.5), so that it can be treated as an internal point by the known equation (3.76).

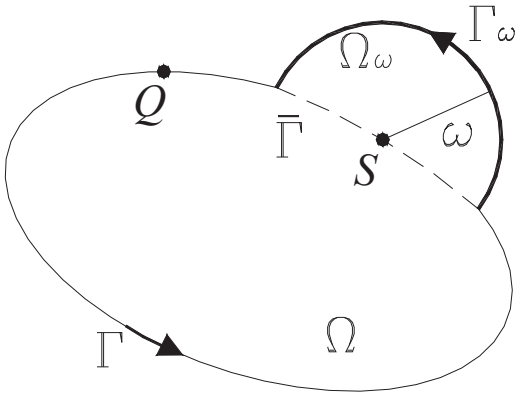

Figure 3.5 – Inclusion of the infinitesimal complementary domain

Redefining (3.76), considering the inclusion of the infinitesimal domain, we obtain

$$u_i(S) = \int_{\Gamma-\bar{\Gamma}} T_k(Q)u_{ik}^*(S,Q)d\Gamma + \int_{\Gamma_\omega} T_k(Q)u_{ik}^*(S,Q)d\Gamma - \int_{\Gamma-\bar{\Gamma}} T_{ik}^*(S,Q)u_k(Q)d\Gamma$$
$$- \int_{\Gamma_\omega} T_{ik}^*(S,Q)u_k(Q)d\Gamma + \int_{\Omega} \delta_{jk}p(q)\varepsilon_{ijk}^*(S,q)d\Omega + \int_{\Omega_\omega} \delta_{jk}p(q)\varepsilon_{ijk}^*(S,q)d\Omega \qquad (3.77)$$
$$+ \int_{\Omega} b_k(q)u_{ik}^*(S,q)d\Omega + \int_{\Omega_\omega} b_k(q)u_{ik}^*(S,q)d\Omega$$

To characterize S as a boundary point, we evaluate the equation (3.77) considering the limit as ω tends to zero. Applying the limit, the integral containing the fundamental solution u_{ik}^* over $\Gamma - \bar{\Gamma}$ is regular, however, the one that contains T_{ik}^* should be evaluated in a Cauchy principal value sense. The integrals over Ω_ω and Γ_ω vanishe to zero, except the one that contains the displacements on the infinitesimal boundary, which has a singularity of $1/r$ and should be evaluated in the sense of Cauchy principal value. Thus, the Somigliana equation adapted to the boundary points results in

$$C_{ik}u_k(S) = \int_{\Gamma} T_k(Q)u_{ik}^*(S,Q)d\Gamma - \int_{\Gamma} T_{ik}^*(S,Q)u_k(Q)d\Gamma + \int_{\Omega} b\delta_{jk}p(q)\varepsilon_{ijk}^*(S,q)d\Omega$$
$$+ \int_{\Omega} \sigma_{kj}^d(q)\varepsilon_{ijk}^*(S,q)d\Omega + \int_{\Omega} b_k(q)u_{ik}^*(S,q)d\Omega \qquad (3.78)$$

The evaluation of the free-term C_{ik} depends on the geometry of the boundary where the source point is located. Consider the possibilities of a soft boundary, defined by with a unique tangent through the point, and angular boundary (see Figure 3.6). The values are defined as:

$$C_{ik} = \frac{1}{2}\delta_{ik} \text{ (soft)} \qquad (3.79)$$

$$C_{ik} = \begin{bmatrix} \frac{\alpha}{2\pi} + \frac{\cos(2\gamma)\operatorname{sen}(\alpha)}{4\pi(1-\upsilon)} & \frac{\operatorname{sen}(2\gamma)\operatorname{sen}(\alpha)}{4\pi(1-\upsilon)} \\ \frac{\operatorname{sen}(2\gamma)\operatorname{sen}(\alpha)}{4\pi(1-\upsilon)} & \frac{\alpha}{2\pi} - \frac{\cos(2\gamma)\operatorname{sen}(\alpha)}{4\pi(1-\upsilon)} \end{bmatrix} \text{ (angular)} \qquad (3.80)$$

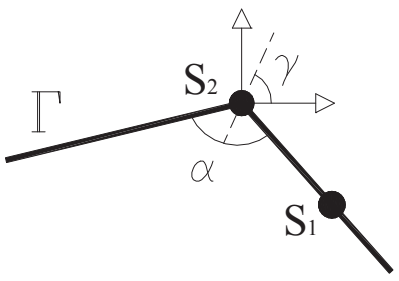

Figure 3.6 – Points S_1 and S_2 in soft and angular boundary, respectively,

Analysis at Internal points. Based on the calculated values on the boundary, the displacements and stresses at internal points can be evaluated. Equation (3.76) provides the displacement values at any given point in the domain. Substituting this integral definition of dislocations in Hooke's law, the stress equation is obtained:

$$\begin{aligned}\sigma_{ij}(s) = &-\int_{\Gamma} S_{ijk}(s,Q)u_k(Q)d\Gamma + \int_{\Gamma} D_{ijk}(s,Q)T_k(Q)d\Gamma + \int_{\Omega} D_{ijk}(s,q)b_k(q)d\Omega \\ &+\int_{\Omega} R_{ijkl}(s,q)\sigma^d_{kl}(q)d\Omega + TL_{ij}\left[\sigma^d_{kl}(s)\right] + \int_{\Omega} b\delta_{kl}R_{ijkl}(s,q)p(q)d\Omega + TL_{ij}\left[b\delta_{kl}p(s)\right]\end{aligned} \tag{3.81}$$

in which the tensors S_{ijk}, D_{ijk} and R_{ijkl} are:

$$\begin{aligned}S_{ijk} = &\frac{G}{2\pi(1-\upsilon)r^2}\left\{2\frac{\partial r}{\partial n}\left[(1-2\upsilon)\delta_{ij}r_{,k} + \upsilon(\delta_{jk}r_{,i} + \delta_{ik}r_{,j}) - 4r_{,i}r_{,j}r_{,k}\right]\right. \\ &\left.+2\upsilon\left(\eta_i r_{,j}r_{,k} + \eta_j r_{,i}r_{,k}\right) + (1-2\upsilon)\left(2\eta_k r_{,i}r_{,j} + \eta_i\delta_{jk} + \eta_j\delta_{ik}\right) - (1-4\upsilon)\eta_k\delta_{ij}\right\}\end{aligned} \tag{3.82}$$

$$D_{ijk} = \frac{1}{4\pi(1-\upsilon)r}\left[(1-2\upsilon)(\delta_{ik}r_{,j} + \delta_{jk}r_{,i} - \delta_{ij}r_{,k}) + 2r_{,i}r_{,j}r_{,k}\right] \tag{3.83}$$

$$\begin{aligned}R_{ijkl} = &\frac{1}{4\pi(1-\upsilon)r^2}\left[(1-2\upsilon)(\delta_{il}\delta_{jk} + \delta_{jl}\delta_{ik} - \delta_{ij}\delta_{kl} + 2\delta_{ij}r_{,k}r_{,l})\right. \\ &\left.+2\upsilon(\delta_{ik}r_{,j}r_{,l} + \delta_{jl}r_{,i}r_{,k} + \delta_{il}r_{,j}r_{,k} + \delta_{jk}r_{,i}r_{,l}) + 2\delta_{kl}r_{,i}r_{,j} - 8r_{,i}r_{,j}r_{,k}r_{,l}\right]\end{aligned} \tag{3.84}$$

and the free terms are written as:

$$TL_{ij}\left[b\delta_{kl}p(s)\right] = -\frac{1}{8(1-\upsilon)}\left\{2\left[\delta_{ij}p(s)\right] + \delta_{ij}(1-4\upsilon)\left[2p(s)\right]\right\} \tag{3.85}$$

$$TL_{ij}\left[\sigma^d_{kl}(s)\right] = -\frac{1}{8(1-\upsilon)}\left\{2\sigma^d_{ij}(s) + \delta_{ij}(1-4\upsilon)\sigma^d_{mm}(s)\right\} \tag{3.86}$$

3.5.2. Integral Formulation for the Fluid Phase

Fundamental Solutions. The equation that defines the problem of fluid conduction, written in the fundamental state, is as follows:

$$p^*_{,ii} = \frac{1}{k}\delta(s,q) \tag{3.87}$$

with k as the permeability coefficient, already defined in the previous chapter. The solution of equation (3.87) is given by:

$$p^*(s,q) = \frac{1}{2\pi k}\ln(r) \tag{3.88}$$

In which r represents the distance between the points s and q. With the pore-pressure fundamental solution, we can write the corresponding solution to the flux:

$$v_i^*(s,q) = \frac{-r_{,i}}{2\pi r} \tag{3.89}$$

Boundary Integral Equation. Similarly to what was presented in 3.5.1, we deduce the integral equation of the pore-pressures from the Betti's reciprocal theorem. The governing equation used is Darcy's law,

$$v_k = k\left(-p_{,k} + f_k\right) \tag{3.90}$$

which relates the relative flow with the pore-pressure gradient. It can be seen in the equation above that v_k and $p_{,k}$ have a linear but not proportional relationship, due to the presence of the part kf_k. Then the proportional flow is defined v_k^{pr}:

$$v_k^{pr} = v_k - kf_k = -kp_{,k} \tag{3.91}$$

It should be noted that the use of this proportional flow is associated to considering a homogeneous transport law, with the constant permeability coefficient k, for the sake of simplicity.

The reciprocity law is written as:

$$\int_\Omega v_k^{pr}(q)p_{,k}^*(s,q)d\Omega = \int_\Omega v_k^*(s,q)p_{,k}(q)d\Omega \tag{3.92}$$

replacing the definition of the proportional flow, we have

$$\int_\Omega \left[v_k - kf_k\right]p_{,k}^*(s,q)d\Omega = \int_\Omega v_k^*(s,q)p_{,k}(q)d\Omega \tag{3.93}$$

in which proceeding the integration by parts, the following expression is reached:

$$\begin{aligned}&\int_\Gamma p^*(s,Q)v_k(Q)\eta_k d\Gamma - \int_\Gamma v_k^*(s,Q)p(Q)\eta_k d\Gamma - \int_\Omega p^*(s,q)v_{k,k}(q)d\Omega \\ &+\int_\Gamma v_{k,k}^*(s,q)p(q)d\Gamma - \int_\Omega p_{,k}^*(s,q)kf_k(q)d\Omega = 0\end{aligned} \tag{3.94}$$

Considering the identity $v^*_{k,k} = -\delta(s,q)$, and Dirac's delta property given in (3.56), the integral equation of the pore-pressures is reached:

$$\begin{aligned} c(s)p(s) &= -\int_\Gamma V^*(s,Q)p(Q)d\Gamma + \int_\Gamma p^*(s,Q)V(Q)d\Gamma \\ &-\int_\Omega p^*(s,q)v_{k,k}(q)d\Omega - \int_\Omega p^*_{,k}(s,q)kf_k(q)d\Omega \end{aligned} \tag{3.95}$$

The continuity equation (3.19), is considered here in its simplified version, ignoring the fluid bulk modulus, in other words:

$$v_{k,k} = -\dot{\phi} \tag{3.96}$$

Rewriting the integral containing $v_{k,k}$, results in:

$$\begin{aligned} c(s)p(s) &= -\int_\Gamma V^*(s,Q)p(Q)d\Gamma + \int_\Gamma p^*(s,Q)V(Q)d\Gamma \\ &+\int_\Omega p^*(s,q)\dot{\phi}(q)d\Omega - \int_\Omega kf_k(q)p^*_{,k}(s,q)d\Omega \end{aligned} \tag{3.97}$$

The term $c(s)$ depends on the position of the source point s.

For sake of convenience, the problem is formulated in terms of the variables ε_{kj} and p, for the solid and fluid, respectively. Then, using equation (3.4), we can write:

$$(\phi - \phi_0) = \frac{(p - p_0)}{M} + b\,\mathrm{Tr}(\varepsilon_{kj}) \tag{3.98}$$

Taking the porosity derivative with respect to time,

$$\dot{\phi} = \frac{1}{M}\dot{p} + b\,\mathrm{Tr}(\dot{\varepsilon}_{kj}) \tag{3.99}$$

equation (3.97) results as follows:

$$\begin{aligned} c(s)p(s) &= -\int_\Gamma V^*(s,Q)p(Q)d\Gamma + \int_\Gamma p^*(s,Q)V(Q)d\Gamma \\ &+\int_\Omega p^*(s,q)\left[\frac{1}{M}\dot{p}(q) + b\,\mathrm{Tr}(\dot{\boldsymbol{\varepsilon}}(q))\right]d\Omega - \int_\Omega kf_k(q)p^*_{,k}(s,q)d\Omega \end{aligned} \tag{3.100}$$

3.5.3. Time-dependent Integral Formulation

The system that defines the pore-damage problem is formed by equations (3.78), (3.81) and (3.100). From this point on, the volume forces acting on the solid matrix and on the fluid are

disregarded. Considering the transient nature of the problem, which is governed by the evolution of different variables over time, it is necessary to write the equations in rates, then we have:

$$\begin{aligned} C_{ik}\dot{u}_k(S) &= \int_\Gamma \dot{T}_k(Q)u^*_{ik}(S,Q)d\Gamma - \int_\Gamma T^*_{ik}(S,Q)\dot{u}_k(Q)d\Gamma + \int_\Omega b\delta_{jk}\dot{p}(q)\varepsilon^*_{ijk}(S,q)d\Omega \\ &+ \int_\Omega \dot{\sigma}^d_{jk}(q)\varepsilon^*_{ijk}(S,q)d\Omega \end{aligned} \tag{3.101}$$

$$\begin{aligned} \dot{\sigma}_{ij}(s) &= -\int_\Gamma S_{ijk}(s,Q)\dot{u}_k(Q)d\Gamma + \int_\Gamma D_{ijk}(s,Q)\dot{T}_k(Q)d\Gamma + \int_\Omega R_{ijkl}(s,q)\dot{\sigma}^d_{kl}(q)d\Omega \\ &+ TL_{ij}\left[\dot{\sigma}^d_{kl}(s)\right] + \int_\Omega b\delta_{kl}R_{ijkl}(s,q)\dot{p}(q)d\Omega + TL_{ij}\left[b\delta_{kl}\dot{p}(s)\right] \end{aligned} \tag{3.102}$$

$$\begin{aligned} c(s)p(s) &= -\int_\Gamma \mathcal{V}^*(s,Q)p(Q)d\Gamma + \int_\Gamma p^*(s,Q)\mathcal{V}(Q)d\Gamma \\ &+ \int_\Omega \frac{1}{M}p^*(s,q)\dot{p}(q)d\Omega + \int_\Omega bp^*(s,q)Tr\left(\dot{\boldsymbol{\varepsilon}}(q)\right)d\Omega \end{aligned} \tag{3.103}$$

Let us admit two time instants, t_1 and t_2, separated by a time step $\Delta t = t_2 - t_1$. The integration of the equations throughout this interval is written as:

$$\begin{aligned} C_{ik}\int_{t_1}^{t_2}\dot{u}_k(S)dt &= \int_{t_1}^{t_2}\int_\Gamma \dot{T}_k(Q)u^*_{ik}(S,Q)d\Gamma dt - \int_{t_1}^{t_2}\int_\Gamma T^*_{ik}(S,Q)\dot{u}_k(Q)d\Gamma dt \\ &+ \int_{t_1}^{t_2}\int_\Omega b\delta_{jk}\dot{p}(q)\varepsilon^*_{ijk}(S,q)d\Omega dt + \int_{t_1}^{t_2}\int_\Omega \dot{\sigma}^d_{jk}(q)\varepsilon^*_{ijk}(S,q)d\Omega dt \end{aligned} \tag{3.104}$$

$$\begin{aligned} \int_{t_1}^{t_2}\dot{\sigma}_{ij}(s)dt &= -\int_{t_1}^{t_2}\int_\Gamma S_{ijk}(s,Q)\dot{u}_k(Q)d\Gamma dt + \int_{t_1}^{t_2}\int_\Gamma D_{ijk}(s,Q)\dot{T}_k(Q)d\Gamma dt \\ &+ \int_{t_1}^{t_2}\int_\Omega R_{ijkl}(s,q)\dot{\sigma}^d_{kl}(q)d\Omega dt + \int_{t_1}^{t_2} TL_{ij}\left[\dot{\sigma}^d_{kl}(s)\right]dt \\ &+ \int_{t_1}^{t_2}\int_\Omega b\delta_{kl}R_{ijkl}(s,q)\dot{p}(q)d\Omega dt + \int_{t_1}^{t_2} TL_{ij}\left[b\delta_{kl}\dot{p}(s)\right]dt \end{aligned} \tag{3.105}$$

$$\begin{aligned} c(s)\int_{t_1}^{t_2}p(s)dt &= -\int_{t_1}^{t_2}\int_\Gamma \mathcal{V}^*(s,Q)p(Q)d\Gamma dt + \int_{t_1}^{t_2}\int_\Gamma p^*(s,Q)\mathcal{V}(Q)d\Gamma dt \\ &+ \int_{t_1}^{t_2}\int_\Omega \frac{1}{M}p^*(s,q)\dot{p}(q)d\Omega dt + \int_{t_1}^{t_2}\int_\Omega bp^*(s,q)Tr\left(\dot{\boldsymbol{\varepsilon}}(q)\right)d\Omega dt \end{aligned} \tag{3.106}$$

With a generic finite interval given by $\Delta t_n = t_{n+1} - t_n$, the evolution of any given variable associated with Δt_n, in finite step, is expressed as $\Delta(\bullet) = \bullet_{n+1} - \bullet_n$ Thus, the system (3.104) - (3.106) results as follows.

$$C_{ik}\Delta u_k(S) = \int_\Gamma \Delta T_k(Q) u^*_{ik}(S,Q)d\Gamma - \int_\Gamma T^*_{ik}(S,Q)\Delta u_k(Q)d\Gamma + \int_\Omega b\delta_{jk}\Delta p(q)\varepsilon^*_{ijk}(S,q)d\Omega + \int_\Omega \Delta\sigma^d_{jk}(q)\varepsilon^*_{ijk}(S,q)d\Omega \tag{3.107}$$

$$\Delta\sigma_{ij}(s) = -\int_\Gamma S_{ijk}(s,Q)\Delta u_k(Q)d\Gamma + \int_\Gamma D_{ijk}(s,Q)\Delta T_k(Q)d\Gamma + \int_\Omega R_{ijkl}(s,q)\Delta\sigma^d_{kl}(q)d\Omega + TL_{ij}\left[\Delta\sigma^d_{kl}(s)\right] + \int_\Omega b\delta_{kl}R_{ijkl}(s,q)\Delta p(q)d\Omega + TL_{ij}\left[b\delta_{kl}\Delta p(s)\right] \tag{3.108}$$

$$c(s)p(s) = -\int_\Gamma V^*(s,Q)p(Q)d\Gamma + \int_\Gamma p^*(s,Q)V(Q)d\Gamma + \frac{1}{\Delta t}\int_\Omega \frac{1}{M}p^*(s,q)\Delta p(q)d\Omega + \frac{1}{\Delta t}\int_\Omega b p^*(s,q)Tr\left(\Delta\boldsymbol{\varepsilon}(q)\right)d\Omega \tag{3.109}$$

This system of equations results nonlinear, due to the presence of the damage correction term, which is calculated at each increment.

3.5.4. Algebraic System

For purposes of using the Boundary Element Method, the system presented above must be discretized, in order to obtain the approximate values of the variables in question at the boundary points and inside the domain.

Based on the concepts presented in the previous section, concerning the Boundary Element Method, system (3.107) - (3.109) is written in a discrete way, on the boundary elements and the domain cells, as follows:

$$C_{ik}\Delta u_k(S) = \sum_{e=1}^{N_e}\int_{\Gamma_e} u^*_{ik}(S,Q)\varphi_n(Q)\Delta T^n_k d\Gamma_e - \sum_{e=1}^{N_e}\int_{\Gamma_e} T^*_{ik}(S,Q)\varphi_n(Q)\Delta u^n_k d\Gamma_e + \sum_{c=1}^{N_c}\int_{\Omega_c}\varepsilon^*_{ijk}(S,q)\varphi_n(q)b\delta_{jk}\Delta p^n d\Omega_c + \sum_{c=1}^{N_c}\int_{\Omega_c}\varepsilon^*_{ijk}(S,q)\varphi_n(q)\Delta\sigma^{d\ n}_{jk}d\Omega_c \tag{3.110}$$

$$\Delta\sigma_{ij}(s) = -\sum_{e=1}^{N_e}\int_{\Gamma_e} S_{ijk}(s,Q)\varphi_n(Q)\Delta u_k^n d\Gamma_e + \sum_{e=1}^{N_e}\int_{\Gamma_e} D_{ijk}(s,Q)\varphi_n(Q)\Delta T_k^n d\Gamma_e$$
$$+\sum_{c=1}^{N_c}\int_{\Omega_c} R_{ijkl}(s,q)\varphi_n(q)\Delta\sigma_{kl}^{d\,n} d\Omega_c + TL_{ij}\left[\Delta\sigma_{kl}^{d\,s}\right] \qquad (3.111)$$
$$+\sum_{c=1}^{N_c}\int_{\Omega_c} b\delta_{kl}R_{ijkl}(s,q)\varphi_n(q)\Delta p^n d\Omega_c + TL_{ij}\left[b\delta_{kl}\Delta p^s\right]$$

$$c(s)p(s) = -\sum_{e=1}^{N_e}\int_{\Gamma_e} \mathbf{V}^*(s,Q)\varphi_n(Q)p^n d\Gamma_e + \sum_{e=1}^{N_e}\int_{\Gamma_e} p^*(s,Q)\varphi_n(Q)\mathbf{V}^n d\Gamma_e$$
$$+\frac{1}{\Delta t}\sum_{c=1}^{N_c}\int_{\Omega_c}\frac{1}{M}p^*(s,q)\varphi_n(q)\Delta p^n d\Omega_c + \frac{1}{\Delta t}\sum_{c=1}^{N_c}\int_{\Omega_c} bp^*(s,q)\varphi_n(q)\mathrm{Tr}\left(\Delta\boldsymbol{\varepsilon}^n\right)d\Omega_c \qquad (3.112)$$

The indices e and c are associated with the boundary elements and internal cells, respectively, so that N_e and N_c represent the number of elements and cells. The interpolations are made by the functions φ_n, for the node n of the element or cell.

To follow, the algebraic representation of the aforementioned equations is presented. Let N_n be the number of boundary nodes and N_i the number of internal nodes. The dimensions of the matrices and vectors used are indicated. Considering the two degrees of freedom in displacements for the two-dimensional problem, we write $2N_n$ algebraic equations based on (3.110), that is:

$$\underset{2N_n,2N_n}{[H]}\ \underset{2N_n,1}{\{\Delta u\}} = \underset{2N_n,2N_n}{[G]}\ \underset{2N_n,1}{\{\Delta T\}} + \underset{2N_n,3N_i}{[Q]}\ \underset{3N_i,1}{\left\{\Delta\sigma^d\right\}} + b\ \underset{2N_n,3N_i}{[Q]}\ \underset{3N_i,N_i}{[IK]}\underset{N_i,1}{\left\{\Delta p_{(i)}\right\}} \qquad (3.113)$$

Matrix $[IK]$ corresponds to the Kronnecker delta.

The stress equations (3.111) give rise to $3N_i$ algebraic equations, as follows:

$$\underset{3N_i,1}{\left\{\Delta\sigma\right\}} = -\underset{3N_i,2N_n}{[HL]}\underset{2N_n,1}{\{\Delta u\}} + \underset{3N_i,2N_n}{[GL]}\underset{2N_n,1}{\{\Delta T\}} + \underset{3N_i,3N_i}{[QL]}\underset{3N_i,1}{\left\{\Delta\sigma^d\right\}} + b\underset{3N_i,3N_i}{[QL]}\underset{3N_i,N_i}{[IK]}\underset{N_i,1}{\left\{\Delta p_{(i)}\right\}} \qquad (3.114)$$

Additionally, $2N_i$ equations of displacements in the internal points are written as:

$$\underset{2N_i,1}{\left\{\Delta u_{(i)}\right\}} = -\underset{2N_i,2N_n}{\left[H_{(i)}\right]}\underset{2N_n,1}{\{\Delta u\}} + \underset{2N_i,2N_n}{\left[G_{(i)}\right]}\underset{2N_n,1}{\{\Delta T\}} + \underset{2N_i,3N_i}{\left[Q_{(i)}\right]}\underset{3N_i,1}{\left\{\Delta\sigma^d\right\}} + b\underset{2N_i,3N_i}{\left[Q_{(i)}\right]}\underset{3N_i,N_i}{[IK]}\underset{N_i,1}{\left\{\Delta p_{(i)}\right\}} \qquad (3.115)$$

With the inclusion of boundary conditions referring to $\{\Delta u\}$ and $\{\Delta T\}$, it is convenient to rearrange the matrix of the three equations, so that the unknown and prescribed values are isolated. Rearranging the matrices columns, the equations can be rewritten as:

$$\underset{2N_n,2N_n}{[A]}\ \underset{2N_n,1}{\{\Delta xu\}} = \underset{2N_n,1}{\{\Delta yu\}} + \underset{2N_n,3N_i}{[Q]}\ \underset{3N_i,1}{\{\Delta\sigma^d\}} + b\ \underset{2N_n,3N_i}{[Q]}\ \underset{3N_i,N_i}{[IK]}\ \underset{N_i,1}{\{\Delta p_{(i)}\}} \tag{3.116}$$

$$\underset{3N_i,1}{\{\Delta\sigma\}} = -\underset{3N_i,2N_n}{[AL]}\ \underset{2N_n,1}{\{\Delta xu\}} + \underset{3N_i,1}{\{\Delta ys\}} + \underset{3N_i,3N_i}{[QL]}\ \underset{3N_i,1}{\{\Delta\sigma^d\}} + b\ \underset{3N_i,3N_i}{[QL]}\ \underset{3N_i,N_i}{[IK]}\ \underset{N_i,1}{\{\Delta p_{(i)}\}} \tag{3.117}$$

$$\underset{2N_i,1}{\{\Delta u_{(i)}\}} = -\underset{2N_i,2N_n}{[A_{(i)}]}\ \underset{2N_n,1}{\{\Delta xu\}} + \underset{2N_i,1}{\{\Delta yu_{(i)}\}} + \underset{2N_i,3N_i}{[Q_{(i)}]}\ \underset{3N_i,1}{\{\Delta\sigma^d\}} + b\ \underset{2N_i,3N_i}{[Q_{(i)}]}\ \underset{3N_i,N_i}{[IK]}\ \underset{N_i,1}{\{\Delta p_{(i)}\}} \tag{3.118}$$

In which $\{\Delta xu\}$ is the vector of unknown boundary values and $\{\Delta yu\}$ and $\{\Delta ys\}$ group the prescribed boundary values in the equations of displacements and stresses, respectively. Isolating $\{\Delta xu\}$ in equation (3.116), we have:

$$\underset{2N_n,1}{\{\Delta xu\}} = \underset{2N_n,2N_n}{[A]^{-1}}\ \underset{2N_n,1}{\{\Delta yu\}} + \underset{2N_n,2N_n}{[A]^{-1}}\ \underset{2N_n,3N_i}{[Q]}\ \underset{3N_i,1}{\{\Delta\sigma^d\}} + b\ \underset{2N_n,2N_n}{[A]^{-1}}\ \underset{2N_n,3N_i}{[Q]}\ \underset{3N_i,N_i}{[IK]}\ \underset{N_i,1}{\{\Delta p_{(i)}\}} \tag{3.119}$$

which can be replaced in the other two equations, resulting in:

$$\begin{aligned}\underset{3N_i,1}{\{\Delta\sigma\}} = &-\underset{3N_i,2N_n}{[AL]}\ \underset{2N_n,2N_n}{[A]^{-1}}\ \underset{2N_n,1}{\{\Delta yu\}} + \underset{3N_i,1}{\{\Delta ys\}} - \left[\underset{3N_i,2N_n}{[AL]}\ \underset{2N_n,2N_n}{[A]^{-1}}\ \underset{2N_n,3N_i}{[Q]} - \underset{3N_i,3N_i}{[QL]}\right]\underset{3N_i,1}{\{\Delta\sigma^d\}} \\ &-b\left[\underset{3N_i,2N_n}{[AL]}\ \underset{2N_n,2N_n}{[A]^{-1}}\ \underset{2N_n,3N_i}{[Q]} - \underset{3N_i,3N_i}{[QL]}\right]\underset{3N_i,N_i}{[IK]}\ \underset{N_i,1}{\{\Delta p_{(i)}\}}\end{aligned} \tag{3.120}$$

$$\begin{aligned}\underset{2N_i,1}{\{\Delta u_{(i)}\}} = &-\underset{2N_i,2N_n}{[A_{(i)}]}\ \underset{2N_n,2N_n}{[A]^{-1}}\ \underset{2N_n,1}{\{\Delta yu\}} + \underset{2N_i,1}{\{\Delta yu_{(i)}\}} - \left[\underset{2N_i,2N_n}{[A_{(i)}]}\ \underset{2N_n,2N_n}{[A]^{-1}}\ \underset{2N_n,3N_i}{[Q]} - \underset{2N_i,3N_i}{[Q_{(i)}]}\right]\underset{3N_i,1}{\{\Delta\sigma^d\}} \\ &-b\left[\underset{2N_i,2N_n}{[A_{(i)}]}\ \underset{2N_n,2N_n}{[A]^{-1}}\ \underset{2N_n,3N_i}{[Q]} - \underset{2N_i,3N_i}{[Q_{(i)}]}\right]\underset{3N_i,N_i}{[IK]}\ \underset{N_i,1}{\{\Delta p_{(i)}\}}\end{aligned} \tag{3.121}$$

Simplifying equation (3.120), we obtain:

$$\underset{3N_i,1}{\{\Delta\sigma\}} = \underset{3N_i,1}{\{\Delta Ns\}} + \underset{3N_i,3N_i}{[QS]}\ \underset{3N_i,1}{\{\Delta\sigma^d\}} + b\ \underset{3N_i,3N_i}{[QS]}\ \underset{3N_i,N_i}{[IK]}\ \underset{N_i,1}{\{\Delta p_{(i)}\}} \tag{3.122}$$

whose terms are:

$$\begin{aligned}\underset{3N_i,1}{\{\Delta Ns\}} &= -\underset{3N_i,2N_n}{[AL]}\,\underset{2N_n,2N_n}{[A]^{-1}}\,\underset{2N_n,1}{\{\Delta yu\}}+\underset{3N_i,1}{\{\Delta ys\}}\\ \underset{3N_i,3N_i}{[Qs]} &= -\underset{3N_i,2N_n}{[AL]}\,\underset{2N_n,2N_n}{[A]^{-1}}\,\underset{2N_n,3N_i}{[Q]}+\underset{3N_i,3N_i}{[QL]}\end{aligned} \tag{3.123}$$

The equation of the pore-pressures (3.112) written for the boundary points leads to N_n algebraic equations, as follows:

$$\underset{N_n,N_n}{[HP]}\,\underset{N_n,1}{\{p\}} = \underset{N_n,N_n}{[GP]}\,\underset{N_n,1}{\{V\}}+\frac{1}{M\Delta t}\underset{N_n,N_i}{[QP]}\,\underset{N_i,1}{\{\Delta p_{(i)}\}}+\frac{b}{\Delta t}\underset{N_n,N_i}{[QP]}\,\underset{N_i,3N_i}{[Tr]}\,\underset{3N_i,1}{\{\Delta\varepsilon\}} \tag{3.124}$$

and for internal points,

$$\underset{N_i,1}{\{p_{(i)}\}} = -\underset{N_i,N_n}{\left[HP_{(i)}\right]}\,\underset{N_n,1}{\{p\}}+\underset{N_i,N_n}{\left[GP_{(i)}\right]}\,\underset{N_n,1}{\{V\}}+\frac{1}{M\Delta t}\underset{N_i,N_i}{\left[QP_{(i)}\right]}\,\underset{N_i,1}{\{\Delta p_{(i)}\}}+\frac{b}{\Delta t}\underset{N_i,N_i}{\left[QP_{(i)}\right]}\,\underset{N_i,3N_i}{[Tr]}\,\underset{3N_i,1}{\{\Delta\varepsilon\}} \tag{3.125}$$

matrix $[Tr]$ plays as the operator trace of a tensor.

Rearranging the columns of $[HP]$ and $[GP]$ in (3.124) and of $\left[HP_{(i)}\right]$ and $\left[GP_{(i)}\right]$ in (3.125), leads to:

$$\underset{N_n,N_n}{[AP]}\,\underset{N_n,1}{\{xp\}} = \underset{N_n,1}{\{yp\}}+\frac{1}{M\Delta t}\underset{N_n,N_i}{[QP]}\,\underset{N_i,1}{\{\Delta p_{(i)}\}}+\frac{b}{\Delta t}\underset{N_n,N_i}{[QP]}\,\underset{N_i,3N_i}{[Tr]}\,\underset{3N_i,1}{\{\Delta\varepsilon\}} \tag{3.126}$$

$$\underset{N_i,1}{\{p_{(i)}\}} = -\underset{N_i,N_n}{\left[AP_{(i)}\right]}\,\underset{N_n,1}{\{xp\}}+\underset{N_i,1}{\{yp_{(i)}\}}+\frac{1}{M\Delta t}\underset{N_i,N_i}{\left[QP_{(i)}\right]}\,\underset{N_i,1}{\{\Delta p_{(i)}\}}+\frac{b}{\Delta t}\underset{N_i,N_i}{\left[QP_{(i)}\right]}\,\underset{N_i,3N_i}{[Tr]}\,\underset{3N_i,1}{\{\Delta\varepsilon\}} \tag{3.127}$$

The vector $[xp]$ can then be written as

$$\underset{N_n,1}{\{xp\}} = \underset{N_n,N_n}{[AP]^{-1}}\,\underset{N_n,1}{\{yp\}}+\frac{1}{M\Delta t}\underset{N_n,N_n}{[AP]^{-1}}\,\underset{N_n,N_i}{[QP]}\,\underset{N_i,1}{\{\Delta p_{(i)}\}}+\frac{b}{\Delta t}\underset{N_n,N_n}{[AP]^{-1}}\,\underset{N_n,N_i}{[QP]}\,\underset{N_i,3N_i}{[Tr]}\,\underset{3N_i,1}{\{\Delta\varepsilon\}} \tag{3.128}$$

being replaced in the pore-pressure equation at the internal points (3.127):

$$\begin{aligned}\underset{N_i,1}{\{p_{(i)}\}} &= -\underset{N_i,N_n}{\left[AP_{(i)}\right]}\underset{N_n,N_n}{[AP]^{-1}}\,\underset{N_n,1}{\{yp\}}+\frac{1}{M\Delta t}\left[-\underset{N_i,N_n}{\left[AP_{(i)}\right]}\underset{N_n,N_n}{[AP]^{-1}}\,\underset{N_n,N_i}{[QP]}+\underset{N_i,N_i}{\left[QP_{(i)}\right]}\right]\underset{N_i,1}{\{\Delta p_{(i)}\}}\\ &+\frac{b}{\Delta t}\left[-\underset{N_i,N_n}{\left[AP_{(i)}\right]}\underset{N_n,N_n}{[AP]^{-1}}\,\underset{N_n,N_i}{[QP]}+\underset{N_i,N_i}{\left[QP_{(i)}\right]}\right]\underset{N_i,3N_i}{[Tr]}\,\underset{3N_i,1}{\{\Delta\varepsilon\}}+\underset{N_i,1}{\{yp_{(i)}\}}\end{aligned} \tag{3.129}$$

The condensation of the terms in equation (3.129) allows writing:

$$\begin{aligned}\underset{N_i,1}{\{p_{(i)}\}} &= \underset{N_i,1}{\{Np\}} + \frac{1}{M\Delta t}\underset{N_i,N_i}{\left[\overline{QP}_{(i)}\right]}\underset{N_i,1}{\{\Delta p_{(i)}\}} \\ &+ \frac{b}{\Delta t}\underset{N_i,N_i}{\left[\overline{QP}_{(i)}\right]}\underset{N_i,3N_i}{[Tr]}\underset{3N_i,1}{\{\Delta\varepsilon\}}\end{aligned} \tag{3.130}$$

with:

$$\begin{aligned}\underset{N_i,1}{\{Np\}} &= -\underset{N_i,N_n}{\left[AP_{(i)}\right]}\underset{N_n,N_n}{[AP]^{-1}}\underset{N_n,1}{\{yp\}} + \underset{N_i,1}{\{yp_{(i)}\}} \\ \underset{N_i,N_i}{\left\{\overline{QP}_{(i)}\right\}} &= -\underset{N_i,N_n}{\left[AP_{(i)}\right]}\underset{N_n,N_n}{[AP]^{-1}}\underset{N_n,N_i}{[QP]} + \underset{N_i,N_i}{\left[QP_{(i)}\right]}\end{aligned} \tag{3.131}$$

Thus, the poro-damage problem is defined by equations (3.122) and (3.130). Based on these, it is appropriate to explain the unknowns $\Delta\varepsilon$ and $\Delta p_{(i)}$, in order to condense the system into a single equation, which will done to follow.

The stress tensor of the problem, written algebraically in rates, is given by

$$\underset{3N_i,1}{\{\Delta\sigma\}} = \underset{3N_i,3N_i}{[E]}\underset{3N_i,1}{\{\Delta\varepsilon\}} - \underset{3N_i,3N_i}{[D]}\underset{3N_i,3N_i}{[E]}\underset{3N_i,1}{[\Delta\varepsilon]} - b\underset{3N_i,N_i}{[IK]}\underset{N_i,1}{\{\Delta p_{(i)}\}} \tag{3.132}$$

which is modified by defining the stress associated with damage:

$$\underset{3N_i,1}{\{\Delta\sigma\}} = \underset{3N_i,3N_i}{[E]}\underset{3N_i,1}{\{\Delta\varepsilon\}} - \underset{3N_i,1}{\{\Delta\sigma^d\}} - b\underset{3N_i,N_i}{[IK]}\underset{N_i,1}{\{\Delta p_{(i)}\}} \tag{3.133}$$

Replacing this in (3.122) leads to

$$\underset{3N_i,3N_i}{[E]}\underset{3N_i,1}{\{\Delta\varepsilon\}} = \underset{3N_i,1}{\{\Delta Ns\}} + \left[\underset{3N_i,3N_i}{[QS]} + \underset{3N_i,3N_i}{[I]}\right]\underset{3N_i,1}{\{\Delta\sigma^d\}} + b\left[\underset{3N_i,3N_i}{[QS]} + \underset{3N_i,3N_i}{[I]}\right]\underset{3N_i,N_i}{[IK]}\underset{N_i,1}{\{\Delta p_{(i)}\}} \tag{3.134}$$

the simplification $\underset{3N_i,3N_i}{\left[\overline{QS}\right]} = \left[\underset{3N_i,3N_i}{[QS]} + \underset{3N_i,3N_i}{[I]}\right]$ is introduced.

Using the time discretization, the equation of the fluid (3.130) takes the following form.

$$\{p_{(i)}\}_n = \{Np\}_n + \frac{1}{M\Delta t_n}\left[\overline{QP}_{(i)}\right]\{\Delta p_{(i)}\}_n + \frac{b}{\Delta t_n}\left[\overline{QP}_{(i)}\right][Tr]\{\Delta\varepsilon\}_n \tag{3.135}$$

The pore-pressure value in the previous step $\{p_{(i)}\}_{n-1}$ can be subtracted, on both sides of the equation:

$$\begin{aligned}&\left\{\mathrm{p}_{(\mathrm{i})}\right\}_{\mathrm{n}}-\left\{\mathrm{p}_{(\mathrm{i})}\right\}_{\mathrm{n}-1}=\left\{\mathrm{Np}\right\}_{\mathrm{n}}-\left\{\mathrm{p}_{(\mathrm{i})}\right\}_{\mathrm{n}-1}\\&+\frac{1}{M\Delta\mathrm{t}_{\mathrm{n}}}\left[\overline{\mathrm{QP}}_{(\mathrm{i})}\right]\left\{\Delta\mathrm{p}_{(\mathrm{i})}\right\}_{\mathrm{n}}+\frac{b}{\Delta\mathrm{t}_{\mathrm{n}}}\left[\overline{\mathrm{QP}}_{(\mathrm{i})}\right]\left[\mathrm{Tr}\right]\left\{\Delta\varepsilon\right\}_{\mathrm{n}}\end{aligned}\tag{3.136}$$

which allows to express the unknown of interest $\Delta\mathrm{p}_{(\mathrm{i})}$, as shown below:

$$\underset{\mathrm{N_i},1}{\left\{\Delta\mathrm{p}_{(\mathrm{i})}\right\}}=\underset{\mathrm{N_i},1}{\left\{\overline{\mathrm{Np}}\right\}}+\frac{1}{M\Delta\mathrm{t}}\underset{\mathrm{N_i},\mathrm{N_i}}{\left[\overline{\mathrm{QP}}_{(\mathrm{i})}\right]}\underset{\mathrm{N_i},1}{\left\{\Delta\mathrm{p}_{(\mathrm{i})}\right\}}+\frac{b}{\Delta\mathrm{t}}\underset{\mathrm{N_i},\mathrm{N_i}}{\left[\overline{\mathrm{QP}}_{(\mathrm{i})}\right]}\underset{\mathrm{N_i},3\mathrm{N_i}}{\left[\mathrm{Tr}\right]}\underset{3\mathrm{N_i},1}{\left\{\Delta\varepsilon\right\}}\tag{3.137}$$

being $\underset{\mathrm{N_i},1}{\left\{\overline{\mathrm{Np}}\right\}}=\left\{\underset{\mathrm{N_i},1}{\left\{\mathrm{Np}\right\}}-\underset{\mathrm{N_i},1}{\left\{\mathrm{p}_{(\mathrm{i})}\right\}}_{\mathrm{n}-1}\right\}$.

Rearranging equation (3.137), we arrive at:

$$\left[\left[\mathrm{I}\right]-\frac{1}{M\Delta\mathrm{t}}\underset{\mathrm{N_i},\mathrm{N_i}}{\left[\overline{\mathrm{QP}}_{(\mathrm{i})}\right]}\right]\underset{\mathrm{N_i},1}{\left\{\Delta\mathrm{p}_{(\mathrm{i})}\right\}}=\underset{\mathrm{N_i},1}{\left\{\overline{\mathrm{Np}}\right\}}+\frac{b}{\Delta\mathrm{t}}\underset{\mathrm{N_i},\mathrm{N_i}}{\left[\overline{\mathrm{QP}}_{(\mathrm{i})}\right]}\underset{\mathrm{N_i},3\mathrm{N_i}}{\left[\mathrm{Tr}\right]}\underset{3\mathrm{N_i},1}{\left\{\Delta\varepsilon\right\}}\tag{3.138}$$

Finally, the system is composed by equations (3.134) and (3.138). It may be appropriate to formulate the problem in terms of a single equation, depending only on $\Delta\varepsilon$ and $\Delta\sigma^{\mathrm{d}}$. Substituting the definition of $\Delta\mathrm{p}_{(\mathrm{i})}$ in (3.134).

$$\underset{3\mathrm{N_i},3\mathrm{N_i}}{\left[\overline{\mathrm{E}}\right]}\underset{3\mathrm{N_i},1}{\left[\Delta\varepsilon\right]}=\underset{3\mathrm{N_i},1}{\left\{\Delta\mathrm{Ns}\right\}}+\underset{3\mathrm{N_i},1}{\left\{\overline{\overline{\mathrm{Np}}}\right\}}+\underset{3\mathrm{N_i},3\mathrm{N_i}}{\left[\overline{\mathrm{QS}}\right]}\underset{3\mathrm{N_i},1}{\left\{\Delta\sigma^{\mathrm{d}}\right\}}\tag{3.139}$$

with the condensed terms defined below:

$$\begin{aligned}&\underset{3\mathrm{N_i},1}{\left\{\overline{\overline{\mathrm{Np}}}\right\}}=b\underset{3\mathrm{N_i},3\mathrm{N_i}}{\left[\overline{\mathrm{QS}}\right]}\underset{3\mathrm{N_i},\mathrm{N_i}}{\left[\mathrm{IK}\right]}\left[\left[\mathrm{I}\right]-\frac{1}{M\Delta\mathrm{t}}\underset{\mathrm{N_i},\mathrm{N_i}}{\left[\overline{\mathrm{QP}}_{(\mathrm{i})}\right]}\right]^{-1}\underset{\mathrm{N_i},1}{\left\{\overline{\mathrm{Np}}\right\}}\\&\underset{3\mathrm{N_i},3\mathrm{N_i}}{\left[\overline{\mathrm{E}}\right]}=\left[\underset{3\mathrm{N_i},3\mathrm{N_i}}{\left[\mathrm{E}\right]}-\frac{b^2}{\Delta\mathrm{t}}\underset{3\mathrm{N_i},3\mathrm{N_i}}{\left[\overline{\mathrm{QS}}\right]}\underset{3\mathrm{N_i},\mathrm{N_i}}{\left[\mathrm{IK}\right]}\left[\left[\mathrm{I}\right]-\frac{1}{M\Delta\mathrm{t}}\underset{\mathrm{N_i},\mathrm{N_i}}{\left[\overline{\mathrm{QP}}_{(\mathrm{i})}\right]}\right]^{-1}\underset{\mathrm{N_i},\mathrm{N_i}}{\left[\overline{\mathrm{QP}}_{(\mathrm{i})}\right]}\underset{\mathrm{N_i},3\mathrm{N_i}}{\left[\mathrm{Tr}\right]}\right]\end{aligned}\tag{3.140}$$

3.5.5. Solution Procedure

Equation (3.139) represents the balance of the body under analysis, also implicitly considering the compatibility conditions of the problem. The equation is written in terms of the rates of the variables involved, which should be evaluated over time t, by an incremental schema in terms of $\Delta\mathrm{t}$. Due to the presence of the correction terms associated with damage, the equation is non-linear at each increment $\Delta\mathrm{t}$. Thus, it is used an incremental-iterative

solution procedure, based on a Newton-Raphson technique. It basically consists of successive prediction and correction stages, which aim to verify, in an approximate way, the body equilibrium in a time step:

$$\left\{Y\left(\left\{\Delta\varepsilon_n\right\}\right)\right\} = -\underset{3N_i,3N_i}{\left[\overline{E}\right]}\underset{3N_i,1}{\left\{\Delta\varepsilon_n\right\}} + \underset{3N_i,1}{\left\{\Delta Ns\right\}} + \underset{3N_i,1}{\left\{\overline{\overline{Np}}\right\}} + \underset{3N_i,3N_i}{\left[\overline{QS}\right]}\underset{3N_i,1}{\left\{\Delta\sigma_n^d\right\}} = 0 \tag{3.141}$$

Let us define the strain increment, for an iteration $i+1$, in the form:

$$\left\{\Delta\varepsilon_n^{i+1}\right\} = \left\{\Delta\varepsilon_n^i\right\} + \left\{\delta\Delta\varepsilon_n^i\right\} \tag{3.142}$$

The evaluation of $\left\{\delta\Delta\varepsilon_n^i\right\}$ is done through a Taylor expansion about $\left\{Y\left(\left\{\Delta\varepsilon_n^i\right\}\right)\right\}$ in equation (3.141), truncated at the first-order term, in other words:

$$\left\{Y\left(\left\{\Delta\varepsilon_n^i\right\}\right)\right\} + \frac{\partial\left\{Y\left(\left\{\Delta\varepsilon_n^i\right\}\right)\right\}}{\partial\left\{\Delta\varepsilon_n^i\right\}}\left\{\delta\Delta\varepsilon_n^i\right\} = 0 \tag{3.143}$$

Calculating the first variation, we obtain

$$\frac{\partial\left\{Y\left(\left\{\Delta\varepsilon_n^i\right\}\right)\right\}}{\partial\left\{\Delta\varepsilon_n^i\right\}} = -\left[\overline{E}\right] + \left[\overline{QS}\right]\frac{\partial\left\{\Delta\sigma_n^{di}\right\}}{\partial\left\{\Delta\varepsilon_n^i\right\}} \tag{3.144}$$

which allows writing the expansion (3.143) as follows:

$$\left\{Y\left(\left\{\Delta\varepsilon_n^i\right\}\right)\right\} = \left[\overline{E}\right] - \left[\overline{QS}\right]\frac{\partial\left\{\Delta\sigma_n^{di}\right\}}{\partial\left\{\Delta\varepsilon_n^i\right\}}\left\{\delta\Delta\varepsilon_n^i\right\} = 0 \tag{3.145}$$

The matrix that multiplies $\left\{\delta\Delta\varepsilon_n^i\right\}$ is called consistent tangent operator. Usually, this is written with respect to $\Delta\sigma_n^i$. We decided to keep it explicitly written as a function of $\Delta\sigma_n^{di}$, which does not alter in any way its role in the equilibrium equation.

It can be seen that this operator contains the derivatives with respect to the strain increment $\frac{\partial\left\{\Delta\sigma_n^{di}\right\}}{\partial\left\{\Delta\varepsilon_n^i\right\}}$, and thus consistent with the algorithm of the problem, incremental in nature. This operator degenerates into a continuous tangent operator if $\Delta\varepsilon \to 0$ is considered, resulting in $\frac{\partial\left\{\sigma_n^{di}\right\}}{\partial\left\{\varepsilon_n^i\right\}}$.

Deduction of the Consistent Tangent Operator. From the incremental form of the constitutive damage model, the derivative of damage stress with respect to the strain increment can be obtained, as described below.

Let the total stress rate, written in algebraic form, be given by

$$\{\dot{\sigma}\} = (1-\mathrm{D})[\mathrm{E}]\{\dot{\varepsilon}\} - \dot{\mathrm{D}}[\mathrm{E}]\{\varepsilon\} - b[\mathrm{IK}]\{\dot{\mathrm{p}}_{(\mathrm{i})}\} \tag{3.146}$$

from which the stress increment in n is defined as:

$$\{\Delta\sigma_{\mathrm{n}}\} = [\mathrm{E}]\{\Delta\varepsilon_{\mathrm{n}}\} - \mathrm{D}_{\mathrm{n+1}}[\mathrm{E}]\{\Delta\varepsilon_{\mathrm{n}}\} - [\mathrm{E}]\{\varepsilon_{\mathrm{n+1}}\}\Delta\mathrm{D}_{\mathrm{n}} - b[\mathrm{IK}]\{\Delta\mathrm{p}_{\mathrm{n}}\} \tag{3.147}$$

Considering an evolution in a finite step governed by $\Delta(\bullet) = \bullet_{\mathrm{n+1}} - \bullet_{\mathrm{n}}$, we have:

$$\{\Delta\sigma_{\mathrm{n}}\} = [\mathrm{E}]\{\Delta\varepsilon_{\mathrm{n}}\} - (\mathrm{D}_{\mathrm{n}} + \Delta\mathrm{D}_{\mathrm{n}})[\mathrm{E}]\{\Delta\varepsilon_{\mathrm{n}}\} - [\mathrm{E}]\{\varepsilon_{\mathrm{n}} + \Delta\varepsilon_{\mathrm{n}}\}\Delta\mathrm{D}_{\mathrm{n}} - b[\mathrm{IK}]\{\Delta\mathrm{p}_{\mathrm{n}}\} \tag{3.148}$$

in which one can identify the increment of the stress associated to damage:

$$\{\Delta\sigma_{\mathrm{n}}\} = [\mathrm{E}]\{\Delta\varepsilon_{\mathrm{n}}\} - \{\Delta\sigma_{\mathrm{n}}^{\mathrm{d}}\} - b[\mathrm{IK}]\{\Delta\mathrm{p}_{\mathrm{n}}\} \tag{3.149}$$

$$\{\Delta\sigma_{\mathrm{n}}^{\mathrm{d}}\} = \mathrm{D}_{\mathrm{n}}[\mathrm{E}]\{\Delta\varepsilon_{\mathrm{n}}\} + \Delta\mathrm{D}_{\mathrm{n}}[\mathrm{E}]\varepsilon_{\mathrm{n}} + 2\Delta\mathrm{D}_{\mathrm{n}}[\mathrm{E}]\Delta\varepsilon_{\mathrm{n}} \tag{3.150}$$

The differentiation of (3.150) with respect to the strain increment leads to:

$$\frac{\partial\{\Delta\sigma_{\mathrm{n}}^{\mathrm{d}}\}}{\partial\{\Delta\varepsilon_{\mathrm{n}}\}} = \mathrm{D}_{\mathrm{n}}[\mathrm{E}] + [\mathrm{E}]\varepsilon_{\mathrm{n}}\frac{\partial\Delta\mathrm{D}_{\mathrm{n}}}{\partial\{\Delta\varepsilon_{\mathrm{n}}\}} + 2\Delta\mathrm{D}_{\mathrm{n}}[\mathrm{E}] + 2[\mathrm{E}]\Delta\varepsilon_{\mathrm{n}}\frac{\partial\Delta\mathrm{D}_{\mathrm{n}}}{\partial\{\Delta\varepsilon_{\mathrm{n}}\}} \tag{3.151}$$

The definition of $\Delta\mathrm{D}_{\mathrm{n}}$ is obtained directly from the incremental equations obtained from Marigo's model (1981). The damage evolution is defined by equation $\dot{\mathrm{D}} = \frac{\dot{Y}}{A}$, which can be written as follows:

$$\Delta\mathrm{D}_{\mathrm{n}} = \frac{\Delta Y_{\mathrm{n}}}{A} \tag{3.152}$$

The increment of the thermodynamic force associated to damage can be calculated by the variation $\Delta Y_{\mathrm{n}} = Y_{\mathrm{n+1}} - Y_{\mathrm{n}}$, which leads to the following expression:

$$\Delta Y_{\mathrm{n}} = \frac{1}{2}\{\varepsilon_{\mathrm{n+1}}\}[\mathrm{E}]\{\varepsilon_{\mathrm{n+1}}\} - \frac{1}{2}\{\varepsilon_{\mathrm{n}}\}[\mathrm{E}]\{\varepsilon_{\mathrm{n}}\} \tag{3.153}$$

whose expansion leads to the following result:

$$\Delta Y_{\mathrm{n}} = \frac{1}{2}\{\varepsilon_{\mathrm{n}}\}[\mathrm{E}]\{\Delta\varepsilon_{\mathrm{n}}\} + \frac{1}{2}\{\Delta\varepsilon_{\mathrm{n}}\}[\mathrm{E}]\{\varepsilon_{\mathrm{n}}\} + \frac{1}{2}\{\Delta\varepsilon_{\mathrm{n}}\}[\mathrm{E}]\{\Delta\varepsilon_{\mathrm{n}}\} \tag{3.154}$$

Considering the symmetry of the elastic tensor, due to isotropy, allows writing:

$$\Delta Y_{\mathrm{n}} = \{\varepsilon_{\mathrm{n}}\}[\mathrm{E}]\{\Delta\varepsilon_{\mathrm{n}}\} + \frac{1}{2}\{\Delta\varepsilon_{\mathrm{n}}\}[\mathrm{E}]\{\Delta\varepsilon_{\mathrm{n}}\} \tag{3.155}$$

The increment of the damage variable is then defined by (3.152), and its derivative with respect to $\Delta\varepsilon_{\mathrm{n}}$ is:

$$\frac{\partial\Delta\mathrm{D}_{\mathrm{n}}}{\partial\{\Delta\varepsilon_{\mathrm{n}}\}} = \frac{1}{A}[\mathrm{E}]\left(\{\varepsilon_{\mathrm{n}}\} + \{\Delta\varepsilon_{\mathrm{n}}\}\right) \tag{3.156}$$

Thus, the difference in (3.151) can be explained as:

$$\begin{aligned}\frac{\partial\{\Delta\sigma_{\mathrm{n}}^{\mathrm{d}}\}}{\partial\{\Delta\varepsilon_{\mathrm{n}}\}} &= \mathrm{D}_{\mathrm{n}}[\mathrm{E}] + 2\Delta\mathrm{D}_{\mathrm{n}}[\mathrm{E}] + \frac{1}{A}[\mathrm{E}]\{\varepsilon_{\mathrm{n}}\}[\mathrm{E}]\{\varepsilon_{\mathrm{n}}\} \\ &+ \frac{3}{A}[\mathrm{E}]\{\varepsilon_{\mathrm{n}}\}[\mathrm{E}]\{\Delta\varepsilon_{\mathrm{n}}\} + \frac{2}{A}[\mathrm{E}]\{\Delta\varepsilon_{\mathrm{n}}\}[\mathrm{E}]\{\Delta\varepsilon_{\mathrm{n}}\}\end{aligned} \tag{3.157}$$

3.5.6. Algorithm to Evaluate the Damage Level

The incremental-iterative procedure seeks, at every step of the analysis, a configuration in equilibrium with the damage level calculated in this step. In the case of the coupled model proposed herein, an analysis step of the damage model can be taken to correspond to a time step of the poroelastic problem, if deemed appropriate.

The algorithm calculates the variables in $\mathrm{n}+1$ considering their known values from the previous step n. The variable that controls the algorithm is the strain increment $\{\Delta\varepsilon_{\mathrm{n}}\}$ and, consequently, the strain in the current step $\{\varepsilon_{\mathrm{n+1}}\}$.

Table 3.1 –Algorithm to evaluate the damage level

I. ELASTIC PREDICTION		
calculates	$\left\{\delta\Delta\varepsilon_n^1\right\}$	$\left\{\delta\Delta\varepsilon_n^1\right\} = -\left(\dfrac{\partial\left\{Y\left(\left\{\Delta\varepsilon_n^1\right\}\right)\right\}}{\partial\left\{\Delta\varepsilon_n^1\right\}}\right)^{-1}\left\{Y\left(\left\{\Delta\varepsilon_n^1\right\}\right)\right\}$
from	$\dfrac{\partial\left\{Y\left(\left\{\Delta\varepsilon_n^1\right\}\right)\right\}}{\partial\left\{\Delta\varepsilon_n^1\right\}} = -\left[\overline{E}\right] + \left[\overline{QS}\right]\dfrac{\partial\left\{\sigma_n^d\right\}}{\partial\left\{\varepsilon_n\right\}}$,	$\left\{Y\left(\left\{\Delta\varepsilon_n{}^1\right\}\right)\right\} = \left\{\Delta Ns\right\} + \left\{\overline{\overline{Np}}\right\}$
updates	$\left\{\Delta\varepsilon_n^1\right\}, \left\{\varepsilon_{n+1}^1\right\}$	
II. DAMAGE MODEL VERIFICATION		
calculates	F_{n+1}	$F_{n+1} = Y_{n+1} - Y_0 - AD_n$
tests	if $F_{n+1} \le 0$	$\Delta D_n = 0$
	if $F_{n+1} > 0$	calculates ΔD_n
	from	$F_{n+1} = Y_{n+1} - Y_0 - A\left(D_n + \Delta D_n\right) = 0$
updates	$\left\{\Delta\sigma_n^d\right\}$ (3.150)	
III. EQUILIBRIUM VERIFICATION		
tests	if $\left\|\left\{Y\left(\left\{\Delta\varepsilon_n\right\}\right)\right\}\right\| \le tol$ (3.141)	updates D_{n+1}, $\left\{\sigma_{n+1}^d\right\}$, $\left\{\sigma_{n+1}\right\}$
	end of step $n+1$	goes to I
	if $\left\|\left\{Y\left(\left\{\Delta\varepsilon_n\right\}\right)\right\}\right\| > tol$ (3.141)	goes to IV
IV. CORRECTION		
calculates	$\left\{\delta\Delta\varepsilon_n^{i+1}\right\}$	$\left\{\delta\Delta\varepsilon_n^{i+1}\right\} = -\left(\dfrac{\partial\left\{Y\left(\left\{\Delta\varepsilon_n^{i+1}\right\}\right)\right\}}{\partial\left\{\Delta\varepsilon_n^{i+1}\right\}}\right)^{-1}\left\{Y\left(\left\{\Delta\varepsilon_n^{i+1}\right\}\right)\right\}$
from	$\dfrac{\partial\left\{Y\left(\left\{\Delta\varepsilon_n^{i+1}\right\}\right)\right\}}{\partial\left\{\Delta\varepsilon_n^{i+1}\right\}} = -\left[\overline{E}\right] + \left[\overline{QS}\right]\dfrac{\partial\left\{\Delta\sigma_n^{di+1}\right\}}{\partial\left\{\Delta\varepsilon_n^{i+1}\right\}}$	$\left\{Y\left(\left\{\Delta\varepsilon_n^{i+1}\right\}\right)\right\}$ (3.141)
updates	$\left\{\Delta\varepsilon_n^{i+1}\right\}, \left\{\varepsilon_{n+1}^{i+1}\right\}$	goes to II

Chapter 4

Numerical Examples

4.1. OVERALL CONSIDERATIONS

This chapter presents some applications for the formulations developed and implemented computationally. First, some examples on poroelasticity and elasticity with damage are examined in order to validate the implementation carried out for the uncoupled problems. Section 4.4 addresses the coupled problem, which is the objective of this work. It should be mentioned that this formulation was implemented in FORTRAN®.

4.2. LINEAR POROELASTICITY EXAMPLES

The poroelastic model implemented in this work is applied to the analysis of classical problems of soil and rock mechanics with known analytical solution, in order to validate its operation. A verification of the model response under different loading conditions is also conducted.

4.2.1. One-dimensional Consolidation

Let us consider the classic problem of one-dimensional consolidation proposed by Terzaghi, which consists of a soil column on a rigid impermeable base (Figure 4.1). A constant heaviside-type unit load is applied to the upper drainage surface and maintained for 100 s. Take a column of 10 m in height, consisting of Berea sandstone, completely saturated by water. The material parameters are defined in Detournay and Cheng (1993). The discretization of the problem includes 60 boundary elements and 40 domain cells.

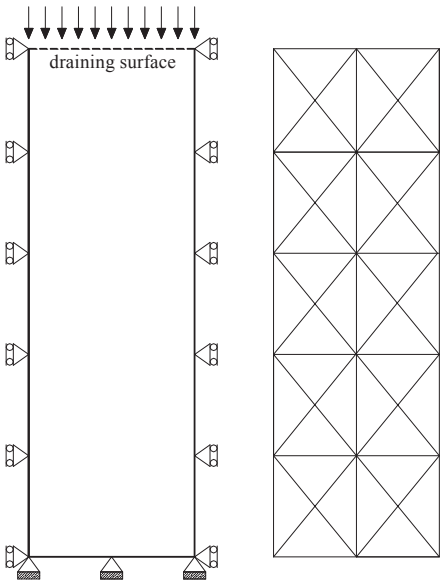

Figure 4.1 - Problem definition, adopted cells mesh

From Figure 4.2, we can observe that the response at the initial times is characterized by the highest pore-pressure values, indicating that the fluid phase is highly requested, while the

solid skeleton does not undergo all the loading action. Throughout the fluid draining process there is an increased level of effective stress, accompanied by a proportional pore-pressure decrease, until it vanishes at 100 s.

Table 4.1 - Parameters of the Berea sandstone

Parameter	Value
G	6000 MPa
υ	0.2
υ^u	0.33
K_s	36000 MPa
ϕ_0	0.19
k	1.9 x 10^{-13} m^2
μ	1 x 10^{-9} MPa.s

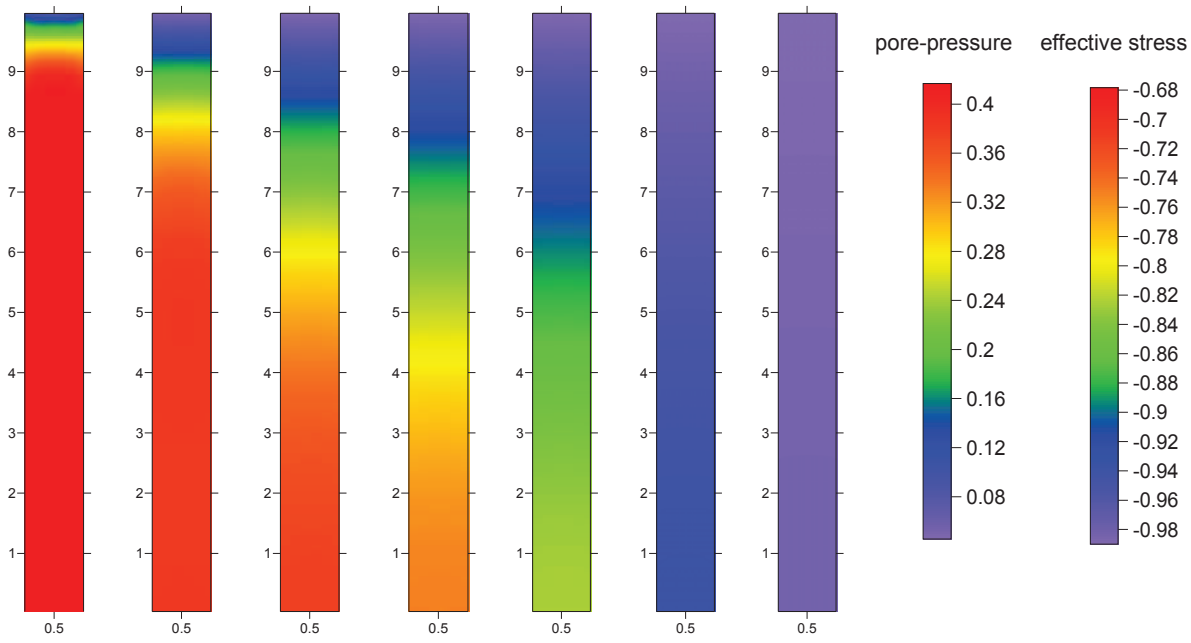

Figure 4.2 - Pore-pressures and vertical effective stress at 0.1 s; 1s; 5s; 10s; 20s; 50s; 100s

Figure 4.3 shows the pore-pressure values at the base of the column over time. Figure 4.4 shows the displacement evolution at the top of the column. Both results indicate the correlation of values obtained with the formulation developed in this work, based on BEM, with the analytical response presented in Detournay and Cheng (1993).

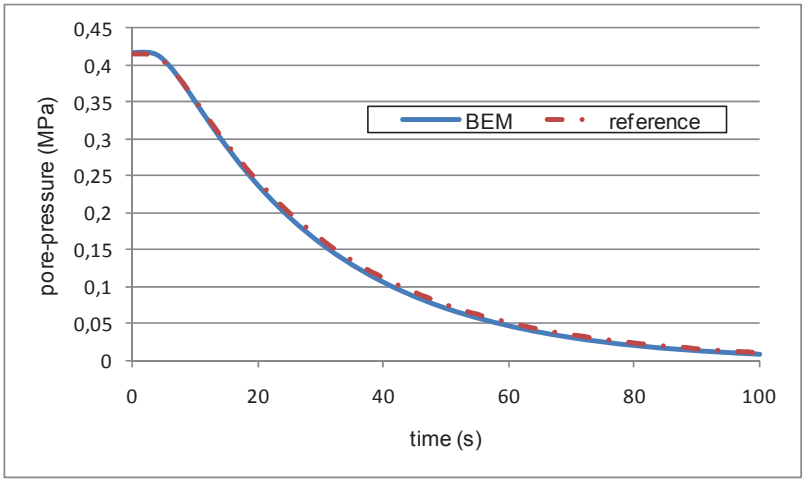

Figure 4.3 - Pore-pressure evolution at the base of the column

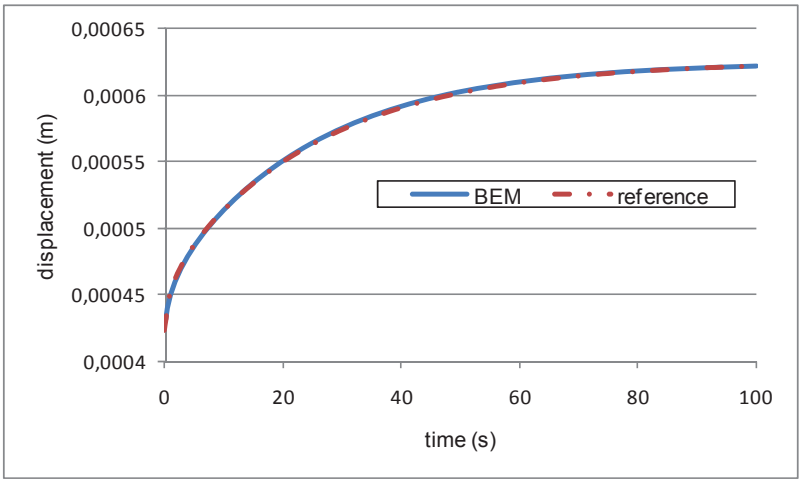

Figure 4.4 - Displacement evolution at the top of the column

It should be noted that in columns of lower height the draining process, and consequently the dissipation of pore-pressures, occurs more rapidly, as shown in Figure 4.5, for a column 3 m in height.

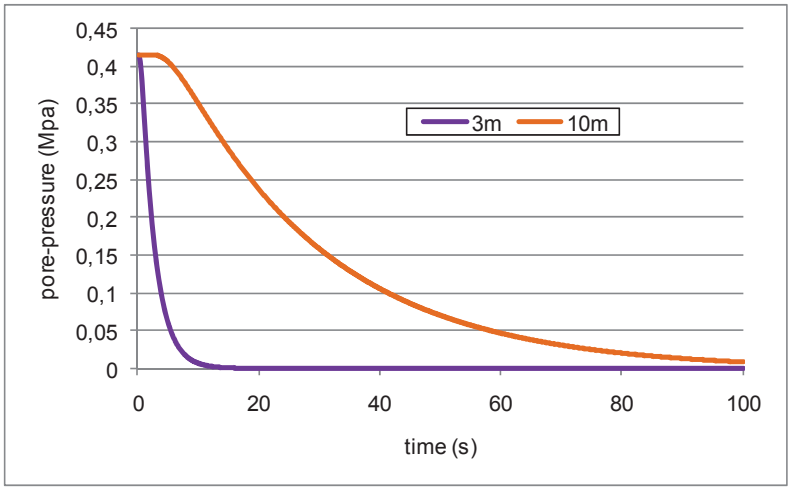

Figure 4.5 - Pore-pressure evolution at the base of the column, for different heights

4.2.2. Plane Consolidation

The problem consists of a semi-infinite plane, saturated by water, subject to a uniform load strip of width 2a. Due to the symmetry of the problem, only half of the domain is analyzed, as shown in Figure 4.6. 34 boundary elements are used, of which 12 are on the symmetry axis, and 161 cells. The loading is applied according to a heaviside function, at t=0, and maintained for 100 s. An analytical solution was proposed in Schiffman *et al.* (1969), in terms of an adjusted time factor, and of the dimensionless values of pore-pressure and total and effective stresses in both coordinate directions:

$$\tau = \frac{(1-\upsilon)}{(1-2\upsilon)}\frac{2Gk}{\gamma_f}t \qquad \bar{p} = \frac{p(\tau)}{p(0)} \qquad \bar{\sigma} = \frac{(\sigma_{11}(\tau)+\sigma_{22}(\tau))}{(\sigma_{11}(0)+\sigma_{22}(0))} \qquad \bar{\sigma}^{ef} = \frac{(\sigma_{11}^{ef}(\tau)+\sigma_{22}^{ef}(\tau))}{(\sigma_{11}^{ef}(\infty)+\sigma_{22}^{ef}(\infty))}$$

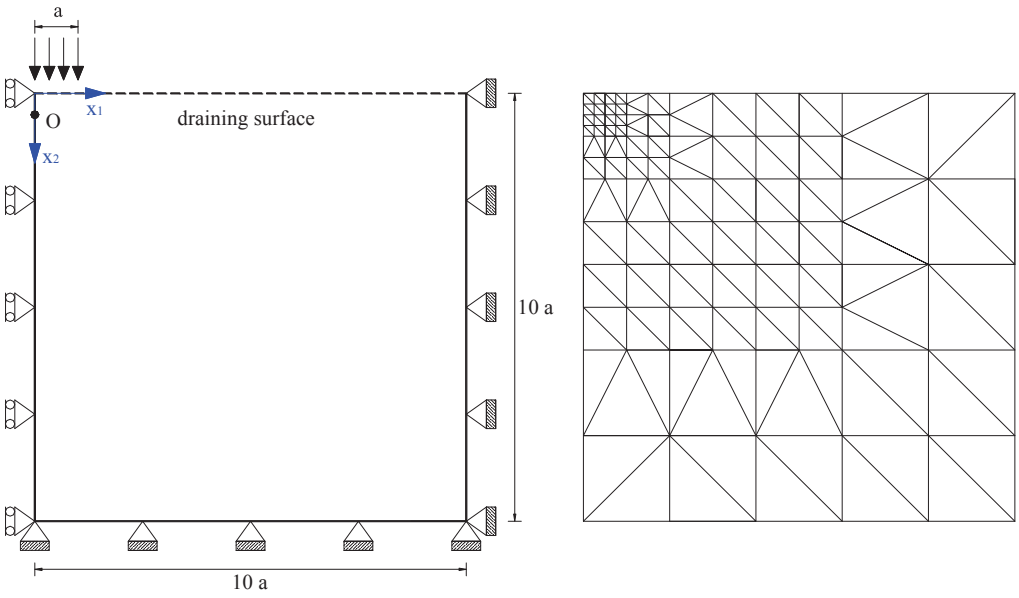

Figure 4.6 - Problem definition, adopted cells mesh

These dimensionless values, measured at point O (0,a/2), are shown in Figure 4.7. The results obtained with the proposed model are compared with those calculated analytically. As in the case of one-dimensional consolidation, the initial slow flow of the fluid induces the largest pore-pressure, while the solid skeleton did not yet undergo significant strain.

Also during the early-time response, the occurrence of the Mandel-Cryer effect (Mandel, 1950, 1953; Cryer, 1963) *apud* Schiffman *et al.* (1969) should be noted, characterized by an increased pore-pressure level, over the initial value. At this stage, the areas next to the surface are quickly drained, undergoing increase in the strain fields and effective stresses.

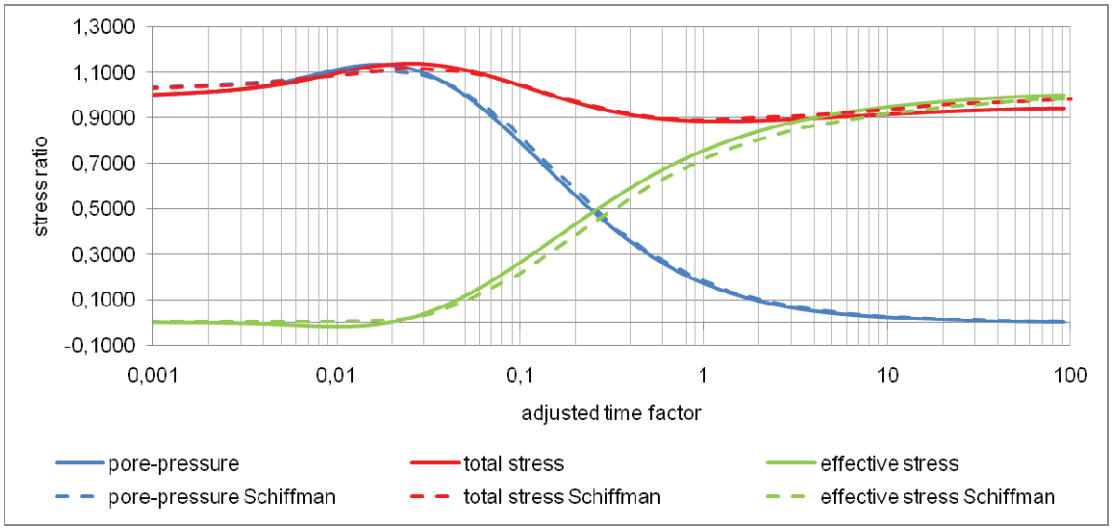

Figure 4.7 - Dimensionless values of pore-pressure, total and effective stress

The volumetric reduction due to this quasi-instantaneous consolidation induces an additional compression in the most inner regions of the body, which then develops additional pore-pressures in the saturating fluid. The effect in question manifests itself at point O (0,a/2), since this is distant from the draining face. During the drainage process, the dissipation of pore-pressure gives rise to increased levels of effective stress, as shown in Figure 4.9.

The normalized values of total and effective stress in the horizontal direction, defined by, $\bar{\sigma}_{11} = \frac{\sigma_{11}(\tau)}{\sigma_{11}(0)}$ and $\bar{\sigma}^{ef}_{11} = \frac{\sigma^{ef}_{11}(\tau)}{\sigma^{ef}_{11}(0)}$, are also defined in the reference analytical solution for the point O (0,a/2). The results obtained using the BEM formulation are in agreement, as shown in Figure 4.8.

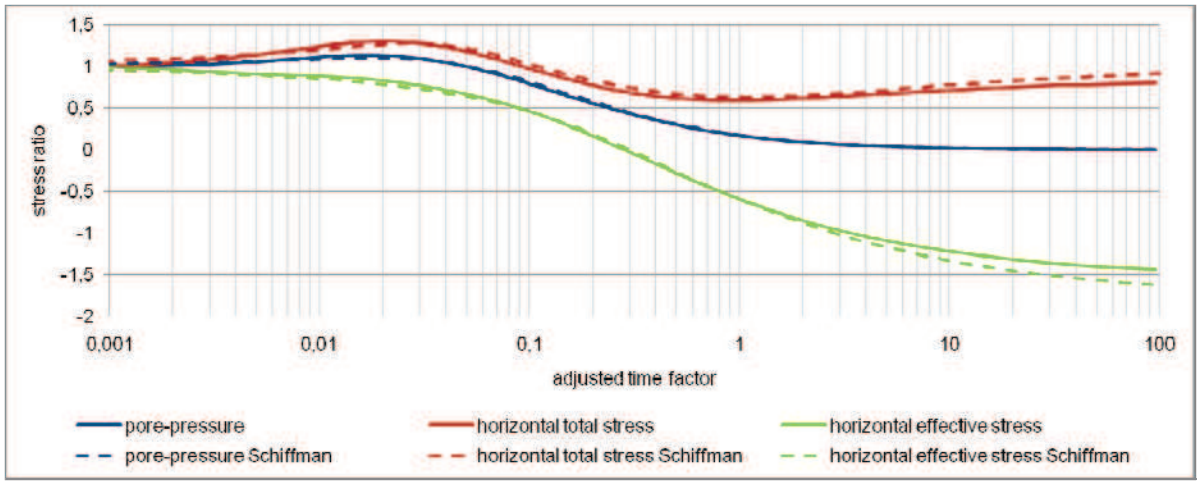

Figure 4.8 - Dimensionless values of pore-pressure and stresses in the horizontal direction

Next are the response in displacement, effective stress and pore-pressure for the whole domain of the problem. In order to illustrate the distribution of these variables on the domain over time, take hypothetical values for some input parameters of the problem, as follows:

Table 4.2 - Hypothetical parameters adopted in example 4.2.2

Parameter	Value
a	1 m
G	0.5 MPa
υ	0
b	1
M	100
k	1

It is assumed that the load has a unit value. The boundary mesh is refined, now containing 136 elements, in order to get a better view of the quantities shown in Figure 4.9. The drainage process is well defined by the equilibrium between pore-pressures and effective stresses on the domain. The loading effects are manifested within a limited area, adjacent to it, in accordance with the Saint-Venant principle.

Note that the pore-pressure levels tend to remain close to zero in the region close to the draining surface, in agreement with the pore-pressure concept placed here, which is related to the differential pressure value compared to the ambient pressure.

Notice that the poroelasticity formulation is not sensitive to the time step adopted. Choosing smaller increments only depends on the interest in quantifying the variables in the initial analysis times. However, this discretization over time does not influence the stability of the response. This confirms the fact that the poroelastic problem can be interpreted as a usual elastic problem, to which additional stiffness and damping are incorporated due to the presence of the fluid phase. This time discretization independence is verified under any loading conditions, either instantaneous or time-distributed, which will be presented in the following Section.

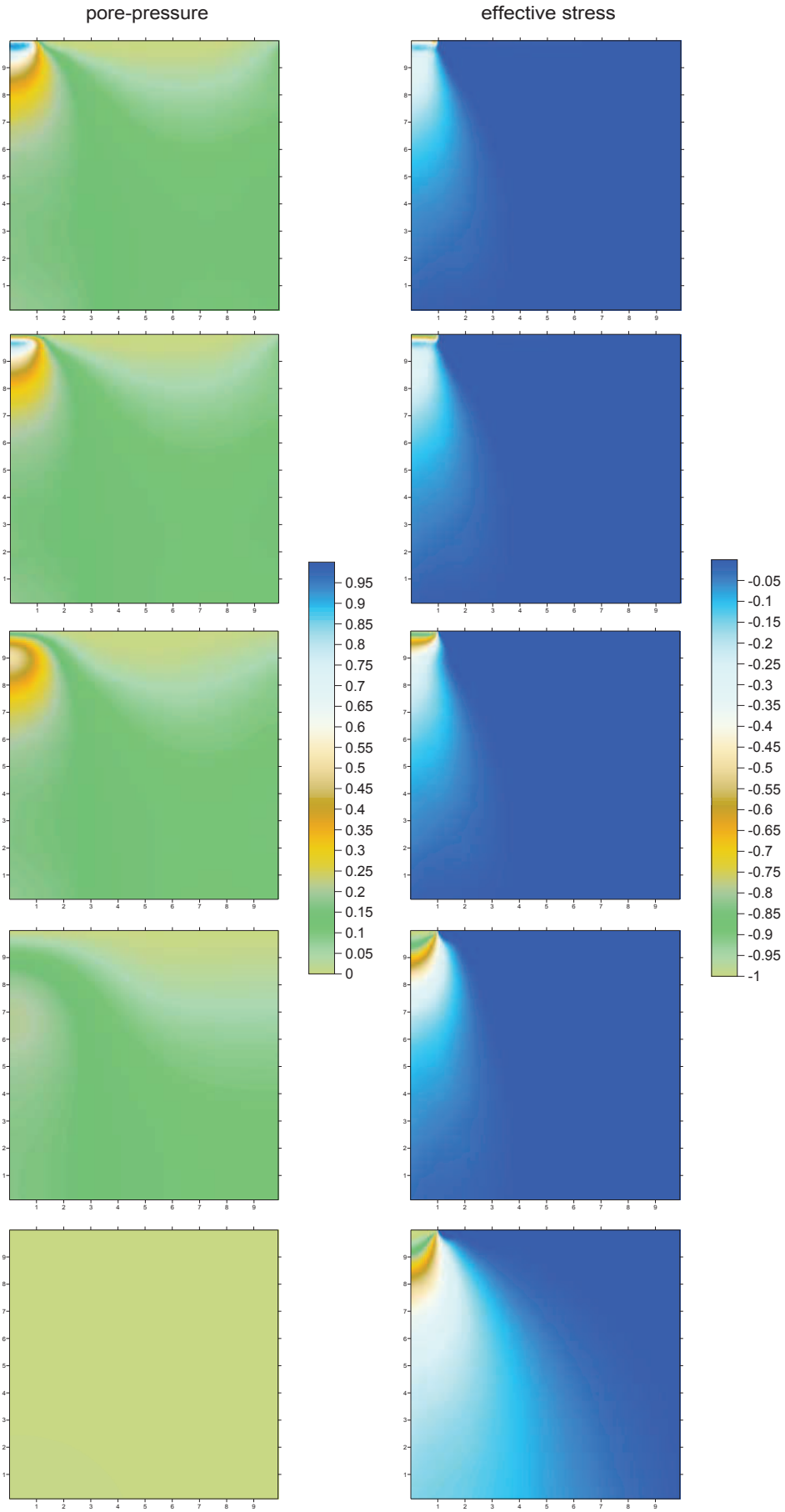

Figure 4.9 - Evolution of poroelastic and vertical effective stresses at 0.001s; 0.01s; 0.2s; 2s; 100s

4.2.3. Poroelastic Response under Different Loading Conditions

Usually, the problems on poroelasticity are characterized by applying an instantaneous loading, with heaviside-type distribution (Figure 4.10). Thus, it is possible to reproduce a condition that does not allow pore-pressure dissipation during the loading process.

Consider a monotonic loading condition, uniformly distributed over a time interval, as illustrated in Figure 4.10.

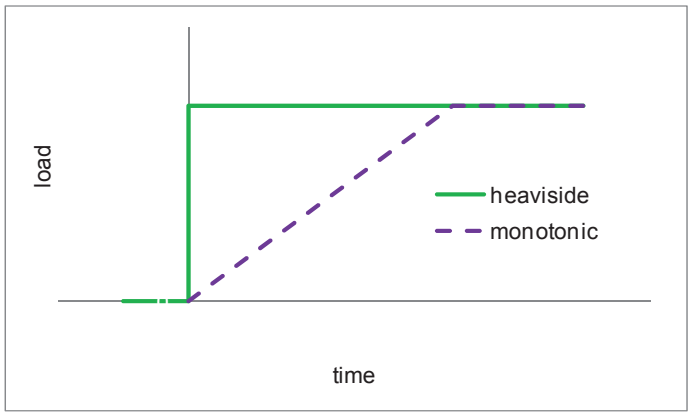

Figure 4.10 - Loading profiles

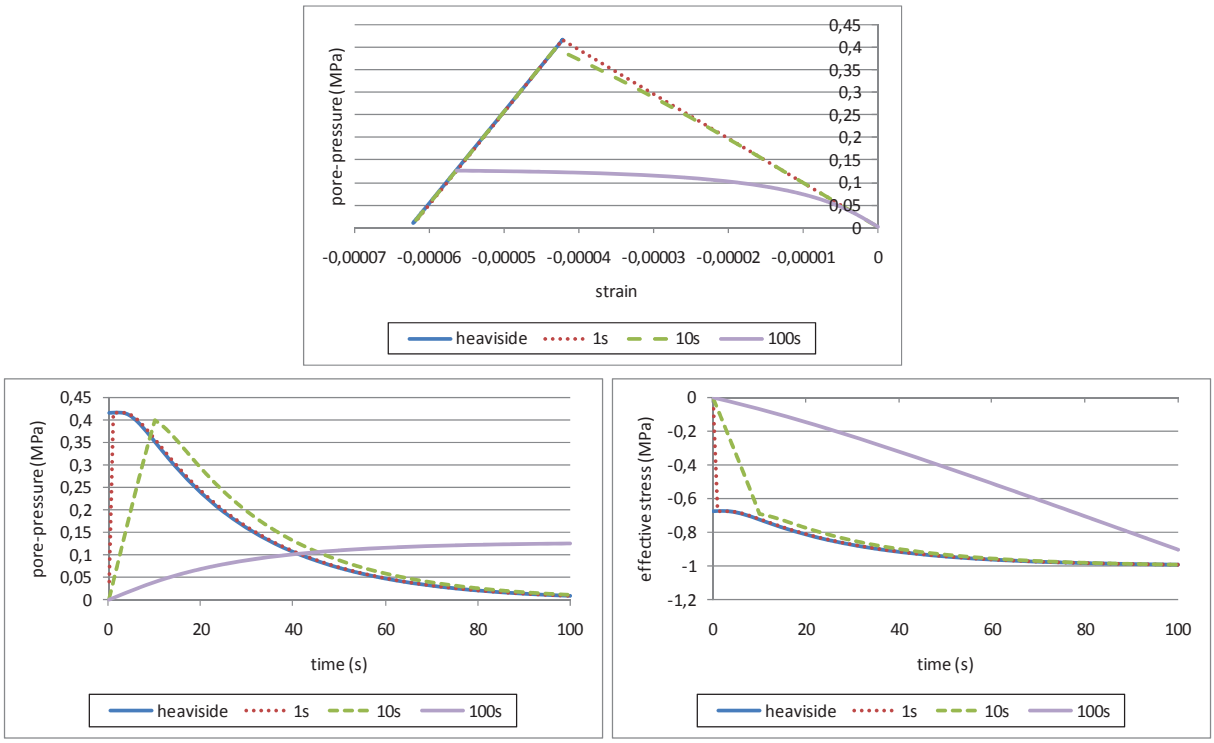

Figure 4.11 - Response at the base of the column for the instantaneous and monotonical loading over 1s, 10s and 100s - a) pore-pressure as a function of vertical strain b) pore-pressure evolution c) vertical effective stress evolution.

The problem of poroelastic column is taken up with a load applied over 1 s, 10 s and 100 s, which is the total time of analysis. According to section 4.2.1, under the instantaneous loading condition, this time is sufficient to dissipate the pore-pressures and for the effective stress to reach its final value, equal to the total stress applied, over the entire domain. Figure 4.11 shows the responses for the different loading application times, compared with the instantaneous application case, at a point at the base of the column.

For the non-instantaneous loadings, the initial values of pore-pressure and effective stress are zero. For loading cases over 1 to 10 s, these values evolve over time, tending to the response for instantaneous loading. However, this is not true for the load distributed over the total time of 100s. In this situation, at the end of the loading process, the drainage is not yet completed, therefore there is residual pore-pressure along the column height, and the effective stress levels have not reached the value of the applied load, as shown in Figure 4.12. This behavior occurs regardless of the applied load value, of the application time or the permeability coefficient of the medium. The level of residual pore-pressure along the column is directly proportional to its height and inversely proportional to the time of application.

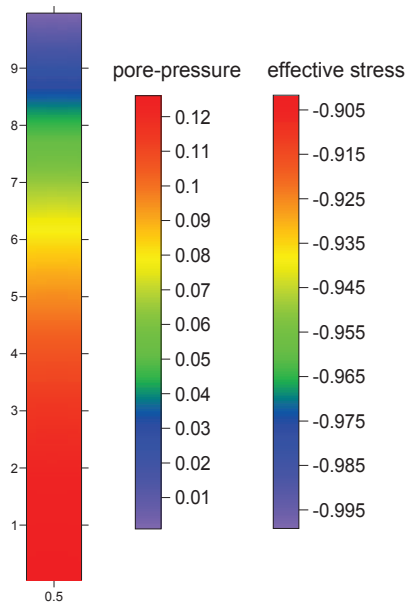

Figure 4.12 - Pore-pressure and effective stress at the end of 100s

4.3. EXAMPLES ON THE ISOTROPIC DAMAGE MODEL ADOPTED

The behavior predicted by Marigo's model (1981) is illustrated, applying the program developed to some simple problems, highlighting the influence of the material parameters in the formulation. The response of the algorithm is treated in load control and displacement control conditions.

4.3.1. Characterization and Parametric Analysis of the Model

As presented in Chapter 2, Marigo's model (1981) represents the behavior of a brittle or quasi-brittle material in the elastic regime subject to damage. The damage criterion is defined by two constants dependent on the material, with a scalar-valued variable that represents the degradation level. Moreover, the model is symmetric with respect to the type of solicitation, providing the same answer to each strain level, whether it is tensile or compressive.

In order to describe the model, let us consider a hypothetical material with a unit longitudinal modulus of elasticity and nil Poisson's coefficient. The damage parameters are taken with the values Y_0=0.05 and A=0.3. Imposing any loading, which induces an evolution of strain at a point, the predicted constitutive answer for the damage model is presented in Figure 4.13.

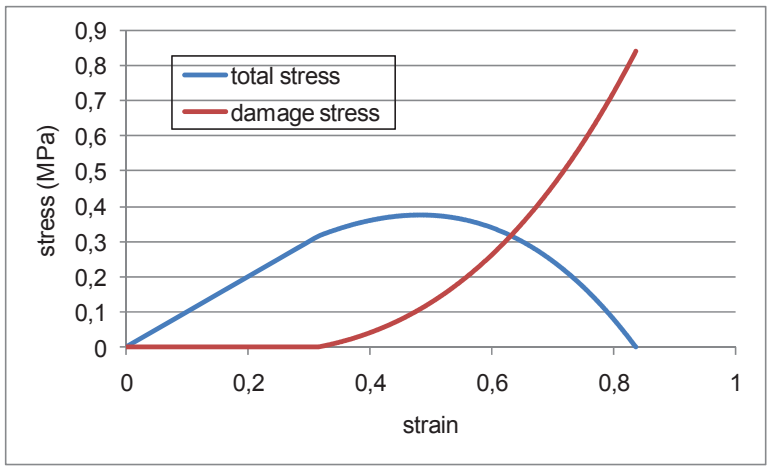

Figure 4.13 - Characteristic curve of the damage constitutive law

The first branch, with linear behavior, corresponds to the elastic regime, in which the total stresses are equal to the effective stresses, and the stresses for the damage are **nil**. Once the damage process begins, these damage stresses start to evolve, reaching the peak value, corresponding to the state of complete degradation, where D=1. Figure 4.14 illustrates the evolution of the damage variable.

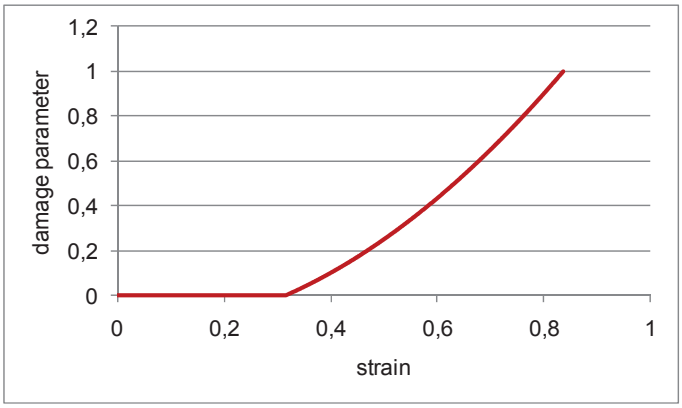

Figure 4.14 - Damage variable evolution

Based on the damage criterion equation, $F(\mathrm{Y},\mathrm{D}) = Y - Y_0 - A\mathrm{D}$, it can be seen that Parameter Y_0 defines the start of the damage process, with *A* responsible for the intensity of the damage evolution. Figures 4.15 and 4.16 describe the influence of these parameters in the constitutive response.

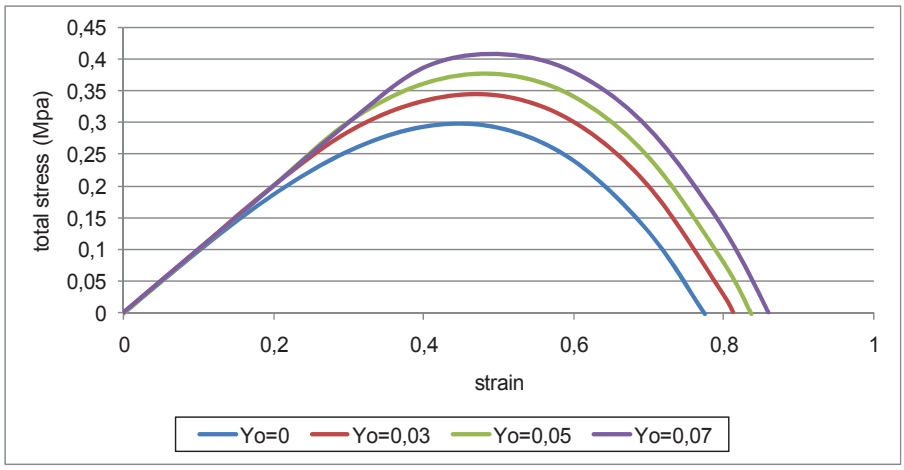

Figure 4.15 - Influence of Y0, on A=0.3

The analysis of the curves shows that for lower values of Y_0, the damage begins earlier, at lower strain values. In the limiting case where Y_0=0, the damage occurs since the beginning of the strain evolving. The smaller values of Parameter *A* correspond to a more pronounced damage effect, with a higher loss of stiffness.

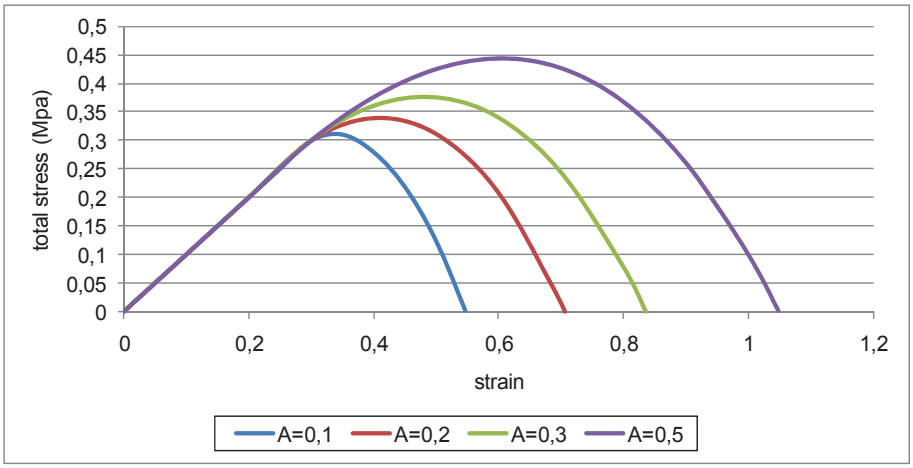

Figure 4.16 - Influence of A, on Y0=0,05

4.3.2. Solid under cyclic loading

Let us assume a rectangular domain, with a unit width base and 2 m in height, as shown in Figure 4.17, made of the material described in Section 4.3.1. A displacement profile defined

by the function plotted in Figure 4.18 is applied to the upper face. The discretization contains 40 cells and 14 boundary elements. Increments of value 0.1 are adopted over analysis time.

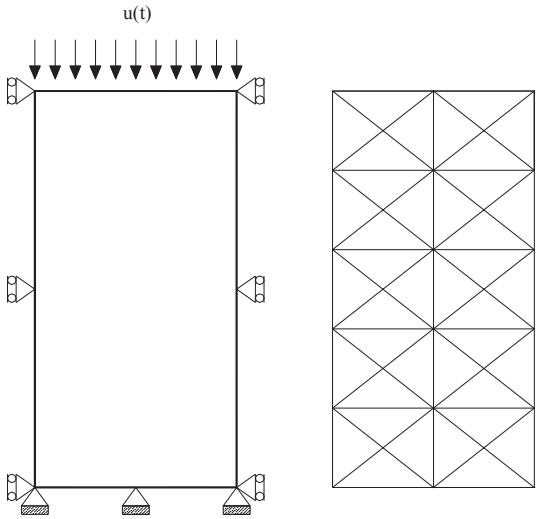

Figure 4.17 - Problem definition, adopted cells mesh

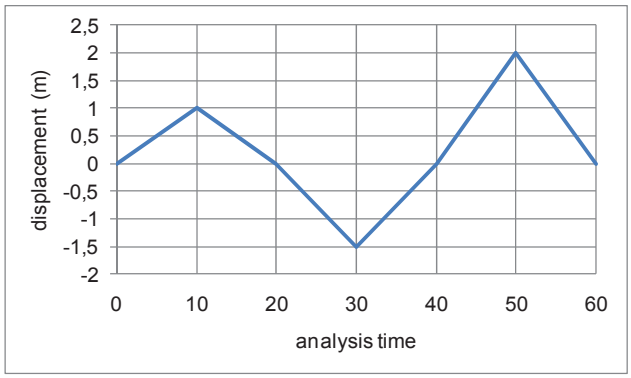

Figure 4.18 - Applied displacement profile

Given that it is a homogeneous solid, with equal elastic and damage parameters on the whole domain, the damage occurs uniformly over the body. Taking any given point, its response is shown in Figure 4.19.

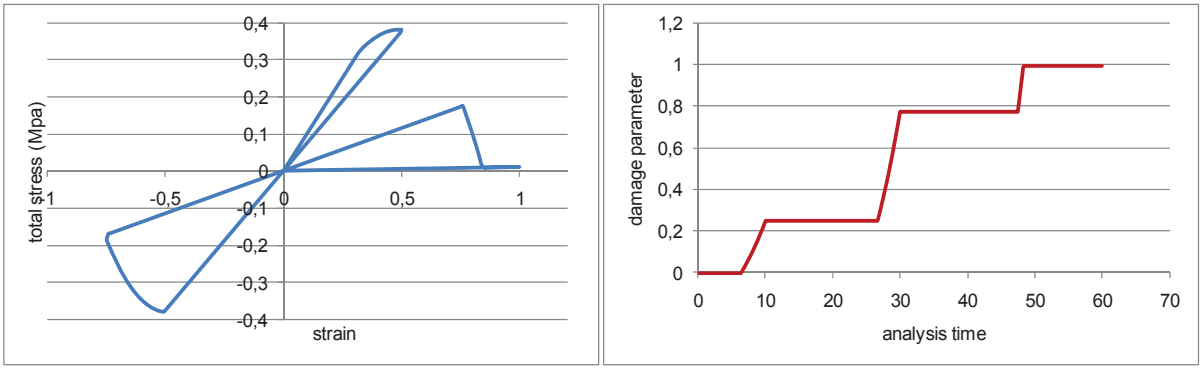

Figure 4.19 - a) Total stress vs. strain, in vertical direction b) damage parameter evolution

Figure 4.19b shows the symmetrical nature of the damage model. At each loading cycle, when there is a change in the sign of the applied displacement, the damage variable evolves. In the unloading cycles, the damage level remains stable.

4.3.3. Solid with Defect under Uniaxial Tension

The rectangular domain shown in Figure 4.20, which has 150 mm in width and 10 mm in height, is subjected to a horizontal displacement of 0.1 mm at its ends. The constituent material has a linear elastic behavior, except for the central region, 30 mm wide, whose material obeys the isotropic damage law. Table 4.3 presents the material parameters. This is a problem in which the phenomenon of localization occurs due to the presence of the defect. The discretization is performed with 64 boundary elements and 60 cells.

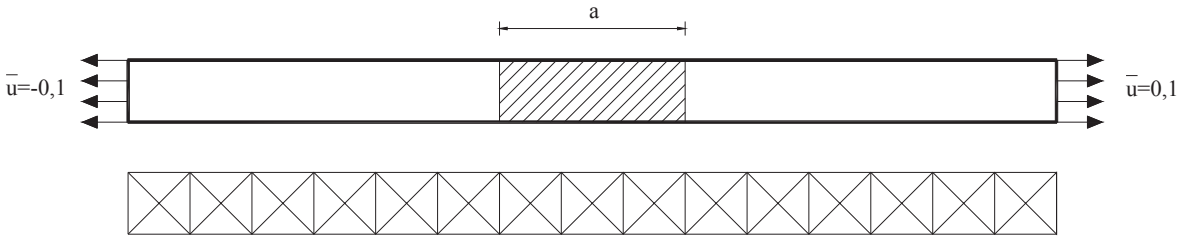

Figure 4.20 - problem definition, adopted cells mesh

Table 4.3 - Parameters adopted in example 4.3.3

Parameter	Value
G	15000 MPa
υ	0
Y_0	0.0016667 MPa
A	0.025 MPa

The displacement is applied gradually, in this case in 1000 steps, and the solid deforms uniformly, until the damage begins in the central region, which starts to develop greater strains than the rest of the body, under the same level of stress (Figure 4.21).

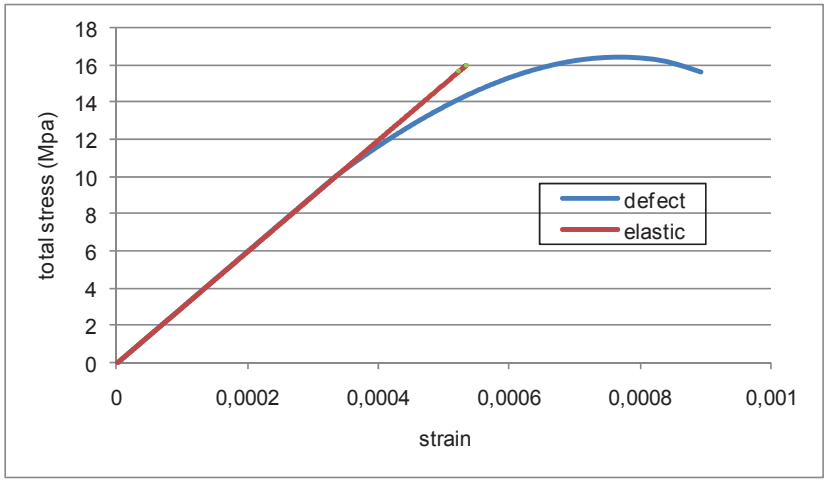

Figure 4.21 - Constitutive response in the elastic and defective regions

As indicated in green in Figure 4.21, from the peak of the stress-strain curve related to the fault, an unloading process begins in the elastic region. This region is proportionally relieved, as the strains in the central defect grow governed by the occurrence of damage.

The loss of convergence of the algorithm can be associated with the localization occurrence, which was intentionally induced in this example, by the introduction of a weak region.

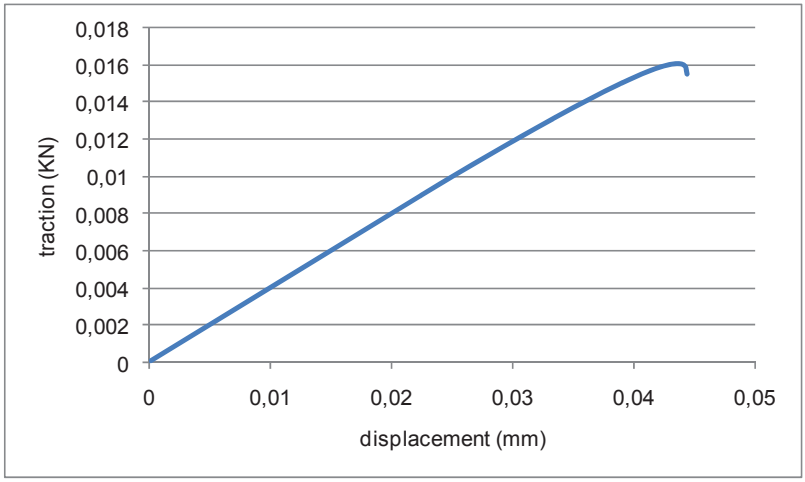

Figure 4.22 - Relationship between the displacement applied and the reaction at the end of the body

The loss of convergence can occur at different instants of the analysis, depending on the value of the applied displacement increment, on the tolerance parameter of the algorithm and on the discretization chosen, with this mesh dependence as one of the biggest drawbacks of localization occurrence. Narrower defective regions induce an earlier loss of convergence. The distributions of horizontal strain and damage variable, referring to the last step of this analysis, are presented in Figures 4.22 and 4.23.

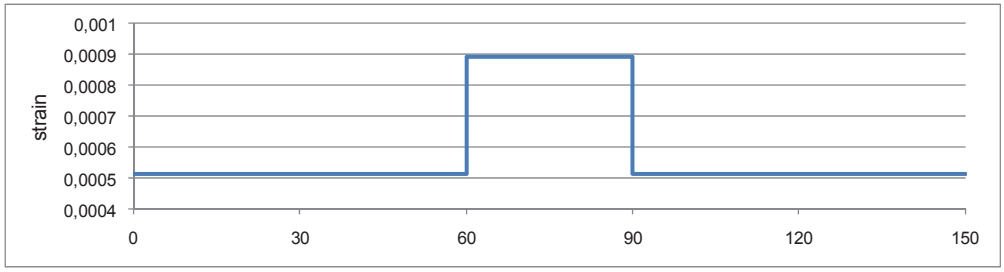

Figure 4.22 - horizontal strain along the width

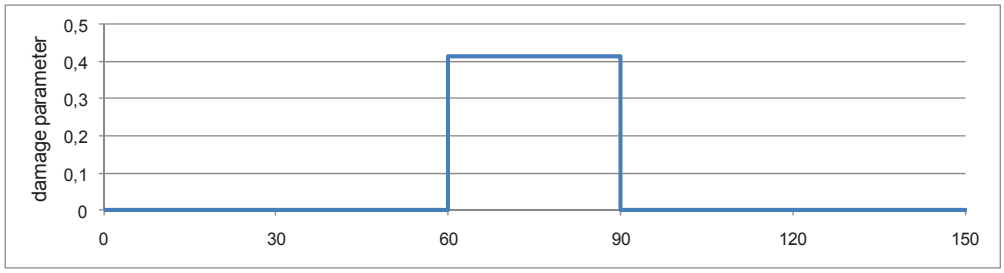

Figure 4.23 - Damage parameter along the width

4.4. EXAMPLES ON POROELASTICITY COUPLED TO DAMAGE

The overall behavior of the porodamage problem is illustrated, identifying the influences of damage in the poroelastic problem, as well as, inversely, regarding the presence of a fluid in a damaged solid problem. To this end, examples inspired in the consolidation problems discussed in Section 4.2.1 are presented.

4.4.1. Poroelastic Column Subject to Damage

Let us accept a column of 10 m in height, unitary width (Figure 4.1), consisting of Berea sandstone, whose parameters are presented in Table 4.1. A distributed loading equal to 15 MN/m is progressively applied over 200 s, on the upper drainage face. The damage parameters estimated for the material are of Y_0=0.001 MPa and A=0.02 MPa. The problem in question is explored by varying the drainage conditions. The incorporation of the effects resulting from the damage process to calculate the mechanical properties of the porous medium, is also considered.

The responses regarding the four possible behaviors of the material are presented: elastic, poroelastic, elastic with damage and poroelastic coupled to damage (porodamage). It can be seen that the highest pore-pressure levels develop at the base of the column, hence strongly manifesting the problem of fluid diffusion, while, at the top of the column the damage problem is prevalent. Figure 4.25 shows the vertical strain curves over time at the base of the column.

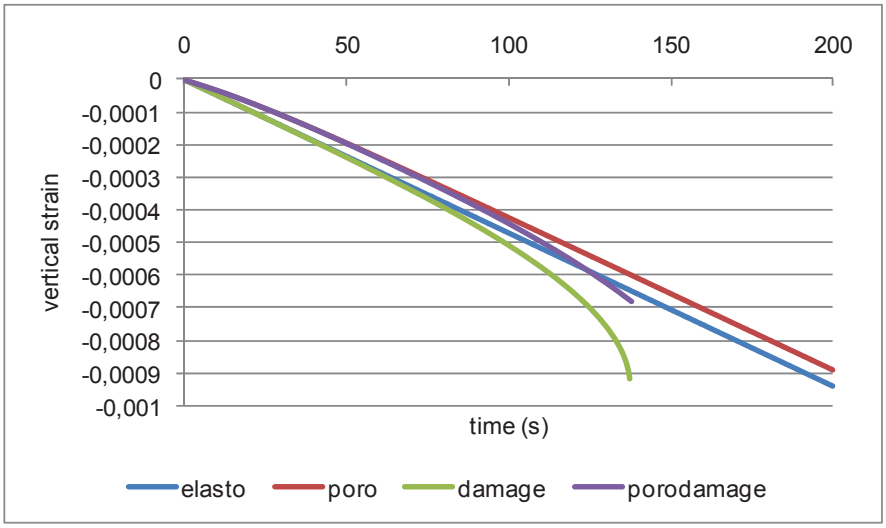

Figure 4.25 - Vertical strain evolution at the base of the column

In the elastic and poroelastic cases, the strains exhibit a similar behavior, except for the section corresponding to the initial 100 s in the poroelastic case, where the flow induces a non-linearity in the strain profile. The difference between these two curves represents the contribution of stiffness of the fluid phase. From the comparison between the cases of damage and porodamage in Figure 4.25, one notes that the presence of the fluid slows the damage process, which can also be seen in Figure 4.26.

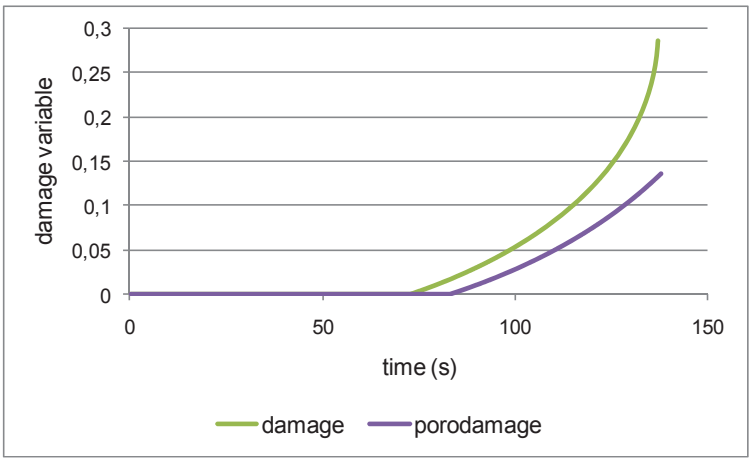

Figure 4.26 - Damage parameter evolution at the base of the column

In the damage and porodamage regimes the analysis is stopped at around 140 s, when the maximum load is reached (Figure 4.27). In future works we intend to implement a load control strategy to capture the post-peak behavior, as for instance the arc-length scheme.

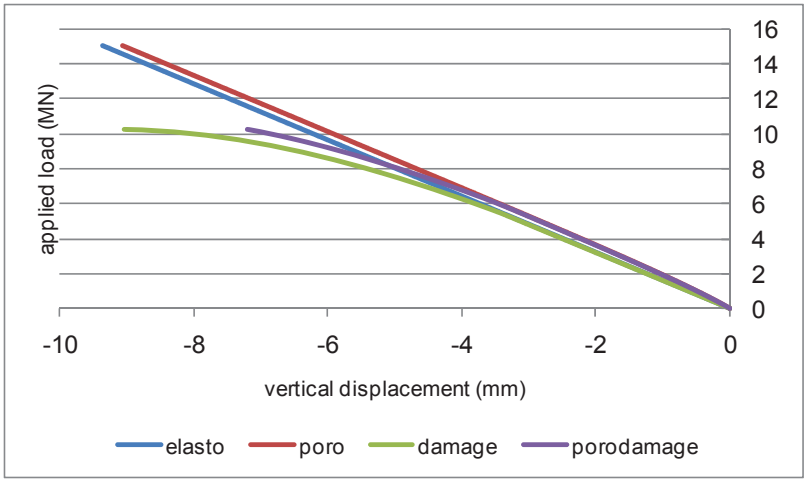

Figure 4.27 - Relationship between the load applied and displacement at the top of the column

It is interesting to note in Figure 4.28 the pore-pressure increase in the presence of damage, beyond the threshold defined in the poroelastic problem. Note in Figure 4.29 that the pore-pressure values are in the order of ten times smaller than the effective stress values at the base of the column.

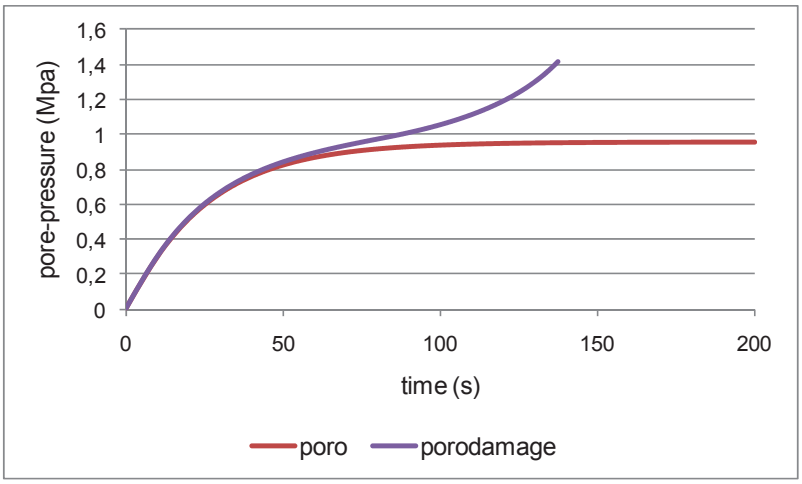

Figure 4.28 - Pore-pressure evolution at the base of the column

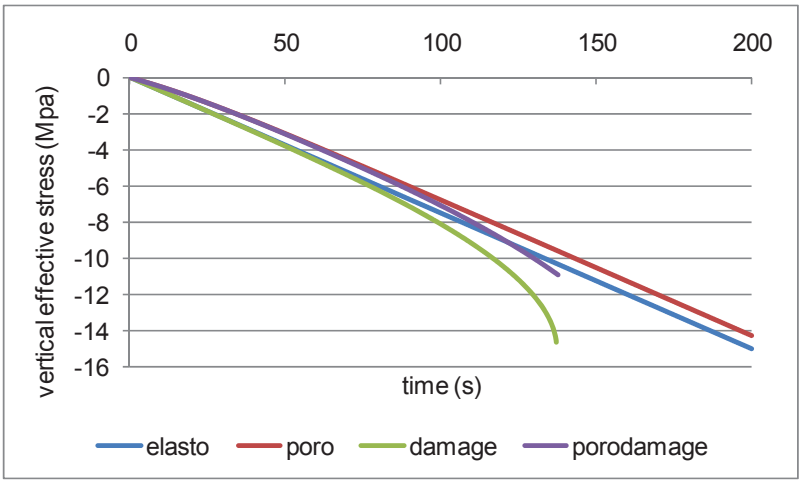

Figure 4.29 -Vertical effective stress evolution at the base of the column.

The overall behavior of the column essentially follows the profiles presented here for a base point, emphasizing that since the areas closer to the top of the column are examined, the damage effects prevail over the effects induced by the fluid flow .

In order to illustrate this general behavior, the distribution of the damage variable at the last instant of the analysis, at around 140 s, is shown in cases of damage and porodamage (Figure 4.30). In the same figure, the pore-pressure distribution in the poroelastic and porodamage case is shown, at the same instant.

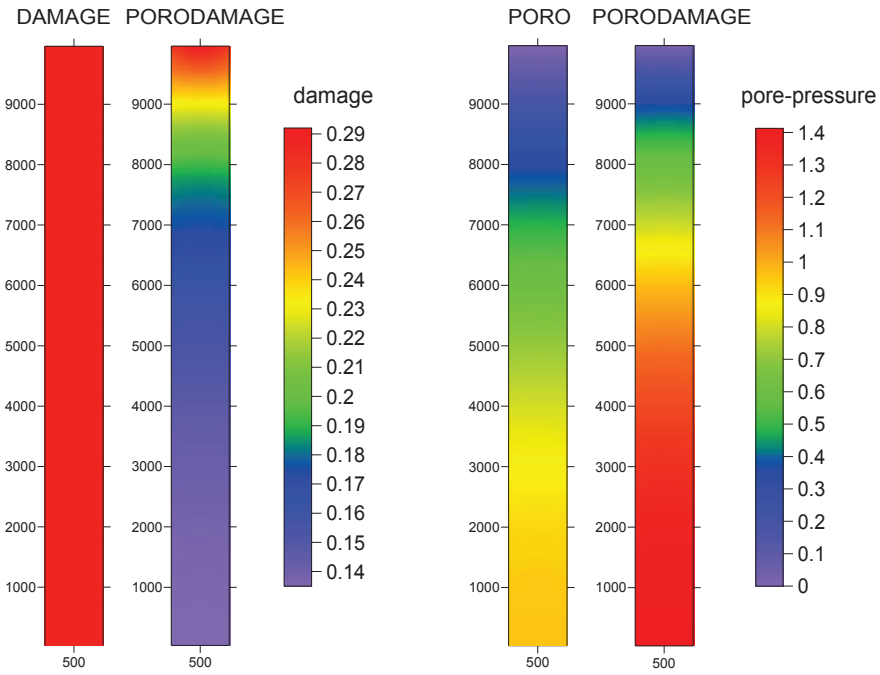

Figure 4.30 - Damage and pore-pressure values (MPa) at 140 s, for different regimes

Damage influence in the poroelastic parameters. In the analysis presented so far, the poroelastic parameters were kept at their nominal values, b=0,7778 and M=12641 MPa, calculated from the properties in Table 4.1.

Using the expressions proposed in Section 3.3, the influence of the material damage level in these parameters is evaluated. Figure 4.31, shows the variations of the parameters with damage at a point on the top of the column, where the damage level is maximum.

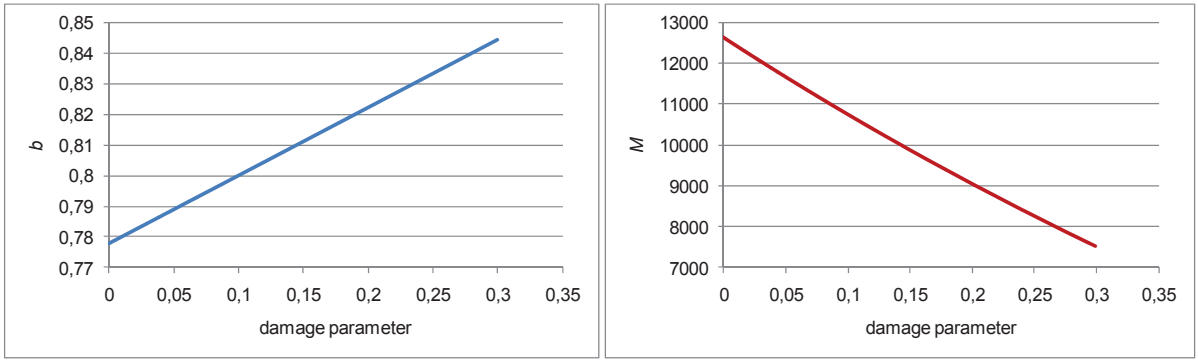

Figure 4.31 - Evolution of poroelastic parameters with the damage at the top of the column

There is a linear increase of the Biot coefficient with the damage parameter, and also a quasi-linear decrease of the Biot modulus. Figure 4.32 exhibits the distribution of the parameters over the column at the end of the analysis.

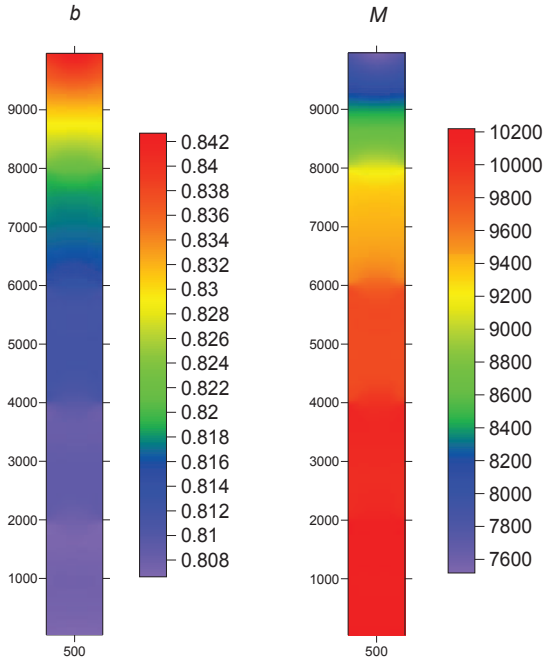

Figure 4.32 - Distribution of the poroelastic parameters at the end of the analysis, considering damage

The re-analysis of the problem of column was carried out, taking into account the evolution of Biot parameters over the analysis. It was found that, for the levels of applied loads, with which about 30% of damage was reached, the response of the problem was not significantly affected.

In order to understand the small influence of this updating of Biot parameters over the damage process in the column response, a limiting case is regarded. Let us assume the values b=0.842 and M=7500 MPa, which are the critical values calculated (see Figure 4.32), as the fixed parameters for the whole domain. The analysis of the problem on the simple poroelastic regime, with monotonic loading, leads to conclude that the problem is in fact not

very sensitive to the Biot parameter values. In the case of instantaneous loading, the influence of these parameters is somewhat more pronounced. This is illustrated in Figure 4.33, for the poroelastic case, comparing the responses obtained with the nominal values of the parameters, and with the penalized values.

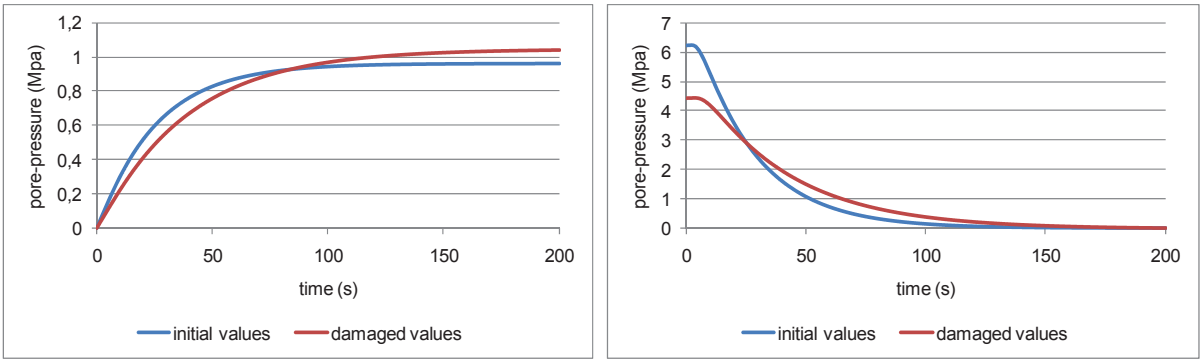

Figure 4.33 - Evolution of pore-pressures for a) monotonic loading and b) instantaneous loading

The analyses presented from this point forward include the updating of poroelastic parameters according to the damage state, along the time.

Analysis of the problem under undrained conditions. Now the analysis of the problem initially presented is proposed, impeding the fluid flow at the top of the column, that is, under undrained conditions. In this situation, regardless of the behavior adopted for the material, the response is uniform throughout the domain.

This type of boundary condition corresponds to the situation in which one can rely on the fluid stiffness throughout the whole loading process.

Considering Figure 4.34, in which the evolution of vertical strains in the column is exhibited, it can be seen that the problem in the porodamage regime is developed up to the end of the 200 s analysis. That is, the critical load defined by the damage model was not reached. The poroelastic response in the presence of damage is significantly defined by the diffusion process, under this fluid containment condition inside the body.

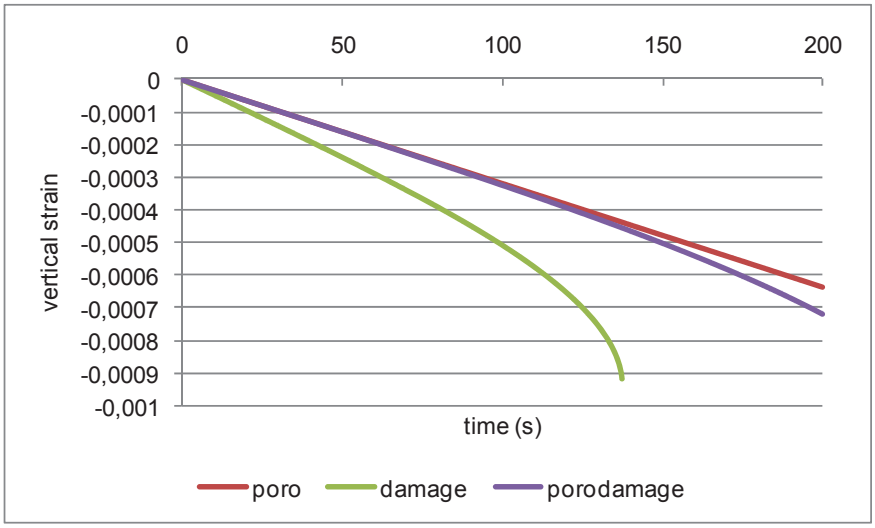

Figure 4.34 - Vertical strain evolution in the column

The smoothing of the damage process over time is seen in Figure 4.35, where the evolution of the state of damage is described, considering or not the presence of the fluid. The level of damage reached at the end of 200 s, around 15%, is similar to the lowest value of damage found in the column in drained conditions (Figure 4.30), within a time of around 140 s.

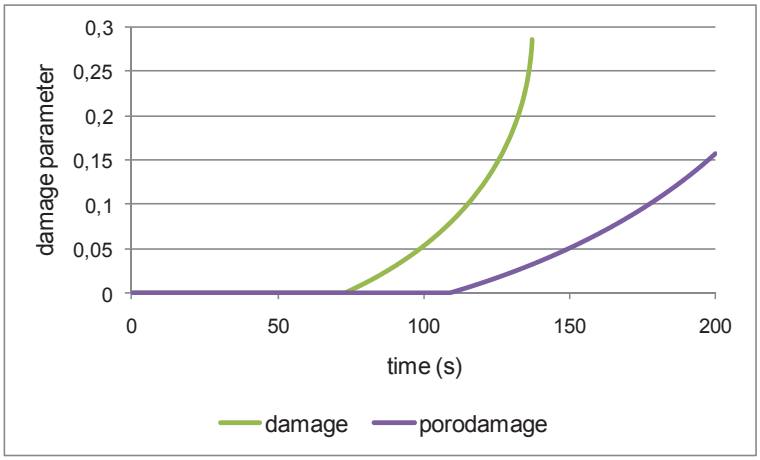

Figure 4.35 - Evolution of the damage variable in the column

It is interesting to note how much higher the values of pore-pressure shown in Figure 4.36 are, when compared to the equivalent under drained conditions, the data is in Figure 4.28.

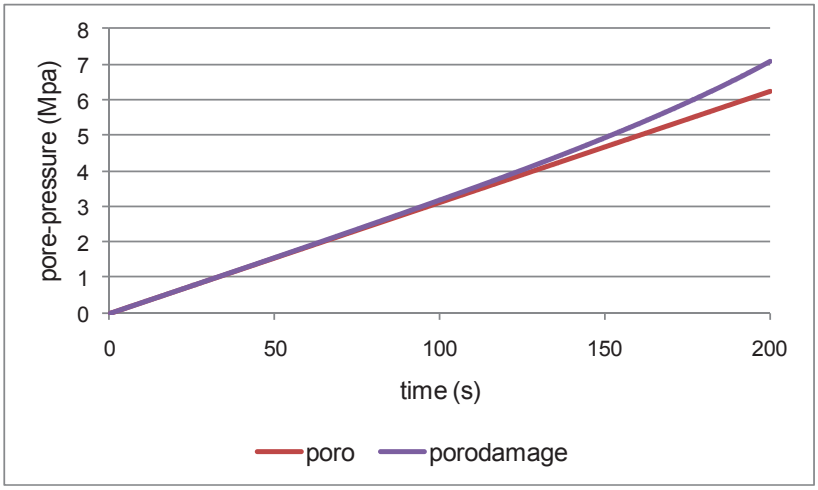

Figure 4.36 - Pore-pressure evolution in the column

4.4.2. Poroelastic Plane Domain subjected to Damage

It is proposed to analyze a plane problem, presented in Figure 4.37. It consists of a rectangular area, with 2 m wide and 1 m in height. A load of 20 MN is applied monotonically over 2 s, on impermeable plates placed on the top and bottom faces. The flow occurs only through the lateral faces. The boundary conditions of the problem are inspired by the problem of consolidation proposed by Mandel (1953). The constituent material is the sandstone already defined in section 4.4.1. The discretization used contains 24 boundary elements and 32 domain cells.

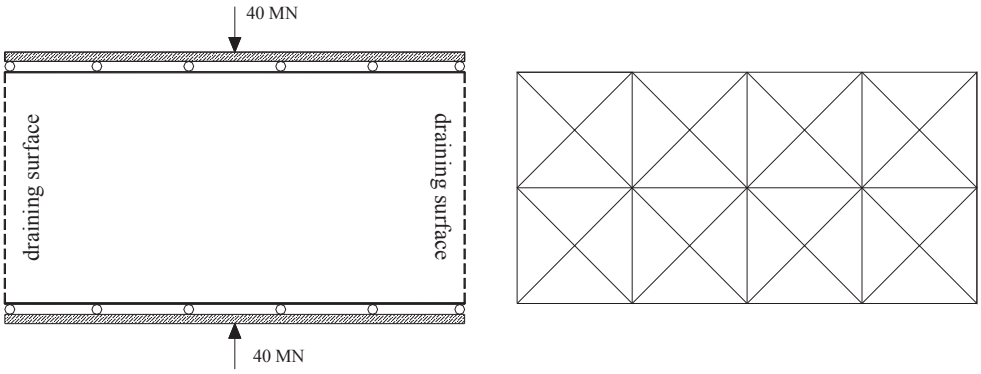

Figure 4.37 - Problem definition, adopted cells mesh

The central point of the domain is taken as reference for the analysis of the problem. Initially, we observe the behavior in the vertical direction along which the load is applied. Based on the graphs concerning to damage and porodamage regimes in Figure 4.38, it can be seen the influence of the fluid as mitigation in the evolution of the strains on the solid skeleton, in the presence of damage.

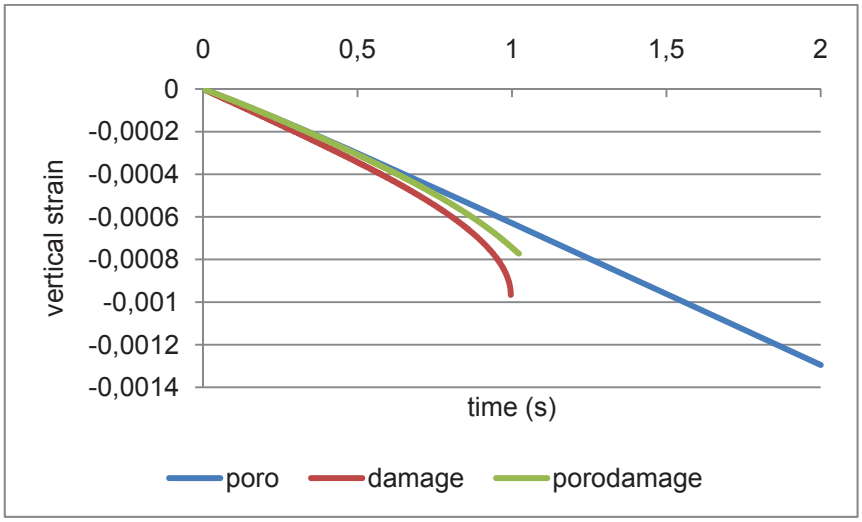

Figure 4.38 - Vertical strain evolution at the central point

The analysis of Figure 4.39 allows to visualize that the coupled behavior (porodamage) is governed initially by the poroelastic regime, going to suffer the effects of damage, which starts at around 0.6 s analysis (see Figure 4.41).

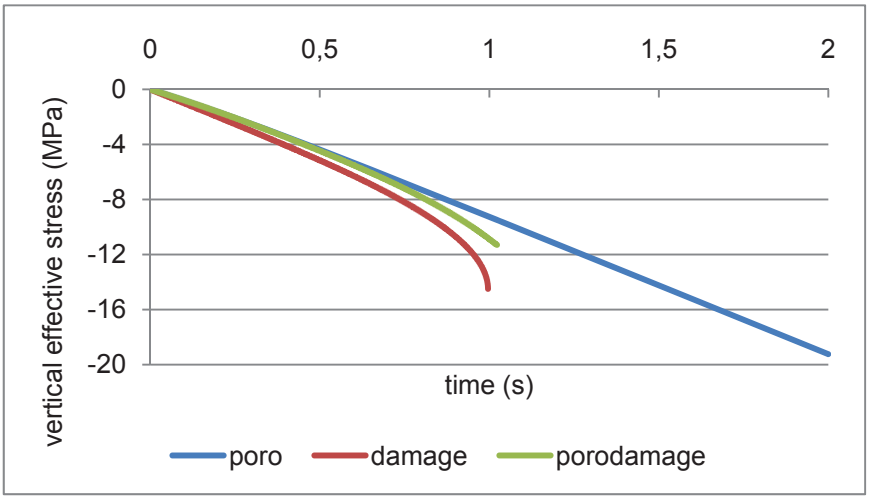

Figure 4.39 - Vertical effective stress evolution at the central point

From around 0.6 s the pore-pressure starts to evolve coupled to the damage level on the material, as shown in Figures 4.40 and 4.41 in which it can be seen that the damage initiation, as well as its intensity, are delayed along the time, in the porodamage regime

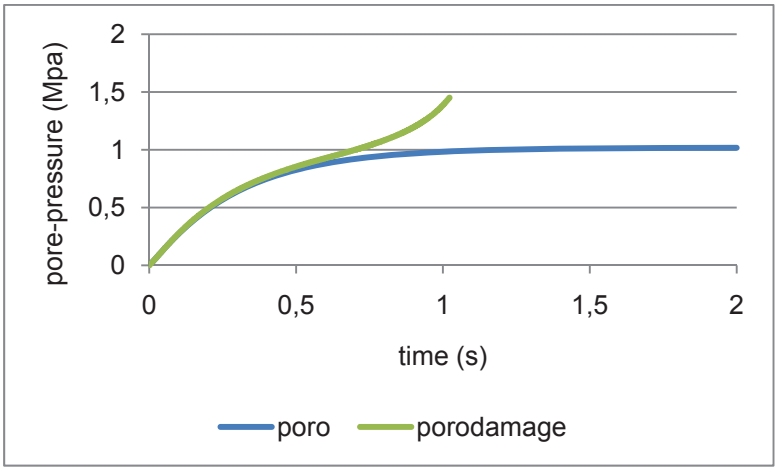

Figure 4.40 – Pore-pressure evolution at the central point

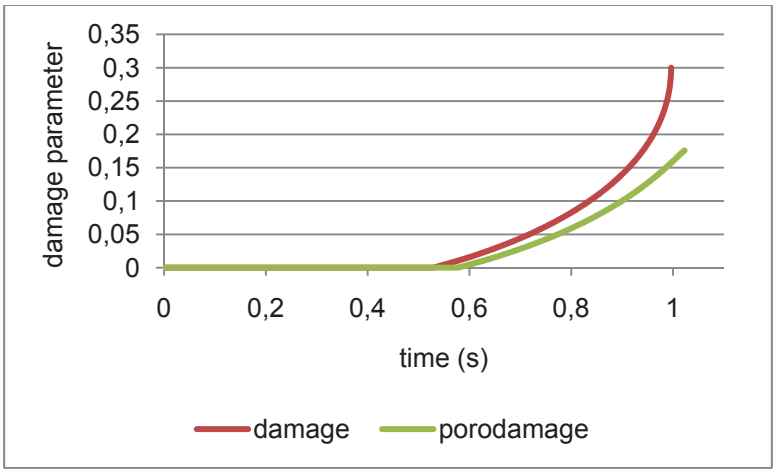

Figure 4.41 – Damage parameter evolution at the central point

Consider now the problem response along the horizontal direction, also measured at the center of the domain. Figure 4.42 shows the evolution of horizontal strain over time, considering the different material behaviors.

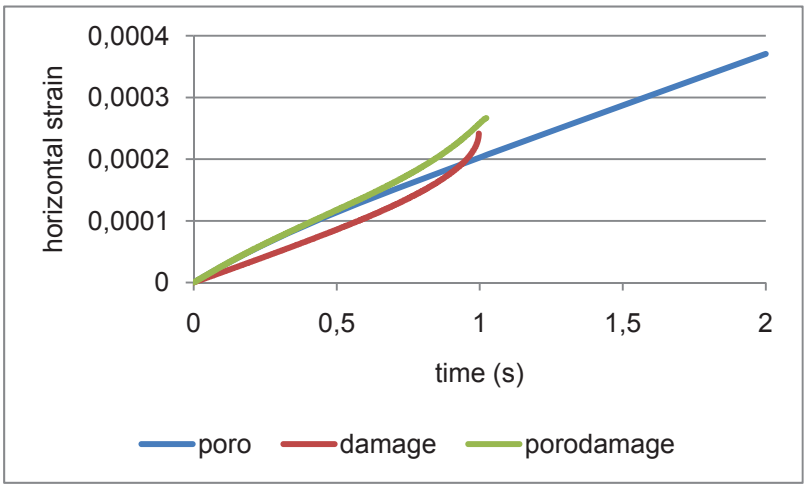

Figure 4.42 – Horizontal strain evolution at the central point

Considering that this is not the direction of load application, the effects of loading are manifested only partially in the horizontal direction, due to Poisson's effect. However, the fluid flows preferentially along horizontal direction, due to the imposed boundary conditions.

The comparison between the strain curves regarding the damage and porodamage regimes in Figure 4.42, allows the verification of the predominance of the effects due to the presence of fluid. The horizontal strains induced in the poroelastic case are higher than those caused in the damage case over the major part of the analysis.

The values of effective stress in horizontal direction are negligible, considering the boundary conditions of the problem. From Figure 4.43 we observe the increase in effective stress caused by the consideration of the damage in poroelastic problem.

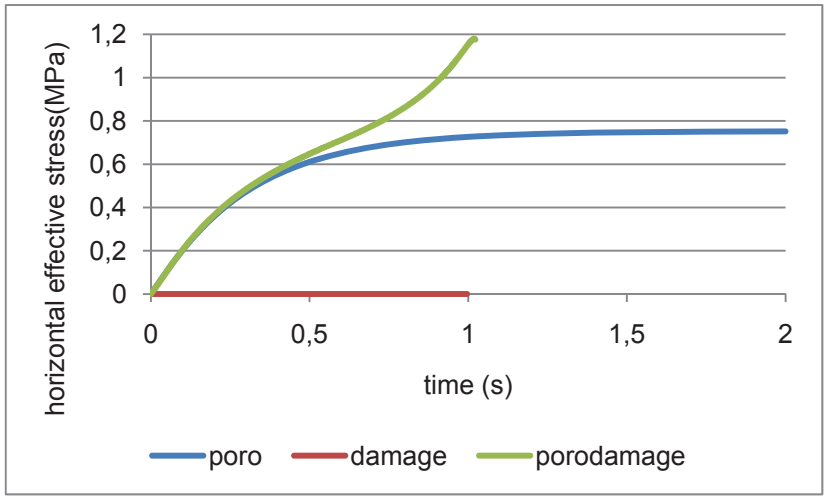

Figure 4.43 – Horizontal effective stress evolution at the central point

In order to illustrate conclusively the difference between the measured responses in the central point along the two coordinate directions, it is presented in Figures 4.44 and 4.45 the evolution of the parts of stress tensor, admitting the porodamage coupled regime. The predominance of the poroelastic behavior along the horizontal direction becomes clear.

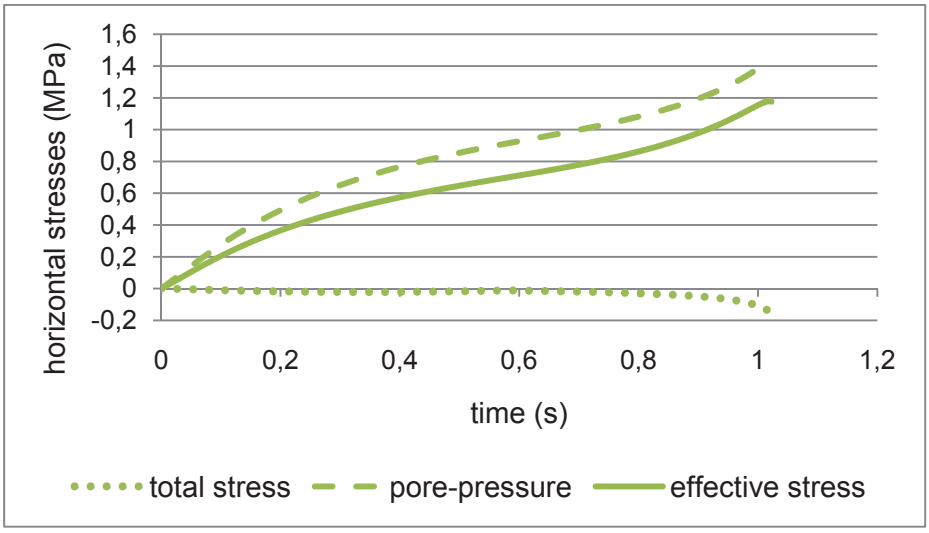

Figure 4.44 – Stress balance in the horizontal direction, at the central point

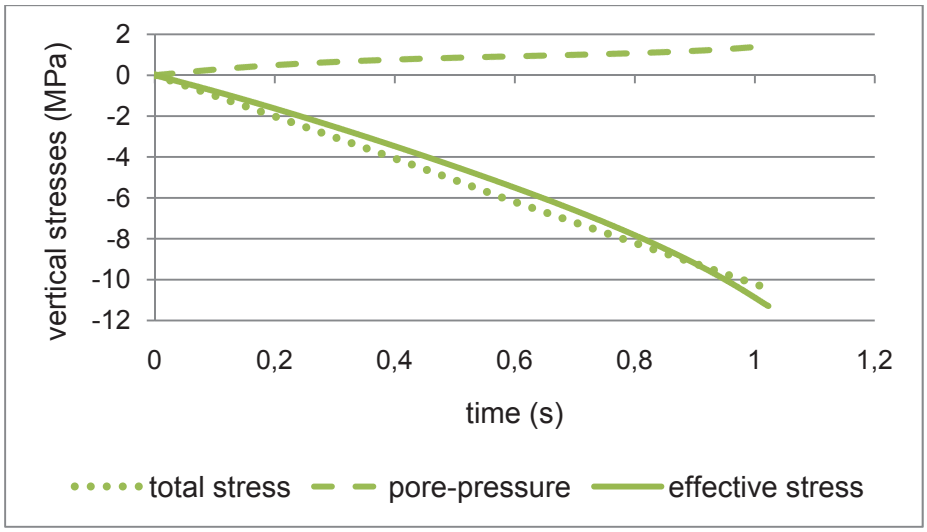

Figure 4.45 – Stress balance in the vertical direction, at the central point

4.4.3. Brief Comments on Shallow and Deep Foundation Structures

Based on Schiffman's problem, presented in 4.2.2, it is proposed here to analyze that semi-infinite domain, subject to a loading of 10 MN / m, applied monotonically over 100 s, considering the effects of damage on the solid matrix. It is assumed that the constituent material is Berea sandstone, and that the domain is saturated by water. It is admitted that this problem reasonably reproduces the conditions of service of a shallow foundation structure along the construction of a building, in a reduced timescale.

A second problem concerning to a deep foundation structure dug in Berea sandstone is also analyzed in order to compare the responses of rock mass in both situations. It is assumed that a single pile transmits the loading at 10 m deep. Analogously to the shallow foundation problem, the simulation is carried out over the half-space, due to the simmetry. Figure 4.46 illustrates the proposed problems.

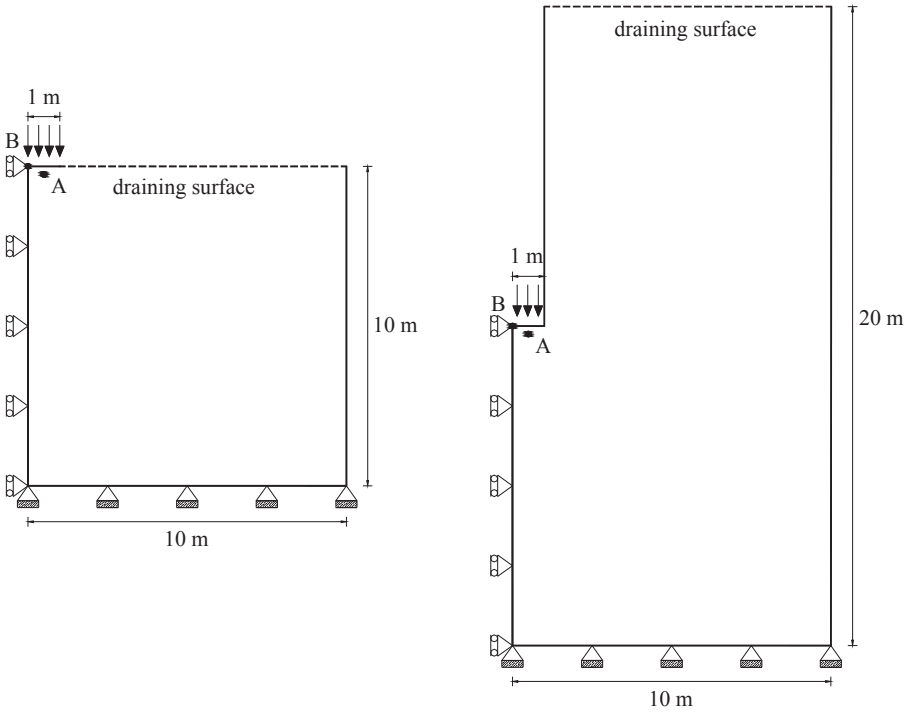

Figure 4.46 - Problem definition for a) shallow foundation and b) deep foundation

The material is considered in the porodamage regime. The points A (0.5,9.75) and B (0,10) are taken as reference. The damage evolution curves of these points are plotted in Figures 4.47 and 4.48, corresponding to the different foundations.

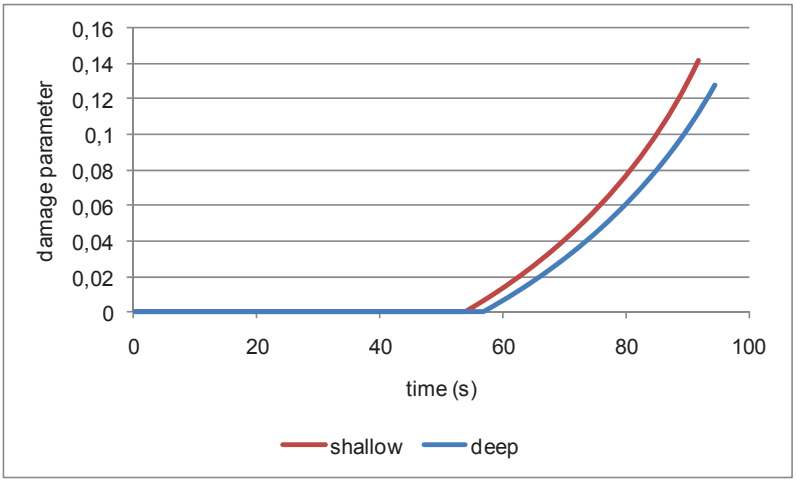

Figure 4.47 - damage evolution at the point A

It can be noted that the damage levels at the both points are higher on the shallow foundation case. The fluid remains more time trapped in the domain corresponding to deep foundation, smoothing the damage process along the time.

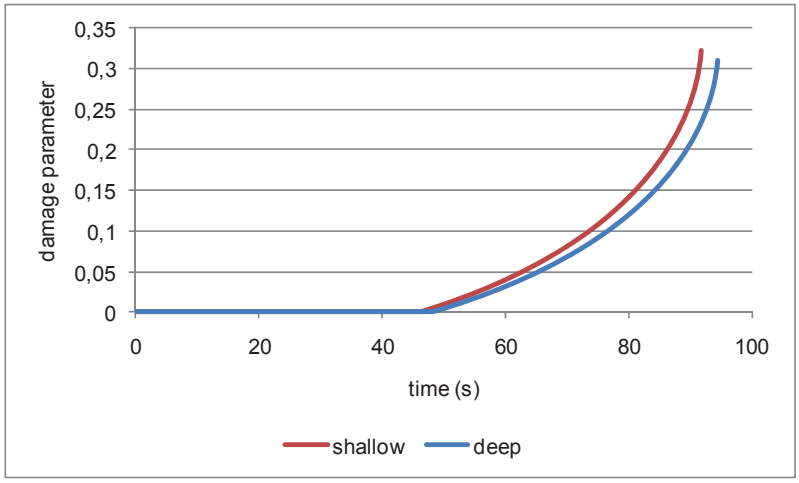

Figure 4.48 - damage evolution at the point B

The point B undergoes the critical level of damage, as can be seen in Figure 4.49, which shows the damage field on the affected region, in the load vicinity, for the two cases considered. From the Figure, it can be note that the damage process starts around 50 s, and reaches the peak value at 91.7 s in the shallow foundation case. At this instant, the damage level induced by the pile, on deep foundation problem, is around 22%. In this case, the peak value of damage parameter is reached at around 95 s of analysis.

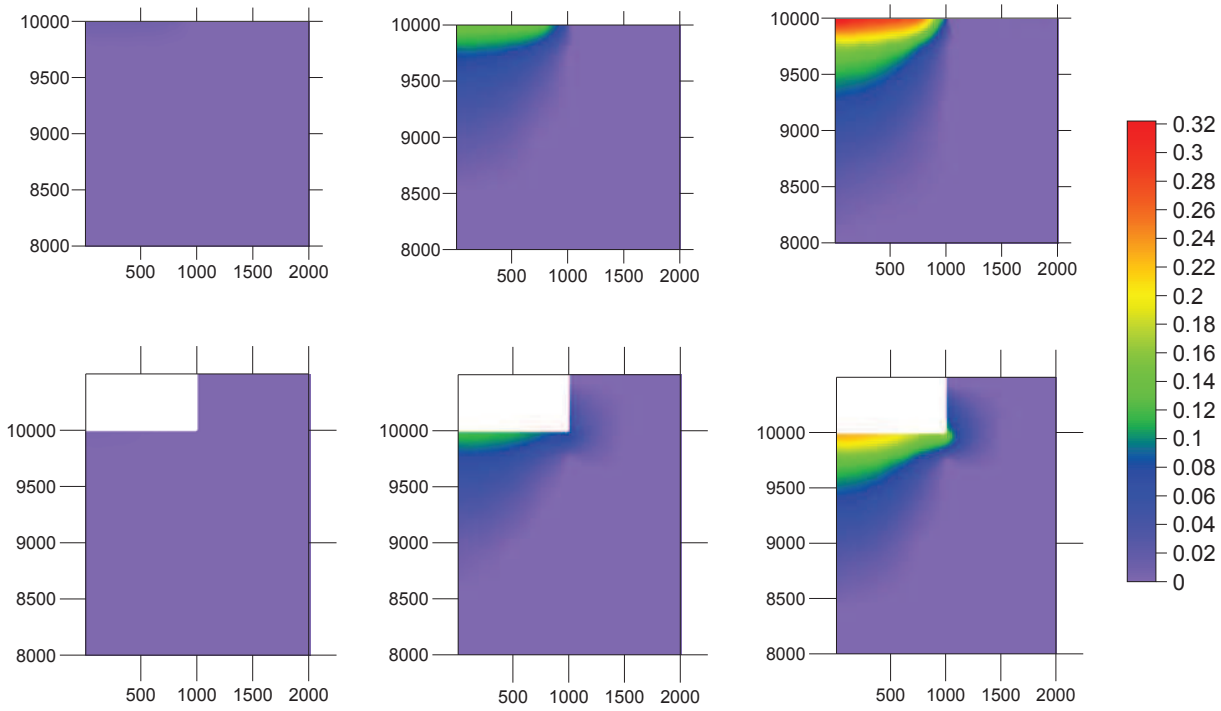

Figure 4.47 - Damage evolution in deep and shallow foundations at 50 s; 80 s; 91.7 s

Conclusions and Perspectives

A linear poroelastic modelling provides good results for the pore-pressure variation and accurately assesses the displacements in a porous medium, under instantaneous loading conditions. However, as shown in experimental studies of rocks and soils, in a loading condition over time (monotonic), the stress-strain relationship is not well represented in the linear poroelasticity theory. Thus, the interest arises to incorporate models of plasticity and/or damage on the poroelastic formulation.

A boundary element method formulation for the analysis of saturated porous media subject to an isotropic damage process was presented. Considering the abundant number of experimental and theoretical studies on the subject, it is understood that one of the contributions of this work was to develop a computational tool that can be applied to the simulation of various engineering problems.

The results show that the presence of fluid in a porous solid matrix subject to damage induces a degree of delay and attenuation in the evolution of the degradation levels. However, considering the damage occurrence in the solid skeleton of the poroelastic problem substantiates increasing the pore-pressure values.

In this study, the damage process in the porous medium was dealt with in a simplistic way, in order to safely perform the coupling technique. Thus, the procedure of how to carry out the coupling between models for poroelasticity and isotropic damage in a BEM formulation was accurately illustrated.

According to the literature, the damage occurs quite differently in various porous materials. For future works, studies on specific classes of materials are indicated, in order to better understand the mechanisms of deformation and rupture of these materials, adopting or proposing suitable nonlinear constitutive models. Throughout this text, some works that can serve as a basis for this purpose were listed, especially those relating to the experimental behavior of soils and rocks.

One of the important features to be explored is the variation of permeability observed during the occurrence of damage. Therefore, another line to be explored in future initiatives is the detailed study and implementation of evolution laws for permeability based on experimental results, giving rise to more complete coupled poro-damage models.

It should be noted that the code generated indicates interesting applications, such as the analysis of the mechanical behavior of building foundations, which are influenced not only by the stiffness of the skeleton, but also by the permeability of the support medium (soil or rock).

BIBLIOGRAPHY[1]

ARAMAKI, G., YASUHARA W. Applications of the boundary element method for axysymmetric Biot's consolidation. *Engineering Analysis with Boundary Elements*, v. 2, 1981, p.184-191.

ARSON, C. *Etude théorique et numérique de l'endommagement thermo-hydro-mécanique des milieux poreux non saturés*. Paris: L'Ecole Nationale des Ponts et Chaussées, 2009, 398 p. Ph.D. Thesis in Geotechnical Sciences.

ARSON, C., GATMIRI, B. A mixed damage model for unsaturated porous media. *Comptes Rendus de Mécanique*, v. 337, série 2, 2009, p. 68-74.

AURIAULT, JL., SANCHEZ-PALENCIA, E. Etude du comportement macroscopique d'un milieu poreux saturé déformable. *Journal de Mécanique*, v. 16, 1977, p. 575-603.

BART, M., SHAO, JF., LYDZBA, D. Poroelastic behaviour of saturated brittle rock with anisotropic damage. *International Journal for Numerical and Analytical Methods in Geomechanics*, v. 24, 2000, p. 1139-1154.

BARY, B. *Etude du couplage hydraulique-mécanique dans le béton endommagé: application au calcul de barrages*. Cachan: L'Ecole Normale Superieure de Cachan, 1996, 156 p. Ph.D. Thesis in Civil Engineering.

BAZANT, ZP. Why Continnum damage is nonlocal : micromechanics arguments. *Journal of Engineering Mechanics*, v. 117, 1991, p. 1070-1087.

BAZANT, ZP., PIJAUDIER-CABOT, G. Nonlocal continuum damage, localization instability and convergence. *Journal of Applied Mechanics*, v. 55, 1988, p. 287-293.

BENALLAL, A., BILLARDON, R., GEYMONAT, G. Some mathematical aspects of the damage softening rate problem. In MAZARS, J., BAZANT, Z.P., ed. *Cracking and Damage*. Amsterdam : Elsevier, 1991, p. 247-258.

BENALLAL, A., BILLARDON, R., GEYMONAT, G. Bifurcation and localization. Rate-independent materials, some general considerations. *CISM Courses and Lectures*, v. 327, 1992, p. 1-44.

[1] According to the International Organization for Standardization

BENALLAL, A., FUDOLI, CA., VENTURINI, WS. An implicit BEM formulation for gradient plasticity and localization phenomena. *International Journal for Numerical Methods in Engineering*, v. 53, 2002, p. 1853-1869.

BENALLAL A., BOTTA AS., VENTURINI, WS. On the description of localization and failure phenomena by the boundary element method. *Computational Methods Applied to Mechanical Engineering*, v. 195, 2006, p. 5833-5856.

BIOT, MA. General theory of three-dimensional consolidation. *Journal of Applied Physics*, v. 12, 1941, p. 155-164.

BIOT, MA. Theory of elasticity and consolidation for a porous anisotropic solid. *Journal of Applied Physics*, v. 26, 1955, p. 182-185.

BIOT, MA., CLINGAN, FM. Consolidation settlement of a soil with an impervious top surface. *Journal of Applied Physics*, v. 12, 1941, p. 578-581.

BIOT, MA., CLINGAN, FM. Bending settlement of a slab resting on a consolidating foundation. *Journal of Applied Physics*, v. 13, 1942, p. 35-40.

BONNET, M., MUKHERJEE, S. Implicit BEM formulation for usual and sensitivity problems in elasto-plasticity using the consistent tangent operator concept. *International Journal of Solids and Structures*, v. 33, 1996, p. 4461-4480.

BORBA, GL. Formulação direta do método dos elementos de contorno para tratamento do estado plano da poroelasticidade acoplada. Campinas: Universidade de Campinas, 1992, 146 p. Ph.D. Thesis in Mechanical Engineering.

BOTTA, AS. Método dos Elementos de Contorno para Análise de Corpos Danificados com Ênfase no Fenômeno da Localização de Deformações. São Carlos: Escola de Enegnahria de São Carlos, 2003, 170 p. Ph.D. Thesis in Civil Engineering.

BOTTA AS., VENTURINI WS., BENALLAL A. BEM applied to damage models emphasizing localization and associated regularization techniques. *Engineering Analysis with Boundary Elements,* v. 29, 2005, p. 814-827.

BREBBIA, CA. *The Boundary element method for engineers.* London: Pentech Press, 1978.

BREBBIA, CA. Weighted residual classification of approximate methods. *Applied Mathematical Modelling*, v. 2. 1978, p. 160-164.

CAVALCANTI, MC., TELLES, JCF. Biot's Consolidation Theory – Application of BEM with time independent fundamental solutions for poro-elastic saturated media. *Engineering Analysis with Boundary Elements*, v. 27, 2003, p. 145-157.

CHATEAU X., DORMIEUX L. Approche micromécanique du comportement d'un milieu poreux non saturé. *Comptes Rendus de l'Académie des Sciences*, v. 326, Série II, 1998, p. 533-538.

CHENG, AH-D., LIGGETT, JA. Boundary integral equation method for linear porous-elasticity with applications to soil consolidation. *International Journal for Numerical Methods in Engineering*, v. 20, 1984, p. 255-278.

CHENG AH-D., LIGGETT JA. Boundary integral equation method for linear porous-elasticity with applications to fracture propagation. *International Journal of Numerical Methods in Engineering*, v. 20, 1984, p. 279-296.

CHENG, AH-D., PREDELEANU, M. Transient boundary element formulation for linear poroelasticity. *International Journal of Applied Mathematical Modelling*, v. 11, 1987, p. 285-290.

CHENG, AH-D., DETOURNAY, E. On singular integral equations and fundamental solutions of poroelasticity. *International Journal of Solids and Structures*, v. 35, 1998, p. 4521-4555.

CHENG H., DUSSEAULT MB. Deformation and diffusion behaviour in a solid experiencing damage: a continous damage model and its numerical implementation. *International Journal of Rock Mechanics and Mining Science and Geomechanics*, v. 30, 1993, p. 1323-1331.

CLEARY, MP. Fundamental solutions for a fluid-saturated porous solid. *International Journal of Solids and Structures*. v. 13, 1977, p. 785-806.

COMI, C., BERTHAUD, Y., BILLARDON, R. On localization in ductile-brittle materials under compressive loadings. *European Journal of Mechanics and Solids*, v. 14, 1995, p. 19-43.

COUSSY, O. *Mechanics of porous continua*. Chichester : John Wiley and Sons, 1995.

COUSSY, O., DORMIEUX, L., DETOURNAY E. From mixture theory to Biot's approach for porous media. *International Journal of Solids and Structures*, v. 35, 1998, p. 4619-4635.

COUSSY, O. *Poromechanics*. Chichester: John Wiley and Sons, 2004.

CRUSE, TA. Numerical solutions in three-dimensional elastostatics. *International Journal of Solids and Structures*, v. 5, 1969, p. 1259-1274.

CRUSE, TA. Aplication of the boundary-integral equation method to three dimensional stress analysis. *Computers and Structures*, v. 3, 1973, p. 509-527.

CRUSE, TA. An improved boundary-integral equation method for three dimensional elastic stress analysis. *Computers and Structures*, v. 4, 1974, p. 741-754.

CRYER, C.W. A comparison of the three-dimensional consolidation theories of Biot and Terzaghi. *Quarterly Jounal of Mechanics and Applied Mathematics*, v. 16, 1963, p. 401-412.

DARGUSH, GF., BANERJEE, PK. A time domain boundary element method for poroelasticity. *International Journal of Numerical Methods in Engineering*, v. 28, 1989, p. 2423-2449.

DARGUSH, GF., BANERJEE, PK. A boundary element method for axisymmetric soil consolidation. *International Journal of Solids and Structures*, v. 28, 1991, p. 897-915.

DETOURNAY, E., CHENG, AH-D. Fundamentals of Poroelasticity. In *Comprehensive Rock Engineering: Principles, Practice and Projects*, v. II, Analysis and Design Method, C. Fairhurst (Ed.), Pergamon Press, 1993.

DORMIEUX L., KONDO, D. Approche micromécanique du couplage perméabilité-endommagement. *Comptes Rendus de Mécanique*, v. 332, 2004, p. 135-140.

DORMIEUX L., KONDO, D., ULM, F. A micromechanical analysis of damage propagation in fluid-saturated cracked media. *Comptes Rendus de Mécanique*, v. 334, 2006, p. 440-446.

FREDHOLM, L. Sur une classe d'equations fonctionelles. *Acta Mathematica*, v.27, 1903, p. 365-390.

FREDHOLM, L. Solution d'un problème fondamental de la theorie de l'élasticité. Arkiv for matematik. *Astromi och Fysik*, v. 2, 1906, p. 3-8.

FUDOLI, CA. *Formulação do método dos elementos de contorno e plasticidade com gradiente*. São Carlos: Escola de Engenharia de São Carlos, Universidade de São Paulo, 1999, 151 p. Ph.D. Thesis in Civil Engineering.

GARCIA R., FLOREZ-LOPEZ J., CERROLAZ M. A boundary element formulation for a class of non-local damage models. *International Journal of Solids and Structures,* v. 36, 1999, p. 3617-3638.

GHABEZLOO, S., SULEM, J., SAINT-MARC, J. Evaluation of a permeability-porosity relationship in a low permeability creeping material using a single transient test. *International Journal of Rock Mechanics and Mining Sciences*, v. 46, 2009, p. 761-768.

HAMIEL Y. *et al.* Stable and unstable damage evolution in rocks with implications to fracturing of granite. *International Journal of Geophysics*, v. 167, 2006, p. 1005-1016.

HERDING U., KUHN G. A field boundary element formulation for damage mechanics. *Engineering Analysis with Boundary Elements*, v. 18**,** 1996, p. 137-147.

JANSON, J.; HULT, J. Fracture mechanics and damage mechanics: a combined approach. *Journal de Mécanique Appliquée*, v. 1, 1977, p. 69-84.

JIRÁSEK, M. Objective modeling of strain localization. *Revue Française de Génie Civil*, v. 6, 2002, p. 1119-1132.

KACHANOV, LM. Time of rupture process under creep conditions. *Izvestia Akademii Nauk*, n. 8, 1958, p. 26-31.

KAMALIAN, M., GATMIRI, B., SHARAHI, M. J. Time domain 3D fundamental solutions for saturated poroelastic media with incompressible constituents. *Communications in Numerical Methods in Engineering*, v. 24, 2008, p. 749-759.

KUROKI T., ITO T., ONISHI K. Boundary Element Method in Biot's Linear Consolidation. *International Journal of Applied Mathematical Modelling*, v. 6, 1982, p. 105-110.

LACHAT, JC. *A Further Development of the Boundary Integral Technique for Elastostatics*. Southampton : Southampton University, 1975. Tese de Doutorado.

LEMAITRE, J. *A Course on Damage Mechanics*. Berlin : Springer-Verlag, 1992.

LEMAITRE, J., CHABOCHE, JL. *Mécanique des Matériaux Solides*. Paris: Dunod, 1985.

LIN, F-B., *et al.* Nonlocal strain-softening model of quasi-brittle materials using boundary element method. *Engineering Analysis with boundary elements*, v. 26, 2002, p. 417-424.

LYDZBA, D., SHAO, JF. Study of poroelasticity material coefficients as response of microstructure. *Mechanics of Cohesive-frictional Materials*, v. 5, 2000, p. 149-171.

MANDEL, J. Etude mathématique de la consolidation des sols. In: *acts du colloque international de mécanique*, Poitier, France, v. 4, 1950. p. 9–19.

MANDEL, J. Consolidation des sols (étude mathématique). *Geotechnique*, v. 3, 1953, p. 287–299

MAGHOUL P., GATMIRI B., DUHAMEL D. Three dimensional transient thermo-hydro-mechanical fundamental solutions of unsaturated soils. *International Journal for Numerical and Analytical Methods in Geomechanics*, v. 34, 2010, p. 297-329.

MARIGO JJ. Formulation d'une loi d'endommagement d'un materiau élastique, *Comptes Rendus de l'Académie des Sciences*, v. 292 série II, 1981, p. 1309-1312.

MCNAMEE, J., GIBSON, RE. Plane strain and axially symmetric problems of the consolidation of a semi-infinite clay stratum. *Quarterly Journal of Mechanics and Applied Mathematics*, v. 13, 1960, p. 210-227.

MCNAMEE, J., GIBSON, RE. A three-dimensional problem of the consolidation of a semi-infinite clay stratum. *Quarterly Journal of Mechanics and Applied Mathematics*, v. 16, 1963, p. 155-127.

NISHIMURA, N., KOBAYASHI, S. A Boundary Integral Equation Method for Consolidation Problems. *International Journal of Solids and Structures*, v. 25, 1989, p. 1-21.

PARK, KH., BANERJEE, PK. Two- and three-dimensional soil consolidation by BEM via particular integral. *Computer Methods Applied Mechanics and Engineering*, v. 191, 2002, p. 3233-3255.

PIJAUDIER-CABOT, G., BENALLAL, A. Strain Localization and Bifurcation in a Nonlocal Continuum. *International Journal of Solids and Structures*, v. 30, 1993, p. 1761-1775.

PIJAUDIER-CABOT, G., BAZANT, ZP. Nonlocal damage theory. *Journal of Engineering Mechanics*, v. 113, 1987, p. 1512-1533.

POON, H., MUKHERJEE, S., BONNET, M. Numerical implementation of a CTO-based implicit approach for the BEM solution of usual and sensitivity problems in elasto-plasticity. *Engineering Analysis with Boundary Elements*, v. 22, 1998, p. 257-269.

PROENÇA, S.P. *Elementos de Mecânica do Dano em Meios Contínuos*. Lecture notes. São Carlos, Universidade de São Paulo, 2001.

RENDULIC, L. Porenziffer und porenwasserdrunk in tonen, *Der Bauingenieur*, v. 17, 1936, p. 559 - 564.

RICE, JR., CLEARY, MP. Some Basic Stress-Diffusion Solutions for Fluid Saturated Elastic Porous Media with Compressible Constituents. *Reviews of Geophysics and Space Physics*, v. 14, 1976, p. 227-241.

RIZZO, FJ. An Integral Equation Approach to Boundary Value Problems of Classical Elastostatics. *Quarterly Applied Mathematics*, v. 25, 1967, p. 83-95.

RIZZO, FJ., SHIPPY, DJ. A Formulation and Solution Procedure for the General Non-Homogeneous Elastic Inclusion Problem. *International Journal of Solids and Structures*, v. 4, 1968, p. 1161-1179.

RUTQVIST, J. Modeling of Damage, Permeability Changes and Pressure Responses during Excavation of the TSX Tunnel in Granitic Rock at URL, Canada. Lawrence Berkeley National Laboratory: Lawrence Berkeley National Laboratory. Paper LBNL-921E, 2009.

SCHIFFMAN RL., CHEN TF., JORDAN JC. An Analysis of Consolidation Theory. *Journal of Soil Mechanics and Foundation Division*, v. 95, 1969, p. 285-309.

SELVADURAI, APS. On the mechanics of damage-susceptible poroelastic media. *Key engineering Materials*, v. 251-252, 2003, p. 363-374.

SELVADURAI, APS., SHIRAZI, A. The Fluid-filled Spherical Cavity in a Damage-susceptible poroelastic medium. *International Journal of Damage Mechanics*, v. 13, 2004, p. 347-370.

SHAO, JF. *et al.* Continous damage modelling in saturated porous media. In *13th ASCE Engineering Mechanics Division Conference*. The Johns Hopkins University Baltimore, MD, USA June 13-16, 1999 , 6 p.

SIMO, JC., TAYLOR, RL. Consistent tangent operators for rate-independent elastoplasticity. *Computer Methods in applied mechanics and Engineering*, n. 48, 1985, p. 101-118.

SIMO, JC., HUGES, TJR. Formulation of finite elasticity with independent rotations. *Computer Methods in applied mechanics and Engineering*, v. 95, 1992, p. 277-288.

SLADEK, J., SLADEK, V., BAZANT, Z. P. Non-local boundary integral formulation for softening damage. *International Journal for Numerical Methods in Engineering*, v. 57, 2003, p. 103-116.

SCHIFFMAN, RL., FUNGAROLI, AA. Consolidation due to tangential loads. In *Proceedings of Sixth International Conference on Soil Mechanics and Foundation Engineering*, Montreal, 1965, v.1, p.188-192.

SOULEY, M., *et al.* Damage-induced permeability changes in granite: a case example at the URL. *Canada International Journal of Rock Mechanics and Mining Sciences*, v. 38, 2001, p. 297-310.

TANG C. A., *et al.* Coupled analysis of flow, stress and damage (FSD) in rock failure. *International Journal of Rock Mechanics and Mining Sciences*, v. 39, 2002, p. 477-489.

TELLES, JCF., BREBBIA, CA. On the application of the boundary element method to plasticity. *Applied Mathematics Modelling*, v. 3, 1979, p. 466-470.

TELLES, JCF., BREBBIA, CA. Elastoplastic boundary element analysis. In *Proceedings of Europe-U.S. Workshop on Nonlinear Finite Element Analysis in Structural Mechanics*, Wunderlich, W. *et al.* (Eds.), Springer-Verlag.1980.

TELLES, JCF., BREBBIA, CA. The Boundary element method in plasticity. *New developments in boundary element methods*, Brebbia, C.A. (Ed.), CML, 1980.

TERZAGHI, K. Die Berechnung der durchlassigkeitsziffer des tones aus dem verlauf der hydrodynamischen spannungserscheinungen. Sitz. Akad. Wissen., Wien Math. Naturwiss. Kl., Abt. IIa, v. 132, 1923, p. 125-138.

VASCONCELOS, RB. *Implementação de modelo de dano isotrópico aplicado a problemas acoplados hidro-geomecânicos*. Recife: Universidade Federal de Pernambuco, 2007, 117 p. M.Sc. Dissertation in Civil Engineering.

VENTURINI, WS. *Application of the boundary element formulation to solve geomechanical problems*. Southampton: University of Southampton, 1982, Ph.D. Thesis in Civil Engineering.

VENTURINI, WS. *Boundary element methods in geomechanics (lectures notes in engineering).* Berlin, Heidelberg, New York and Tokio : Springer-Verlag, 1984.

VENTURINI, WS. Um estudo sobre o método dos elementos de contorno e suas aplicações em problemas de engenharia. São Carlos: Universidade de São Paulo, 1988, Habilitation Thesis.

VENTURINI, WS., BREBBIA, CA. Some applications of the boundary element methods in geomechanics. *International Journal for Numerical and Analytical Methods in Geomechanics*, v. 7, 1983, p. 419-434.

VENTURINI, WS., BREBBIA, CA. Boundary element formulation for nonlinear applications in geomechanics. *Applied Mathematical Modelling*, v. 8, 1988, p. 251-260.

VENTURINI, WS., BOTTA, AS. Reinforced 2d domain analysis using BEM and regularized BEM/FEM combination. *Computer Modeling in Engineering and Sciences,* n. 8, 2005, p. 15-28.

VERRUIJT, A. Elastic storage of aquifers. In De WIEST, R.J.M. ed. *Flow through porous media*, New York : Academic Press, 1969.

VOYIADJIS, GZ., KATTAN, PI. *Damage Mechanics*. Boca Raton : CRC Press, 2005.

WANG, HF. Theory of linear poroelasticity: with applications to geomechanics and hydrogeology. Princeton : University Press, 2000.

WUTZOW, WW. *Formulação do método dos elementos de contorno para materiais porosos reforçados*. São Carlos: Escola de Engenharia de São Carlos, 2008, 316 p. Ph.D. Thesis in Civil Engineering.

ZHOU, J. *Contribution à la modélisation de l'endommagement anisotrope et de la variation de la perméabilité des roches fragiles*. Lille: Université des sciences et technologies de Lille, 2006, 121 p. Ph.D. Thesis in Civil Engineering.